

Master Thesis

# **Balancing System for a 6-Cell-Lithium-Ion Battery Module Including Protection, Display, and Control Equipment**



**Tian Zhi**

**Leoben, December 2013**

## **EIDESSTATTLICHE ERKLÄRUNG**

**Ich erkläre an Eides statt, dass ich diese Arbeit selbständig, andere als die angegebenen Quellen und Hilfsmittel nicht benutzt und mich auch sonst keiner unerlaubten Hilfsmittel bedient habe.**

**Tian Zhi**

**12. DEZ 2013**

## **Task of Master Thesis**

Candidate: Mr. TIAN Zhi

Date of birth: 26 July 1979

Individual Master Study „Environmental Electrical Energy Engineering“

Supervision: Institute of Electrical Engineering

Title:

Balancing System for a 6-Cell-Lithium-Ion Battery Module Including Protection, Display, and Control Equipment

(Balancing-System für ein 6-Zellen-Lithium-Ionen-Batteriemodul mit Schutz-, Anzeige- und Steuereinrichtungen)

Task:

High power and high energy Lithium-ion cells are state of the art for electrical vehicles. These Lithium-ion cells require an extended battery management system with balancing, supervision and monitoring, and especially protection circuits in case of implementing used cells. A continuously operating passive balancer for 6 cells in series with minimum power consumption is to be designed, built, commissioned, and evaluated as prototype. The balancer shall load cells that exhibit a cell voltage being 0.05 Volts or more over average cell voltage. For this balancing system, monitoring and protection circuits are to be added, too, as well a control input for remote turn-off of the balancer. Balancing currents shall be in the range of about 1.5 Amperes. Dissipated power is to be handled by design. Standard components without alignment components such as variable resistors (potentiometers, trimmers) are to be used. Effects from tolerances of components for balancing performance shall be described by measurement results.

The task is defined in coordination with the candidate. The candidate accepts the task to be accomplished.

---

## ACKNOWLEDGEMENTS

Foremost, I would like to express my sincere gratitude to my supervisor Prof.Dr. Helmut Weiss and Dipl.-Ing. Rudolf Krall, for your patience, motivation, enthusiasm, and immense knowledge. Your guidance helped me in all the time of research and writing of this thesis.

Beside my supervisor, I would like to thank Dipl.-Ing. Johann Krenn and Wenzel Maier, for your encouragement, insightful comments and also in correcting this thesis.

Last but not the least, many thanks to all of my friends and to my family: my mother Zhang Zhengzheng, my wife Xia Yuman and my father Anhu, as well as my son Chris. Each of you can share in this accomplishment, for without your support it would not have been possible.

## 致谢

首先，我衷心的感谢我的导师 **Prof.Dr. Helmut Weiss** 先生，您敏锐的洞察力、渊博的知识，给予了我大量的、极其有益的建议和具体的指导。您严谨的治学态度、精益求精的工作作风给我留下了刻骨铭心的印象，使我受益匪浅。

同时感谢 **Dipl.-Ing. Rudolf Krall** 先生，谢谢你热烈的鼓励和有见地的意见，以及对我论文的审阅和纠错。

此外我还要感谢 **Dipl.-Ing. Johann Krenn** 先生对于本文的审稿和纠错，以及 **Wenzel Maier** 先生在论文实验测试过程中的帮助和支持。

最后，我要感谢我的父亲母亲，妻子，我的儿子克里斯，以及所有在雷奥本给予我帮助的朋友们，你们每个人都可以分享此成就，因为没有你们的支持此论文是不可能完成的。

---

## Abstract

The task of this master thesis is to realize a continuously operating passive balancing system for 6 cells in series including cell condition monitoring and protection circuits. For this system, sensors for voltage and temperature measurement are chosen and installed, protection measures (over-temperature, overvoltage) are installed as well a control input for remote turn-off of the balancer. Distributed power supplies are established and operating status of the entire system is displayed. Finally, the entire system is assembled, commissioned, and tested in laboratory. Voltage equalization for battery pack is evaluated. The balancing system loads cells that exhibit a cell voltage being 0.05 Volts or more over average cell voltage by a moderate current until the overvoltage falls under a defined threshold.

---

## Kurzfassung

Ziel dieser Arbeit ist der Entwurf und Aufbau einer kontinuierlich arbeitenden, passiven Balancier-Einrichtung für sechs Batteriezellen in Serie, inklusive Zustandsüberwachung (condition monitoring) und Schutzbeschaltung (protection circuits). Für dieses System werden Sensoren für Spannungs- und Strommessung ausgewählt, sowie Schutzmaßnahmen für Übertemperatur und Überspannung als auch eine Fernabschaltung der Balanciereinheit aufgebaut. Zuletzt wurde das ganze System im Labor aufgebaut, getestet und die korrekte Funktion der Balanciereinheit demonstriert.

---

## Table of Contents

1	Introduction .....	1
1.1	Lithium-Ion-Battery for Electric Vehicles .....	1
1.1.1	Basic Chemical Characteristics of Lithium-Ion Battery .....	2
1.1.2	Performance Characteristic of Lithium-Ion Battery .....	3
1.2	Aim of Battery Balancing and Protection.....	5
1.3	State of Battery Balancing .....	8
1.4	Tasks of the thesis .....	10
2	Electric Circuit Fundamentals.....	12
2.1	Operational Amplifier .....	12
2.1.1	Non-inverting amplifier .....	14
2.1.2	Inverting amplifier.....	15
2.1.3	Difference Amplifier .....	16
2.2	Window Comparator and Schmitt Trigger .....	17
2.3	Temperature sensors .....	20
2.3.1	Silicon Temperature sensors .....	20
2.3.2	Positive temperature coefficient (PTC) thermistor.....	22
2.4	Diode Transistor Logic Circuit.....	23
2.4.1	AND logic gate .....	24
2.4.2	OR logic gate .....	26
2.4.3	NOT logic gate .....	27
2.4.4	RS flip flop circuit .....	29
2.5	Charge pump.....	30
3	Design and Implementation of the Electric Circuit.....	32
3.1	Battery Balancing .....	32
3.1.1	Measurement system for voltages .....	32
3.1.2	Battery regulator.....	43

---

3.2 Measurement System for Temperature.....	47
3.2.1 Temperature measurement circuit.....	47
3.2.2 Over-temperature detection system .....	49
3.3 Monitoring System for Voltage of Batteries .....	54
3.4 Control and Display Module.....	60
3.5 Power Supply Module.....	64
4 Electric Circuit Testing and Commissioning.....	67
4.1 Testing Function Modules .....	67
4.1.1 Battery voltage measurement .....	67
4.1.2 Voltage monitoring module.....	72
4.1.3 Temperature measurement and over-temperature detection .....	74
4.2 Testing Entire Balancing System with Power Supply .....	77
4.3 Balancing System Installation and Commissioning .....	86
5 Conclusion.....	90
6 Directory .....	92
6.1 Literature .....	92
6.2 Tables .....	93
6.3 Figures.....	94
6.4 List of Symbols .....	98



---

# 1 Introduction

Lithium-ion cells have been used of small batteries for consumer products and are now starting to supplant lead-acid batteries and NiMH cells in large packs for applications such as electric vehicles. Lithium battery in over-temperature, over-charge, or over-discharge cases may result in damage, and even occurrence of fire or explosion. It is very important to build up a battery management system. The task of battery management system is to ensure optimum use of the energy inside the battery and to prevent the risk of potential damage. This can be achieved by monitoring and controlling the charging and discharging process of the battery. Usually, control is imposed on individual cell voltages by passive or active balancing.

## 1.1 Lithium-Ion-Battery for Electric Vehicles

The properties required for a battery in electric vehicle applications are as follows [1]:

- High energy density can be attained with one charge to provide a long range or mileage.
- The high energy density makes it possible to achieve stable power with full discharge characteristics to allow acceleration and ascending power capability of the electric vehicles.
- Long cycle life with maintenance free and high safety mechanisms. Battery cycle life is an indicator for the number of times that the battery can be completely charged and discharged [2].
- Wide acceptance as a recyclable battery from the environmental standpoint.
- Sufficient raw materials availability.

### 1.1.1 Basic Chemical Characteristics of Lithium-Ion Battery

The lithium-ion battery is a rechargeable battery. During discharge of a lithium-ion battery, lithium ions move from the negative electrode (Anode in chemical terms) to the positive electrode (Cathode in chemical terms). When the lithium ions reach the cathode, they are quickly incorporated into the cathode material. This process is reversible in charging process.

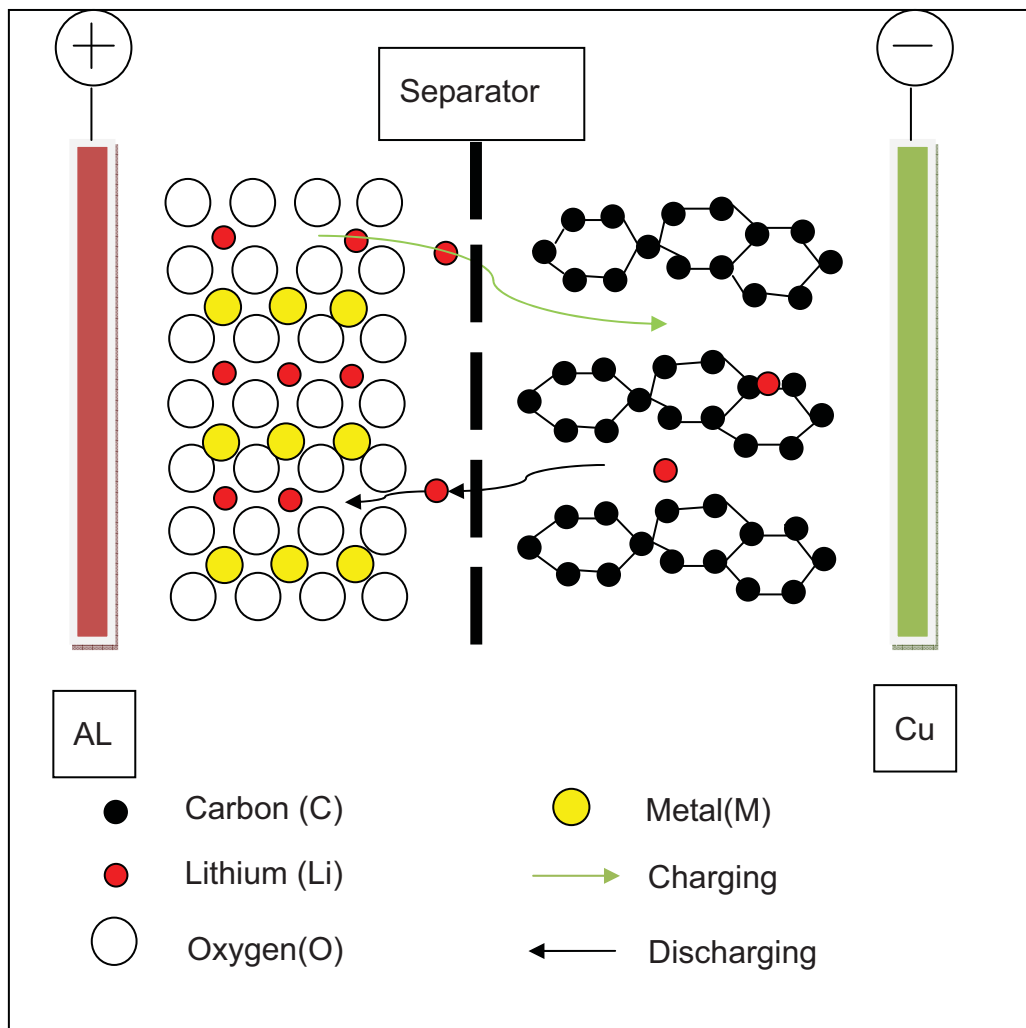


Figure 1.1 Operating Principle of Lithium-ion Battery [3]

In the case of a charge and discharge, as shown in Figure 1.1, the lithium ions which are embedded and prolapsed in the positive and negative materials only

causes changes in the lattice spacing. This will not damage the crystal structure. The memory effect [4] is defined the cell to hold less charge and lose the maximum capacity if it is repeatedly discharged only partway before recharging. Compared with nickel-based batteries, lithium batteries have no memory effect.

During the charging process, the Li-ion cell anode equation is represented as:



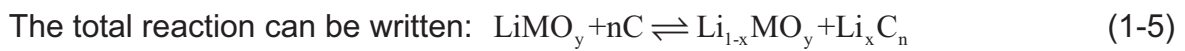
The Li-ion cell cathode equation is represented as:



During the discharging process, the Li-ion cell anode equation is represented as,



The Li-ion cell cathode equation is represented as:



### 1.1.2 Performance Characteristic of Lithium-Ion Battery

Lithium-ion Battery has following performance characteristics.

- Cell voltage

Figure 1.2 shows the equivalent circuit of a lithium-ion battery.

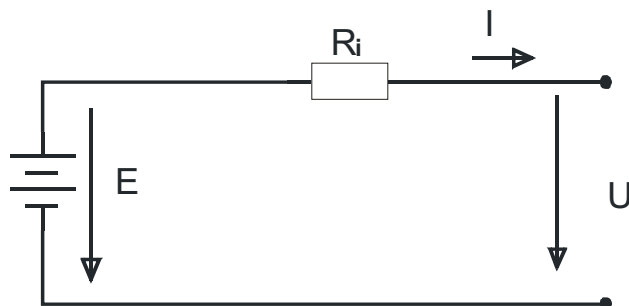


Figure 1.2 equivalent circuit of a lithium-ion battery

The electromotive force, also called emf [5], abbreviated by E, refers to the inner voltage E generated by the cell.

---

The battery terminal voltage  $U$  can be calculated using the following equation:

$$U = E - I * R_i \quad (1-6)$$

Where  $R_i$  is the internal resistance and  $I$  is the actual battery current ( $I$  positive during discharge).

A significant limitation of the effective cell capacity is the point at which charging and discharging is stopped. Cell manufacturers instruct users to stop charging and discharging at given terminal voltages. When the cell voltage reaches the low cutoff discharge level, the cell is considered fully discharged. When the cell voltage reaches the high cutoff charge level, the cell is fully charged. Charging and discharging within these levels prevent cell damage.

- Cell capacity and cell specific capacity

The battery capacity means an integral of current over a defined period of time. The rated capacity is defined as the amount of electric charge which can be delivered under rated conditions. Capacity is measured in units such as amp-hour (A·h). 1Ah means that a battery can deliver one Ampere for 1 hour.

The state of charge (SOC) of the cell is the proportion of the available charge at a certain condition, compared to the total charge available when it is fully charged [8]. The battery capacity can be evaluated using gravimetric specific capacity (A.h/kg) or volumetric specific capacity (A.h/Liter).

- Specific energy

Specific energy is defined as the energy per unit mass. It is also called "energy density." Energy density is the product of the specific capacity and the operating voltage in one full discharge cycle.

Energy density is expressed in  $\frac{\text{Watt.hours}}{\text{Volume}}$  and  $\frac{\text{Watt.hours}}{\text{Weight}}$ .

Table 1.1 Battery Specific energy Comparison [6]

	Pb/SO <sub>4</sub>	NiCd, MiHM	NaS	Li-ion
Battery	Pb(Lead)	Ni(Nickel)	Na(Natrium)	Li(Lithium)
Weight energy density(Wh/kg)	40	60-80	120	180
Volume energy density(Wh/L)	80	150	320	400

A battery directed to the consumer electronics market, especially in the field of electric vehicles, should be as light (high weight energy density) and as small (high volume energy density) as possible. According to table 1.1, conventional batteries such as lead acid and NiCd are heavy and large. NaS operates at about 300 °C and is not considered anymore for standard electric vehicles. In comparison, Lithium-ion battery has four times more energy density than lead acid batteries.

- Internal Resistance

As shown in Figure 1.2, the internal resistance determines the battery's power output and also efficiency. A general requirement is that the internal resistance must be significantly below that of the appliance. It is not a simple ohmic resistance. It depends on the state of charge (SOC), temperature and the current direction [7]. The internal resistance increases when the end of discharge is approached. Large internal resistance will cause lower working voltage and shorter discharge time.

## 1.2 Aim of Battery Balancing and Protection

In a small battery with a few cells in series, the charger voltage is divided rather equally among the cells. In a high-voltage battery with many cells in series, there is a much greater chance that the overall pack voltage is not evenly divided among its cells [8]. A battery with large capacity requires an advanced management system to ensure battery performance. The optimal ambient temperature and cell voltage

---

should be considered. It is important to pay more attention to thermal management, battery reliability, battery life and cell balancing for high-capacity lithium-ion battery pack.

In order to provide sufficient voltage to the device, Lithium battery pack consists of multiple cells in series. The capacity difference between single cells will affect the capacity of the total battery pack. The total capacity of the battery pack is defined by the lowest cell capacity.

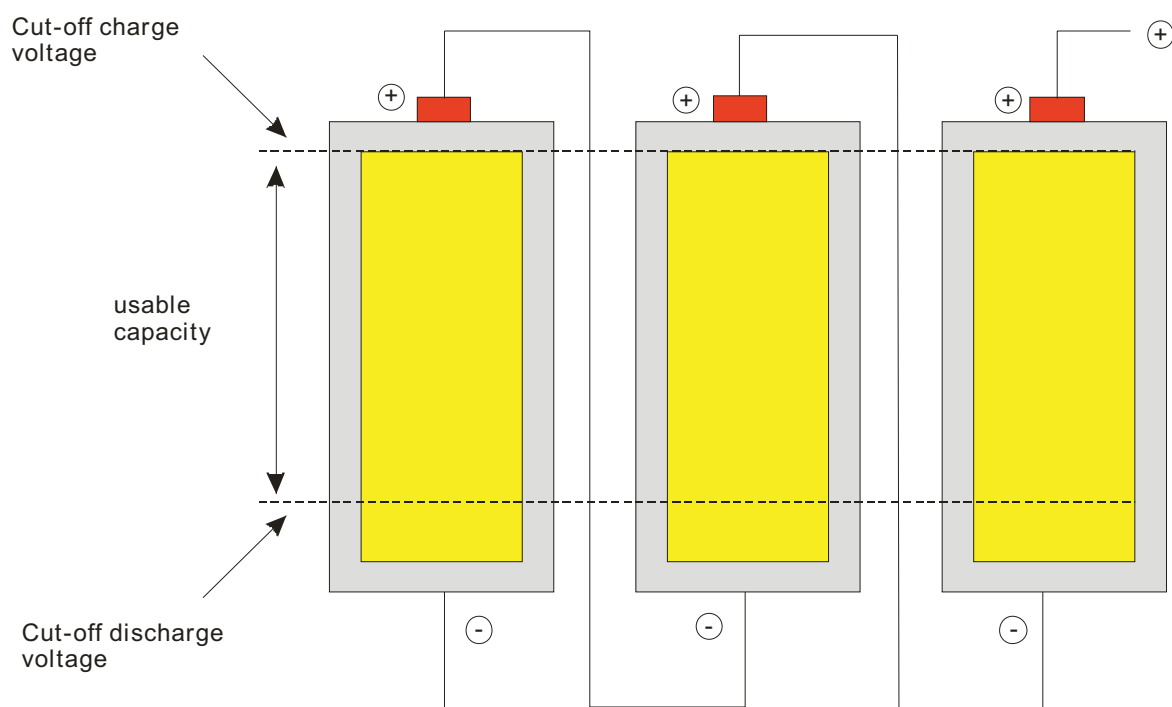


Figure 1.3 3 Battery pack with 3 cells in series

As shown in Figure 1.3, 3 cells are connected in series. Cut-off Charge Voltage and Cut-off discharge Voltage are defined.

Figure 1.4 shows a typical battery discharge without balancing. The Battery in the middle has arrived at cut-off discharge voltage. That is why the whole battery pack has to stop discharge. Otherwise this cell will be damaged.

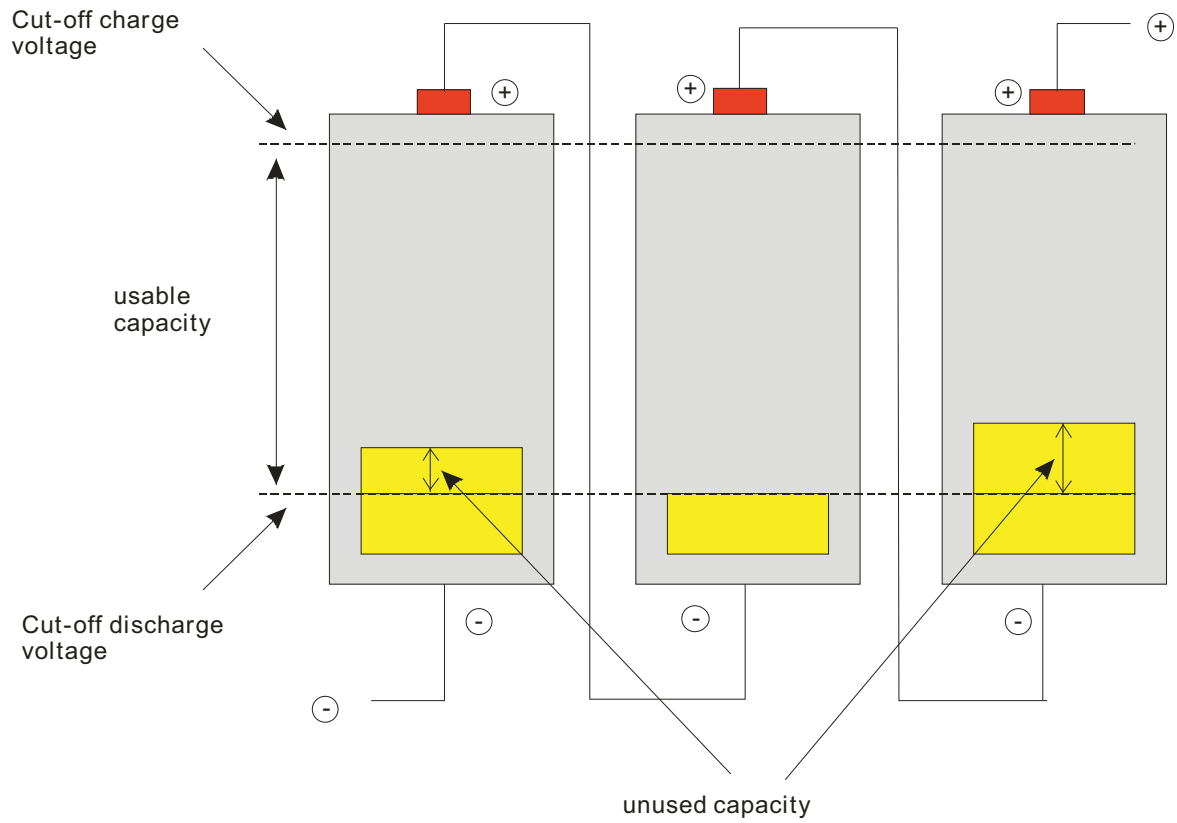


Figure 1.4 Discharging without Battery Balancing

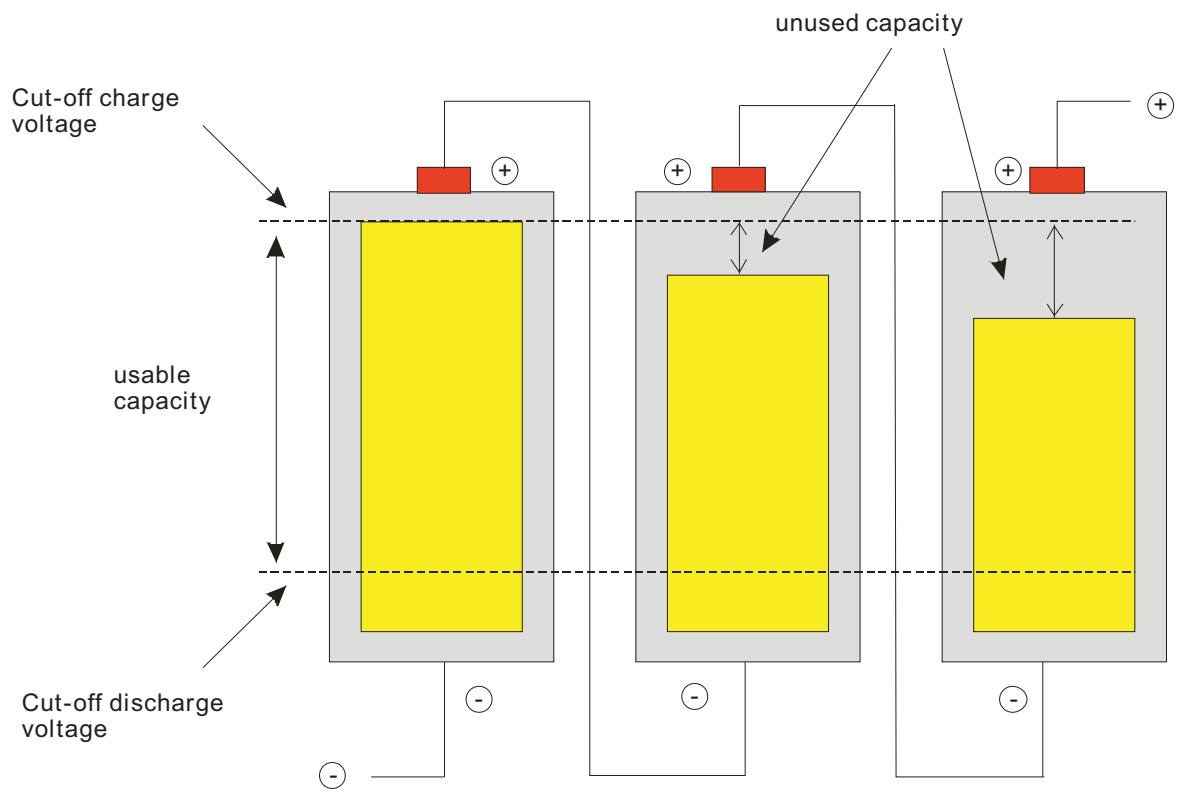


Figure 1.5 Charging without Battery Balancing

---

Figure 1.5 shows one possibility of battery charge without balancing. The battery on the left has arrived at cut-off charge voltage. That means this battery has been fully charged. The charging process of the battery pack should be stopped. However, other 2 batteries have not been fully charged. There are still unused capacities.

There are many reasons for cell imbalance. Because of differences between the individual cells in the battery pack, a certain imbalance in SOC may exist. These cells may have different internal resistance. These differences occur due to manufacturing and will increase because of aging. Another reason could be that some cells become hotter than others. This temperature difference between the cells is influenced by the position of the cells. This effect may be worse for some cells in a battery pack.

In order to solve this cell imbalance problem, a balancing and protection system is needed to rebalance or equalize the battery cells in the battery pack. This will help to maximize battery pack capacity and provide more utilization of the battery which is a critical requirement of an electric vehicle.

### **1.3 State of Battery Balancing**

There are two main methods for battery balancing: passive and active balancing. The active battery balancing methods remove charge from cells with higher charge level and deliver it to cells with lower level.

The passive battery balancing methods dissipate energy through resistors from the cells with higher energy, until the charge matches those of the lower energy cells in the pack or charge reference.

In addition to active and passive balancing methods, balancing system may also be



---

constructed using two architectures: centralized and distributed.

Figure 1.6 shows schematic diagram of a centralized passive battery balancing device. In a centralized architecture, most of the battery management functions are included on a single electronic circuit module. Monitoring, measurement, communication modules and passive balancing power dissipation area are simplified in this centralized electronic circuit. A relatively long wire connects the balancing unit to the battery pack. If the wires are shorted, batteries will be damaged.

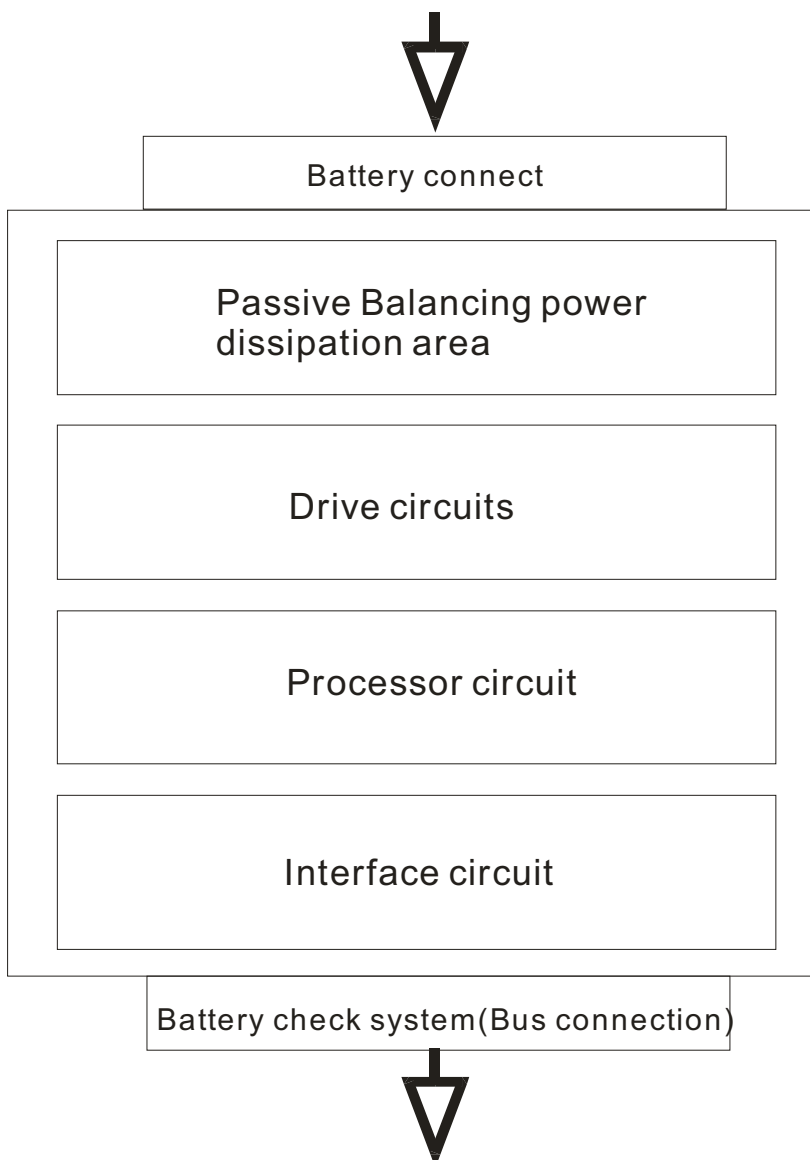


Figure 1.6 Schematic diagram of simple passive Battery balancing device

---

The excess energy can be released by the external circuit connection in parallel to each battery. This circuit consists of a power resistor connected in series with a controlled MOSFET transistor. There is neither potential separation nor short circuit protection. This approach can be used when the physical size of the battery is not too large. It offers less flexibility and safety.

A distributed balancing system increases the number of signal interconnections between modules but reduces power interconnections and allows more flexibility. Monitoring and measuring module are duplicated. The signals from these functions must be communicated to a central process module. Signal communication between modules with potential separation can also be realized. This balancing system is more flexible and safe. Therefore, a distributed balancing system is designed and implemented.

## **1.4 Tasks of the thesis**

Lithium-ion battery is a very important component of electric vehicle. Imbalance of cells in battery system is an essential factor in the battery system life.

Battery balancing system protects the battery system from damage, increases battery life, and maintains the battery system in an accurate and reliable operational condition.

The detailed tasks of this thesis are determined as follows:

### **1. Module arrangement**

The balancing system consists of control module, monitoring module, display module, power supply module and balancing module. The balancing module is mounted directly beside the cell. The control module is located externally and is connected to the balancing module with a cable. A potential separation between control and balancing module is implemented. Further, the balancing function

---

can be activated by an On/Off switch.

2. Protection engineering design (over temperature, voltage monitoring)

An over-temperature protection and a cell voltage monitoring are designed.

3. Design all required functions, include measurement, control, regulation and protection.

4. Implementation

Producing control and balancing circuit. Assembling all function modules of complete circuit.

5. Commissioning in the laboratory

6. Measurement in the laboratory

Measurement of control, monitoring, display and balancing functions.

7. Documentation of hardware layout and measured results.

---

## 2 Electric Circuit Fundamentals

This chapter describes the most important electric components and functional circuits.

### 2.1 Operational Amplifier

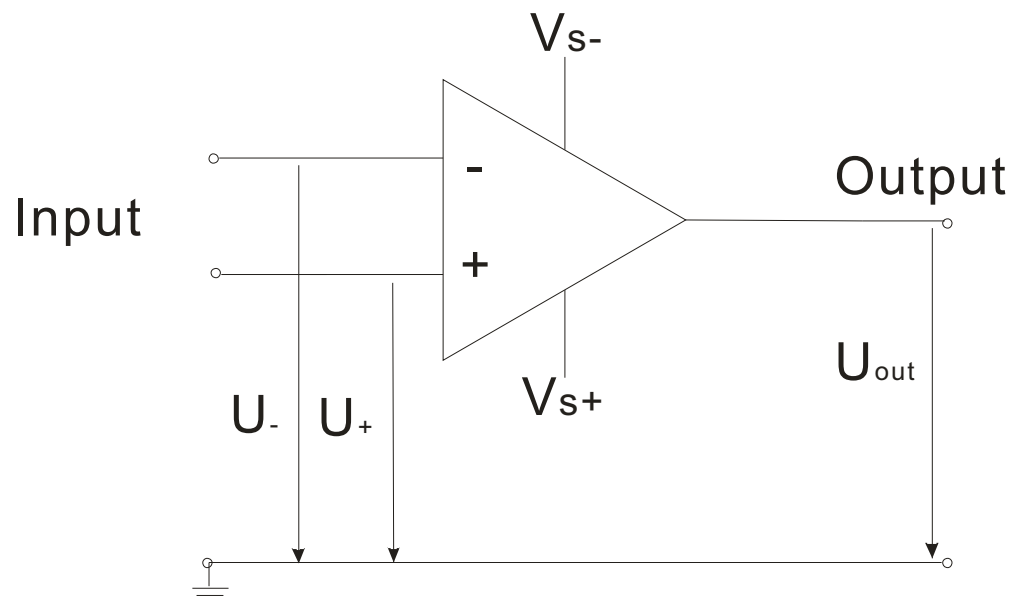


Figure 2.1 Symbol of operational amplifier

Operational amplifier (Op-Amp) has two input terminals, as shown in Figure 2.1, one is called the inverting input ( $U_-$ ) and the other is named as the non-inverting input ( $U_+$ ). The output voltage of the operational amplifier is the difference between the two input terminals, multiplied by the gain  $A$ , which is define by equation (2-1)

$$U_o = A(U_+ - U_-) \quad (2-1)$$

The transfer characteristic of an ideal operational amplifier is shown in Figure 2.2.

As shown in figure 2.2, the output voltage  $U_{out}$  is proportional to the voltage difference  $U_{in}$  in the linear operating range  $-10V < U_{out} < 10V$ .  $V_{o,max}$  is the maximum output voltage and  $V_{o,min}$  is the minimum output voltage. When this limit is reached,

---

a further increase in  $U_{in}$  causes no further increase in  $U_{out}$ . That means, the amplifier is overdriven, or saturated, respectively.

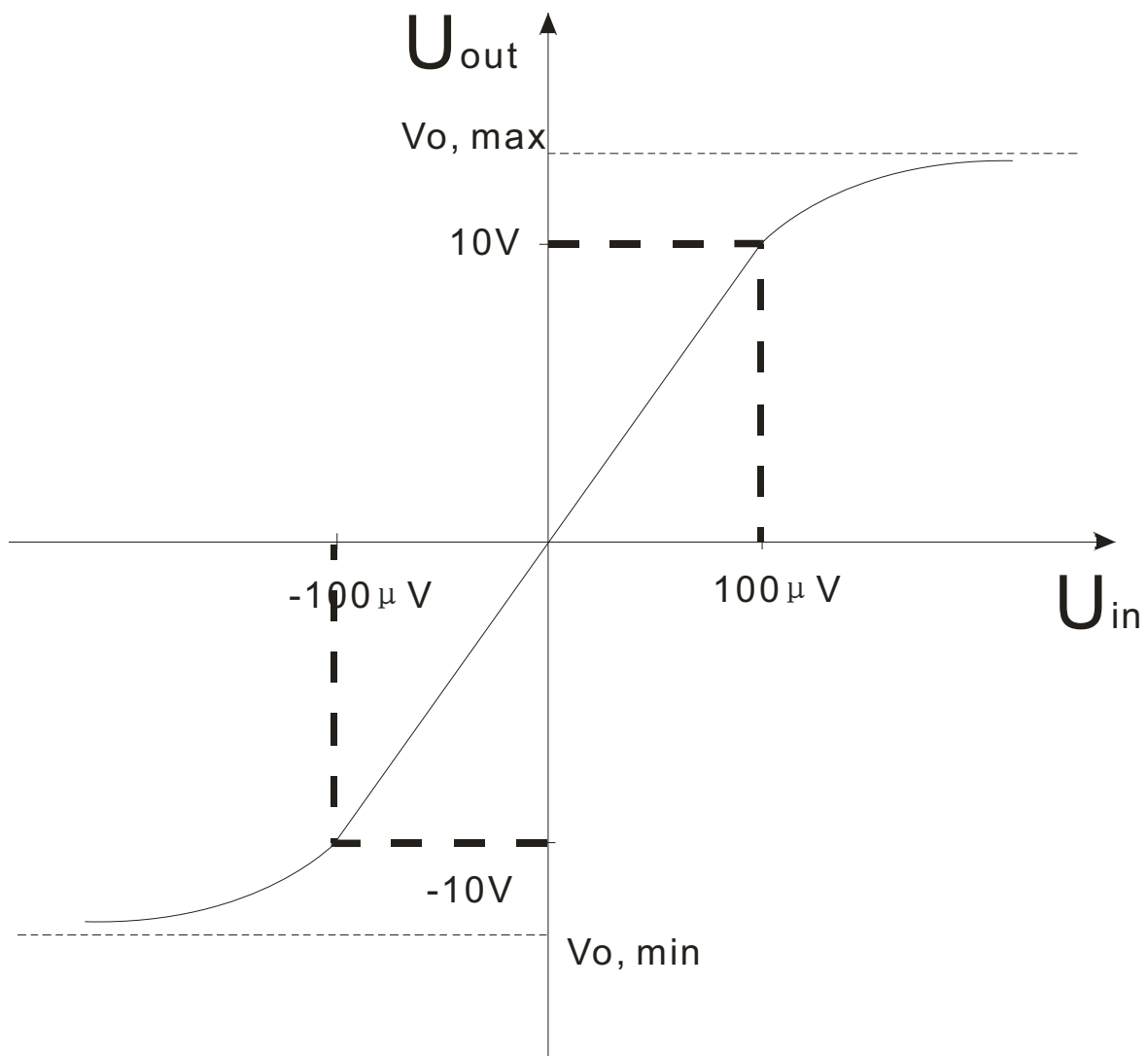


Figure 2.2 Amplifier with voltage output [19]

- Transfer characteristic of an ideal operational amplifier

The Ideal Op-Amp has following characteristics

- The input impedance is infinitely high
- The output impedance is zero
- The open-loop gain ( $A$ ) is infinite.

The real operational amplifier has an open-loop gain with a finite value. This value

is between  $10^4$  and  $10^7$ .

Two basic aspects are used to calculate operational amplifier, behavior under ideal conditions.

1. When negative feedback is applied to the ideal operational amplifier, the difference of input voltage is zero.
2. The current flow into the two input terminals is zero.

### 2.1.1 Non-inverting amplifier

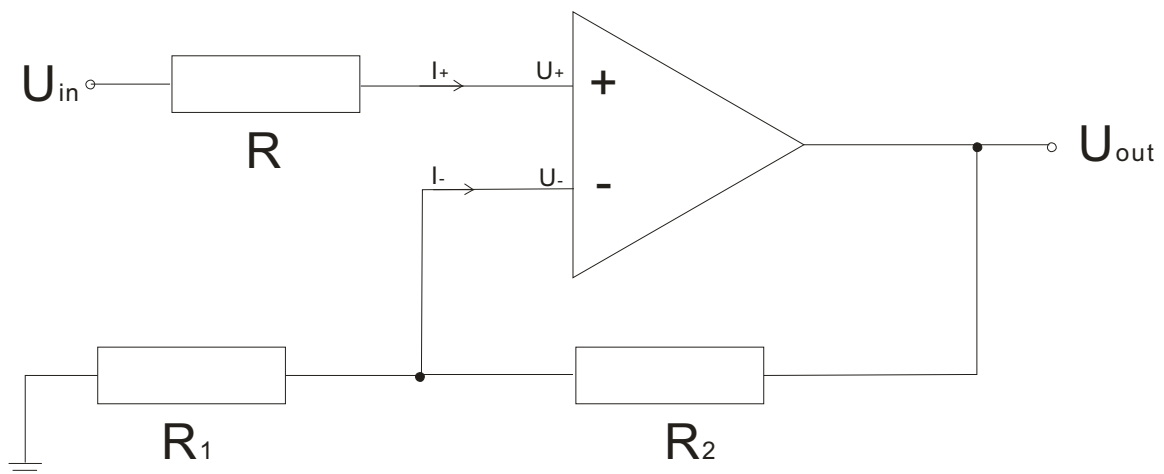


Figure 2.3 Non-inverting amplifier [14]

The non-inverting ideal amplifier, shown in Figure 2.3, has following deductions:

$$U_- = U_+ = U_{in} \quad , \quad I_- = I_+ = 0 \quad , \quad U_- = \frac{R_1}{R_1 + R_2} U_{out} \quad (2-1)$$

The voltage at both inputs must be equal. No current flows into either of the op-amp's input. Potential divider  $R_1$  and  $R_2$  determine the voltage at the inverting input.

$$\Rightarrow \quad U_{out} = \frac{R_1 + R_2}{R_1} U_- = \left(1 + \frac{R_2}{R_1}\right) U_{in} \quad (2-2)$$

Typically,  $R$  is set to zero.  $R$  unequal zero can compensate non-zero input currents of real op-amps. FET-input op-amps are used. Due to their extremely low input

currents, input current effects can be neglected, therefore.

### 2.1.2 Inverting amplifier

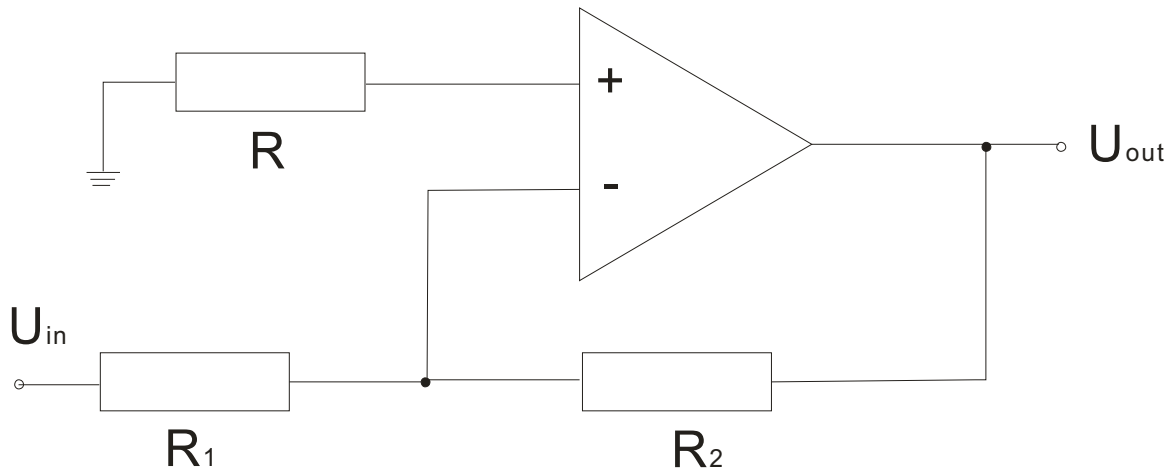


Figure 2.4 Inverting amplifier [14]

The inverting ideal amplifier, shown in Figure 2.4, has following deductions:

$$U_- = U_+ = U_{in}, \quad I_- = I_+ = 0 \quad (2-3)$$

The non-inverting input is connected to ground potential. The inverting input with the negative feedback has the same potential as the non-inverting input. This is known as a virtual earth. Since no current flows into the op-amp input, the current through  $R_1$  and  $R_2$  are equal.

$$\Rightarrow \frac{U_{out} - U_-}{R_2} + \frac{U_{in} - U_-}{R_1} = 0 \quad (2-4)$$

$$\Rightarrow U_{out} = -\frac{R_2}{R_1} U_{in} \quad (2-5)$$

Typically,  $R$  is set to zero.  $R$  unequal zero can compensate non-zero input currents of real op-amps. FET-input op-amps are used. Due to their extremely low input currents, input current effects can be neglected, therefore.

### 2.1.3 Difference Amplifier

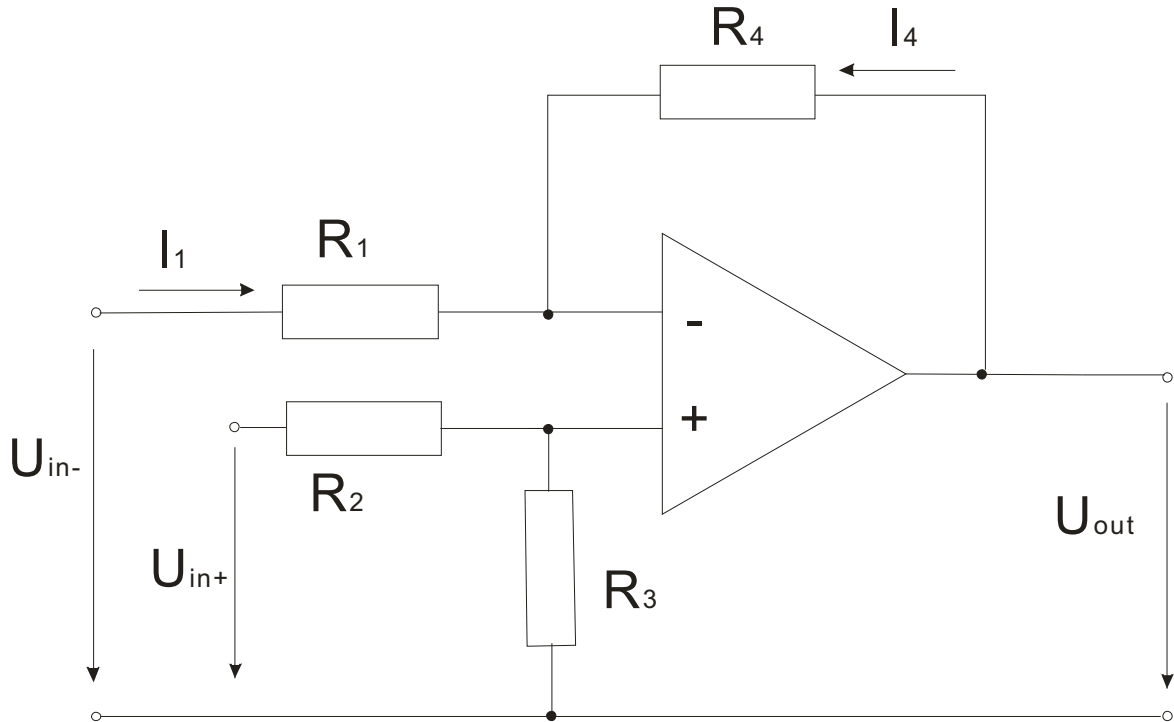


Figure 2.5 Difference Amplifier [15]

The ideal difference amplifier, shown in Figure 2.5, has following deductions:

$$U_- = U_+ , I_1 + I_4 = 0 , I_1 = \frac{U_{in-} - U_-}{R_1} , I_4 = \frac{U_{out} - U_-}{R_4} \quad (2-6)$$

$$U_+ = \frac{R_3}{R_2 + R_3} U_{in+} , U_- = U_{in-} - R_1 I_1 , \quad (2-7)$$

The voltage at both inputs must be equal. No current flows into either of the op-amp's inputs. Potential divider R<sub>1</sub> and R<sub>4</sub> determine the voltage at the inverting input. Potential divider R<sub>2</sub> and R<sub>3</sub> determine the voltage at the non-inverting input.

$$\Rightarrow U_- = \frac{U_{in-} R_4 + U_{out} R_1}{R_1 + R_4} \quad (2-8)$$

$$\Rightarrow U_{out} = \frac{1 + R_4 / R_1}{1 + R_2 / R_3} U_{in+} - \frac{R_4}{R_1} U_{in-} \quad (2-9)$$

$$\text{If } R_1 = R_2 \text{ and } R_3 = R_4 , \quad (2-10)$$



---


$$\Rightarrow U_{\text{out}} = \frac{R_4}{R_1} (U_{\text{in}+} - U_{\text{in}-}) \quad (2-11)$$

The output voltage of the differential amplifier depends on the difference between the voltages applied to the two input terminals and the differential gain.

However, the output of a real differential amplifier has error because of tolerances of resistors. It is necessary to consider the common-mode rejection ratio (CMRR) of a differential amplifier [9]. An ideal differential amplifier would have infinite CMRR.

Formula 2-10 can be changed to:

$$R_3/R_2 = (1+\Delta)R_4/R_1 \quad (2-12)$$

In an idealized situation,  $\Delta$  is 0. But in practice,  $\Delta \neq 0$ , even if the precise resistances are chosen.

For the real situation there is following deduction [9]:

$$\text{CMRR} \approx 20 \cdot \log\left(\frac{1+R_4/R_1}{|\Delta|}\right) \quad [dB]$$

Voltages that are common to both inputs are visible as noise. The more they are amplified, the more the circuit will be inaccurate. The impact of common mode error is tested in chapter 4.

## 2.2 Window Comparator and Schmitt Trigger

The window comparator is a device usually consisting of two voltage comparators. The output of the window comparator indicates whether the measured signal is within the voltage range bounded by two different thresholds (an "upper" threshold and a "lower" threshold).

---

The window comparator circuit schematic is provided in Figure 2.6. Resistor R and diodes form a logical AND circuit. Diodes are required to decouple the op-amp outputs.

The inverting comparator and the non-inverting comparator are combined together in this circuit. The comparator outputs are connected. The input voltage ( $U_{in}$ ) is applied to the positive terminal of one comparator and the negative terminal of the other comparator.

The output is high ( $U_{out}=U_s$ ) when input voltage lies above  $U_{TH-}$  and below  $U_{TH+}$ , otherwise the output is low.

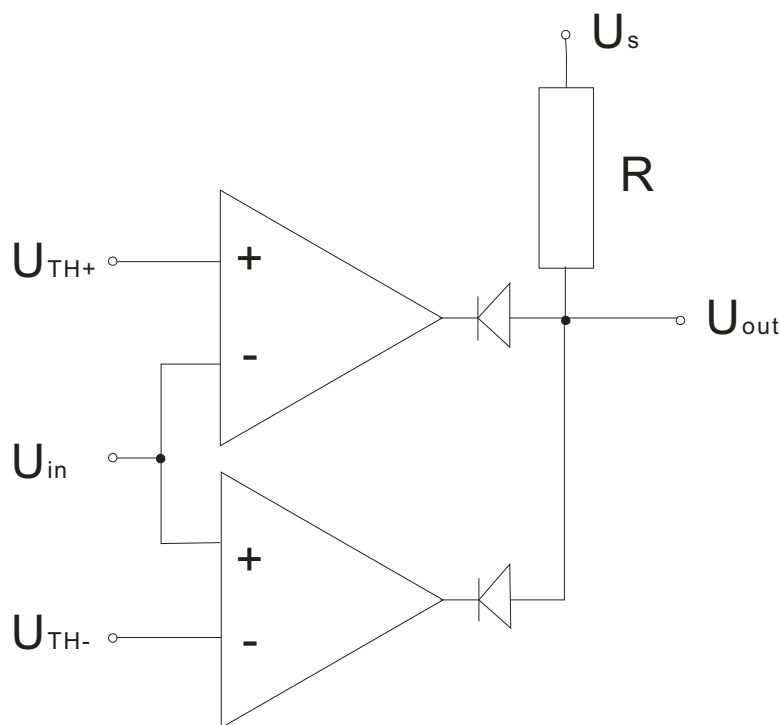


Figure 2.6 function of the window comparator [9]

In this thesis, MAX9065 [10] from Maxim is chosen as window comparator.

The MAX9065 is an ultra-small, low-power, window comparator ideal for a wide variety of electronics applications. The MAX9065 features an input range of -0.3V to +5.5V independent of supply voltage. The upper threshold voltage is 4.2V and the lower threshold voltage is 3.0V. The output is high when input voltage lies above 3.0V and below 4.2V, otherwise the output is low.

In comparators, the operation amplifier is used in open loop mode. The comparator circuit with a positive feedback is called Schmitt trigger [11].

The Figure 2.7 shows the basic Schmitt trigger circuit. The inverting mode produces opposite polarity output. We see positive feedback to the non-inverting input.

When the input voltage  $U_{in}$  is more positive than  $U_{ref}$ , the output gets driven into negative saturation at  $U_{out\_min}$  level. When the input voltage  $U_{in}$  becomes more negative than  $-U_{ref}$ , the output gets driven into positive saturation at  $U_{out\_max}$  level. The output voltage is always at  $U_{out\_max}$  or  $U_{out\_min}$ .

$+U_{ref}$  is called as the upper threshold voltage and  $-U_{ref}$  is called as the lower threshold voltage. The voltage  $U_{ref}$  can be controlled by the voltage divider  $R_1$  and  $R_2$ .

$$\text{Lower threshold voltage } -U_{ref} = \frac{R_1}{R_1 + R_2} U_{out\_min}$$

$$\text{Upper threshold voltage } U_{ref} = \frac{R_1}{R_1 + R_2} U_{out\_max}$$

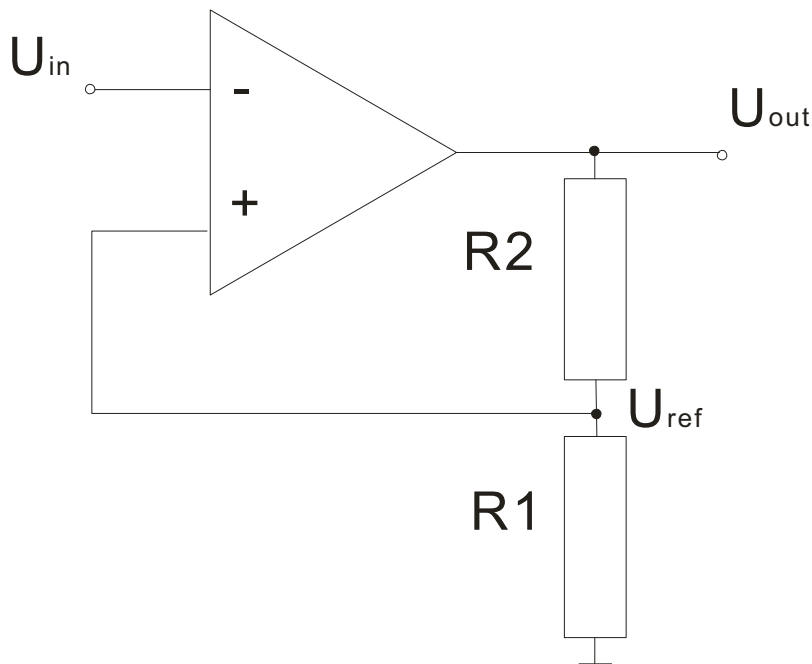


Figure 2.7 Inverting Schmitt Trigger [19]

---

The output voltage remains in a given state until the input voltage exceeds the threshold voltage level either positive or negative.

The corresponding transfer characteristic is shown in Figure 2.8

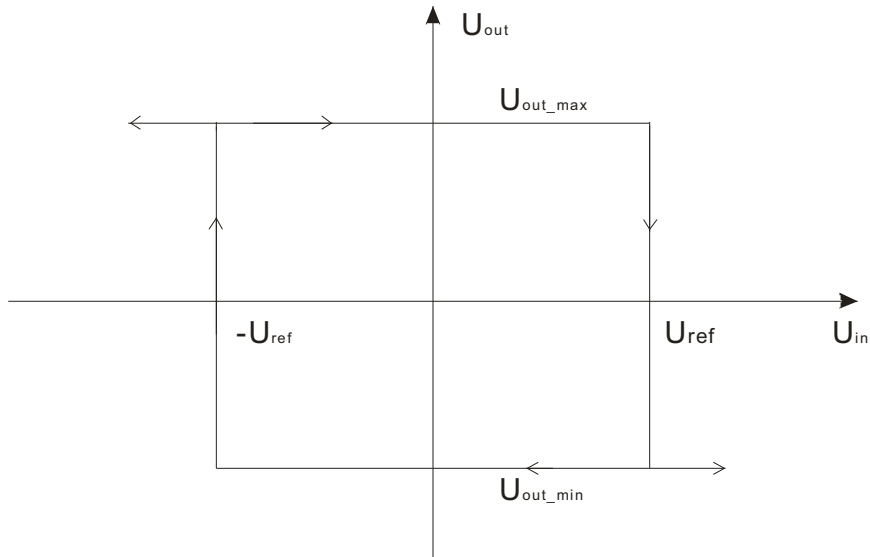


Figure 2.8 Transfer characteristic of Schmitt Trigger

As shown in Figure 2.8, once the output changes the state, it remains there until the input voltage exceeds the other threshold voltage. Hysteresis of Schmitt trigger is given by the difference between  $U_{ref}$  and  $-U_{ref}$ .

## 2.3 Temperature sensors

Electronic components and batteries need a defined operating temperature. If the operating temperature is out of range, they cannot work properly or will even be damaged. Therefore, temperature sensors are used in temperature measurement and control circuits.

### 2.3.1 Silicon Temperature sensors

The molecular silicon is an inherently stable element, especially in its crystalline form. Silicon-based temperature sensors are stable over time and over extreme environmental conditions. Therefore, silicon temperature sensors are used for temperature measurement in automotive applications.

---

Temperature coefficient of a resistance is the measure of the change in electrical resistance of any substance per degree of temperature rise.

Let a conductor having a resistance of  $R_0$  at  $0^\circ\text{C}$  and  $R_t$  at  $T^\circ\text{C}$  respectively.

From the equation of resistance variation with temperature:

$$\frac{R_t}{R_0} = \frac{T_0 + T}{T_0 + 0}$$

$$\Rightarrow R_t = R_0 + \frac{R_0 \cdot T}{T_0}$$

$$\Rightarrow R_t - R_0 = \Delta R = \frac{R_0 \cdot T}{T_0} = \alpha_0 \cdot R_0 \cdot T \quad \text{where} \quad \alpha_0 = \frac{1}{T_0}$$

This  $\alpha_0$  is called temperature coefficient of resistance of that substance at  $T_0$ .

The temperature sensors KTY81 series [12] have a positive temperature coefficient of resistance. If the temperature increases, the resistance increases in the same time. It has a wide operating range from  $-55^\circ\text{C}$  to  $150^\circ\text{C}$ . The required temperature measurement range of balancing system is from  $-50^\circ\text{C}$  to  $100^\circ\text{C}$ . Therefore, it is suitable for use in measurement and control systems.

As shown in Figure 2.9, KTY sensors display a virtually linear temperature coefficient over their operating temperature range, ensuring both simple as well as highly accurate temperature measurements. A resistor can be added additionally for improved linearization. Furthermore, silicon is inherently stable, so KTY sensors are extremely reliable (typically  $\pm 0.05$  K per year [12]) and have very long operational lifetimes.

Fig 2.6 shows R/T curve of KTY81/210

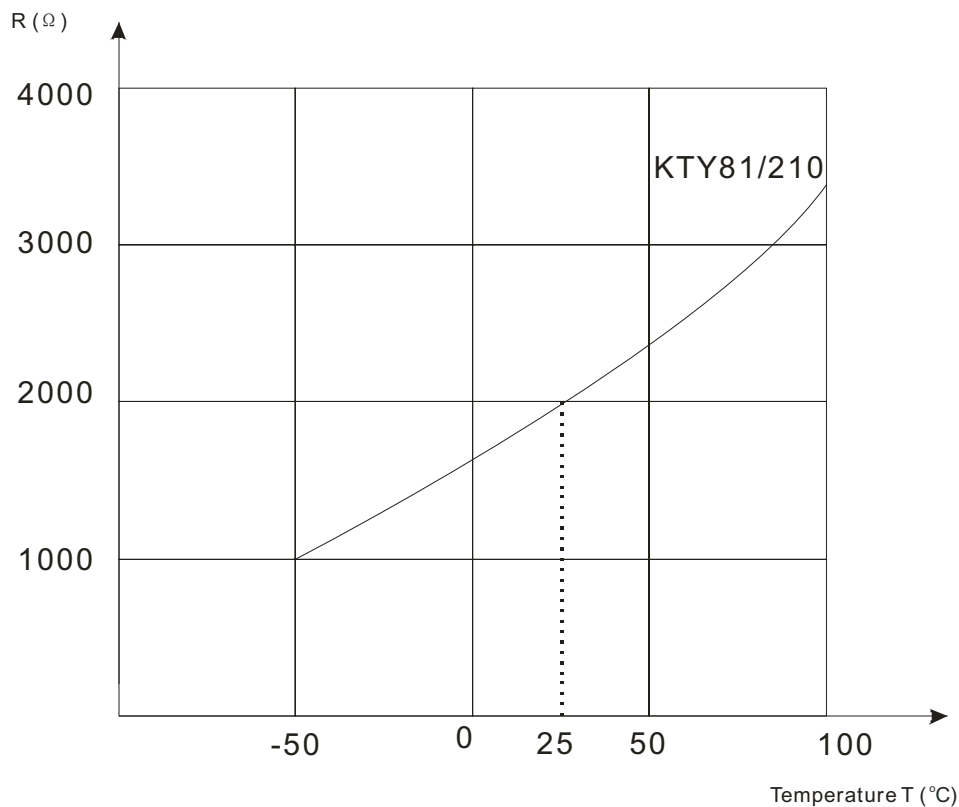


Figure 2.9 R/T curve of KTY81/210

### 2.3.2 Positive temperature coefficient (PTC) thermistor

The PTC thermistor is made of a doped polycrystalline ceramic containing barium titanate ( $\text{BaTiO}_3$ ) and other compounds.

A PTC thermistor has properties like a switch. This means the PTC thermistors have an approximately constant resistance at temperatures below their switch temperature,  $T_s$ , as shown in Figure 2.10. A temperature above  $T_s$ , the resistance increases dramatically. Because of this large change in resistance, PTC thermistors are used as resettable fuses to protect electric circuit or battery from overheating or from damage by sustained excessive currents.

PTC thermistors have a positive temperature coefficient. When the circuit is working properly, the temperature of PTC is the same as room temperature. When the temperature is higher than the switching temperature  $T_s$ , (for example: short

circuit) the resistance of PTC would increase. The increased resistance would break the circuit and allow only a small leakage current.

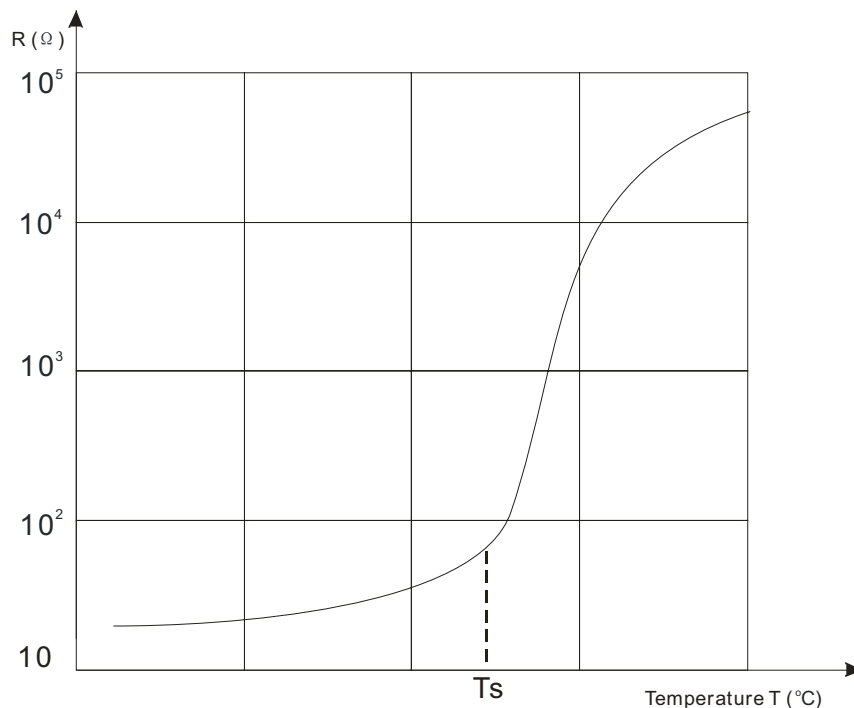


Figure 2.10 RT curve of PTC thermistor

After removing the short, the temperature decreases below the switching temperature  $T_s$  again. PTC 'resets' and allows normal current to flow again. It's a resettable fuse that protects the system.

According to the properties of PTC thermistors, it is suitable to use on battery powered devices that need to protect against high-current accidental discharges.

PTC devices are used as protection components for over-temperature detection independent from the standard temperature measurement.

## 2.4 Diode Transistor Logic Circuit

Logic gates are the basic components of the electric circuit. Any boolean algebra operation can be associated with an electronic circuit in which the inputs and outputs represent the statements of the boolean algebra. Although these circuits may be complex, they may all be constructed from three basic devices. These are

---

the AND gate, the OR gate and the NOT gate.

Diode Transistor Logic (DTL) [13] circuits are built with diodes, transistors, and resistors.

### 2.4.1 AND logic gate

The AND gate is named this way because it operates in the same way as an AND logical operator. The output is 1(high) only when all the inputs are 1(high) and, 0(low) if at least one of the inputs is 0(low). The schematic representation of the AND gate is shown in Figure 2.11

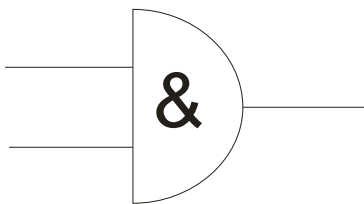


Figure 2.11 The schematic diagram for the two-input AND gate

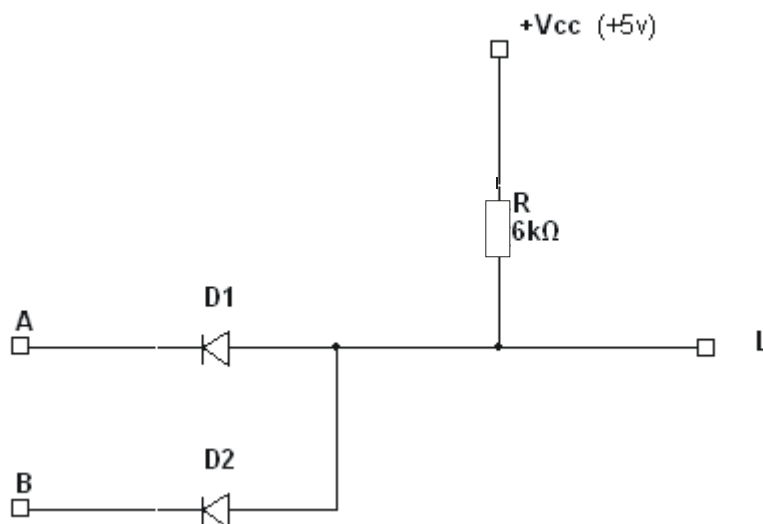


Figure 2.12 Typical DTL Circuit of AND logic gate



Figure 2.12 shows the typical DTL circuit of AND logic gate. Each Input A and B is connected with a diode. Both the diodes are connected in the reverse directions and forward biased by an additional voltage source  $+V_{cc}$  through the pull-up resistor R.

When all the input voltages are high, both diodes are reversely biased. There is no current through diodes and resistor R. This pulls up the output to the supply voltage  $+V_{cc}$  (+5V). Therefore, the output is high.

When the input A is low, and the input B is high, the upper diode is forward-biased (ON) and it pulls the output down to a low voltage. With the input B high, the lower diode goes into reverse bias (OFF).

The following table shows the relationship between input and output voltages.

Table 2.1 input and output voltages of AND logic gate

INPUT		OUTPUT
$V_A(V)$	$V_B(V)$	$V_L(V)$
0	0	0
0	5	0
5	0	0
5	5	5

From this table, the following truth table is obtained.

Table 2.2 Truth table of AND logic gate

INPUT		OUTPUT
A	B	L
0	0	0
0	1	0
1	0	0
1	1	1

---

## 2.4.2 OR logic gate

The output of the OR logic gate is 1(high) if one or both of the inputs are 1(high). If both inputs are 0(low) then the output is 0(low).

Figure 2.13 shows the schematic diagram for the two-input OR gate.

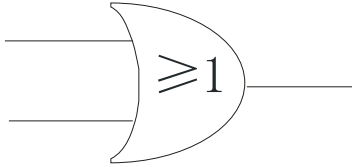


Figure 2.13 The schematic diagram for the two-input OR gate

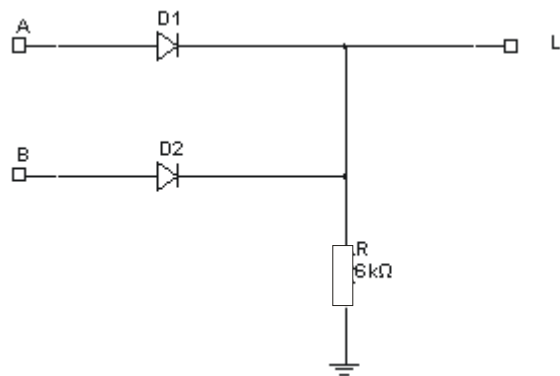


Figure 2.14 Typical DTL Circuit of OR logic gate

Figure 2.14 shows the typical DTL circuit of the AND logic gate. Each Input A and B is connected to a diode. Both diodes are connected in forward direction. A resistor is also connected in the circuit to ground.

When both input voltages are low, the anodes of both diodes are grounded. The diodes are reverse biased and the output voltage is low.

When the input A is low and input B is high, input B forward-biases lower diode, producing an output voltage high. The upper diode D1 is reverse biased. The output voltage is high.

The following table shows the relationship between input and output voltages.

Table 2.3 input and output voltages of OR logic gate

INPUT		OUTPUT
$V_A(V)$	$V_B(V)$	$V_L(V)$
0	0	0
0	5	5
5	0	5
5	5	5

From this table, the following truth table is obtained.

Table 2.4 Truth table of OR logic gate [17]

INPUT		OUTPUT
A	B	L
0	0	0
0	1	1
1	0	1
1	1	1

### 2.4.3 NOT logic gate

The NOT gate is different from other types of electronic inverter devices. It has only one input. It reverses the logic state. Figure 2.15 shows the schematic diagram for the NOT gate.

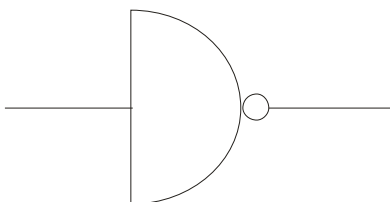


Figure 2.15 Schematic diagram for NOT gate

Figure 2.16 shows the typical circuit of NOT logic gate.

If the voltage of the input source is high, the transistor is turned on through its base current. The output voltage is low.

If the input voltage is low, the transistor does not get a base current and is turned off. The output voltage is high.

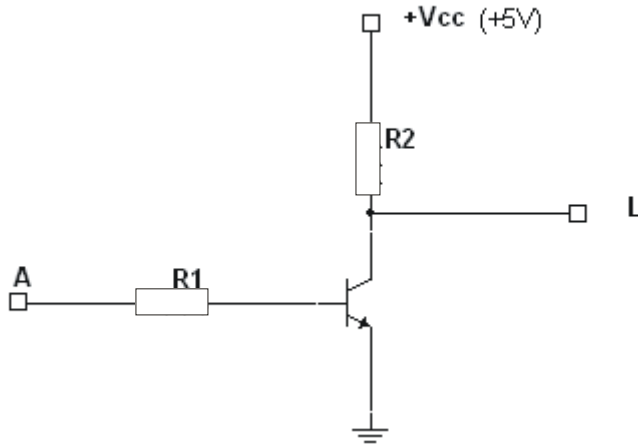


Figure 2.16 Typical DTL Circuit of NOT logic gate

Table 2.5 input and output voltages of NOT logic gate

INPUT	OUTPUT
$V_A(V)$	$V_L(V)$
0	5
5	0

From this table, the following truth table is obtained.

Table 2.6 Truth table of NOT logic gate [17]

INPUT	OUTPUT
A	L
0	1
1	0

---

### 2.4.4 RS flip flop circuit

If it is necessary to save signal status, the RS flip flop circuit can achieve this function. There are two logic or digital circuits for an RS flip flop, one using NAND gates and the other RS flip-flop using NOR gates. Figure 2.17 shows the basic flip-flop circuit with NAND gates. Figure 2.18 shows the basic flip-flop circuit with NOR gates. A connection within the flip-flop is the feedback path from the output of one gate into the input of other gate. This characteristic feedback determines the truth table of the flip-flop as well as its memory property.

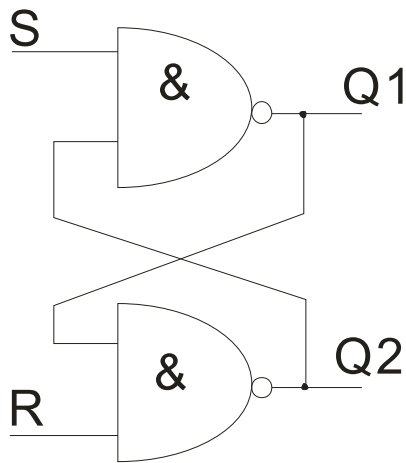


Figure 2.17 Basic flip-flop circuit with NAND gates [16]

Table 2.7 Truth table for RS flip flop using two NAND gates

S	R	Q1	Q2	Action
0	1	1	0	Set
1	1	X	$\bar{X}$	Hold
1	0	0	1	Reset
0	0	1	1	To be avoided

For S=1 and R=1 in “Hold” condition, the output states from previous state are maintained.

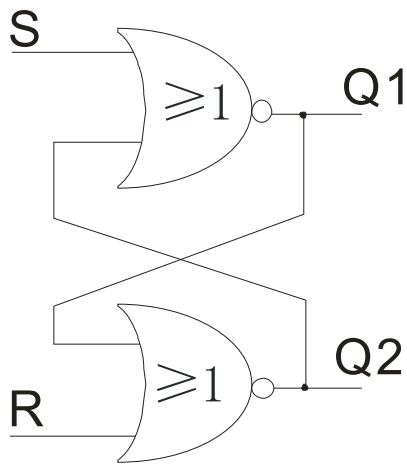


Figure 2.18 Basic flip-flop circuit with NOR gates [16]

Table 2.8 Truth table for RS flip flop using two NOR gates

S	R	Q1	Q2	Action
1	0	0	1	Set
0	0	X	$\bar{X}$	Hold
0	1	1	0	Reset
1	1	0	0	To be avoided

## 2.5 Charge pump

A charge pump is a DC to DC converter that uses capacitors as energy storage elements to create either a higher or lower voltage power source [18]. Charge pumps can be used to invert a voltage, if the current requirement delivered by the load is low [19].

Figure 2.19 and Figure 2.20 show the circuit schematic of charge pump.

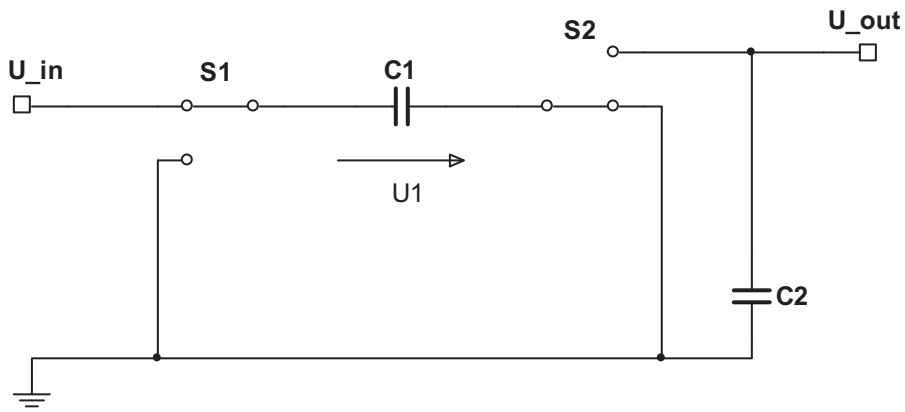


Figure 2.19 Voltage inverter employing the charge pump principle [19], state 1: charging of C1

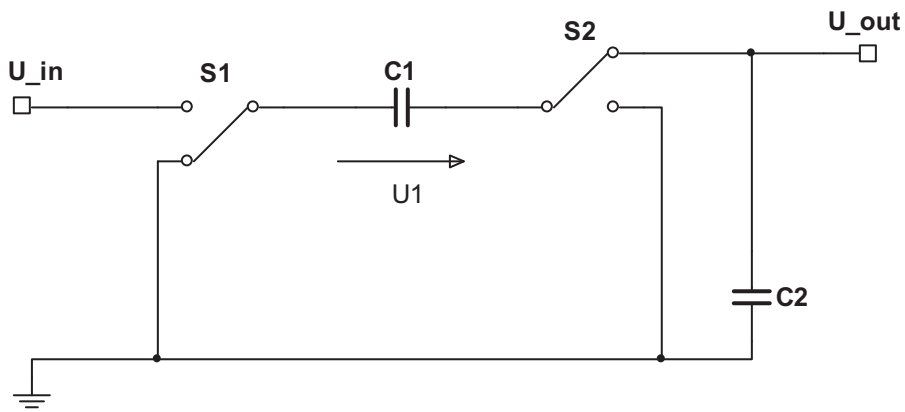


Figure 2.20 Voltage inverter employing the charge pump principle [19], state 2: discharging of C1

In the switch position shown in Figure 2.19, the charge pump capacitor C1 is charged to the input voltage  $U_{in}=U_1$ . During the switching cycle shown in Figure 2.20, the voltage of C1 is inverted and applied to capacitor C2. For perfect switches the output voltage is the negative of the input voltage  $U_{out}=-U_1=-U_{in}$ .

---

## 3 Design and Implementation of the Electric Circuit

On the basis of the theoretical introduction in the chapter above, the electric circuit with the following function modules will be designed and implemented.

1. Battery balancing module
2. Voltage monitoring module
3. Temperature measurement module
4. Control and display module
5. Power supply module

### 3.1 Battery Balancing

The individual cell voltages will differ over time. As a consequence, especially at the end of the charging cycle, battery pack capacity will decrease quickly without battery balancing system and even can be destroyed by overcharging of some cells. Passive balancing methods will be used in this thesis to prevent this problem.

The core concept of this method is removing the excess charge from the cells with high state of charge (SOC) through a power resistor until the SOC matches those of the cells with lower SOC in the pack or the charge reference as we consider the cell voltage being a state of charge indicator.

#### 3.1.1 Measurement system for voltages

There are in total 12 batteries in the battery pack. Always two batteries are connected in parallel. This results in 6 different cell voltages. The connection of the batteries is shown in Figure 3.1



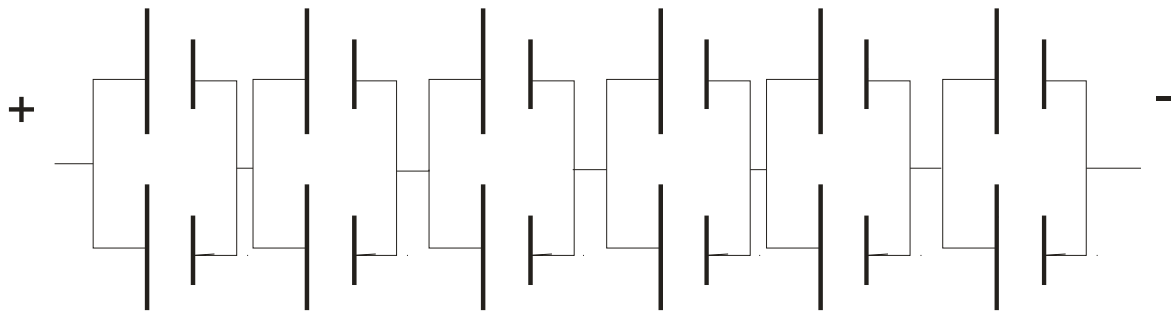


Figure 3.1 Battery pack connection diagram

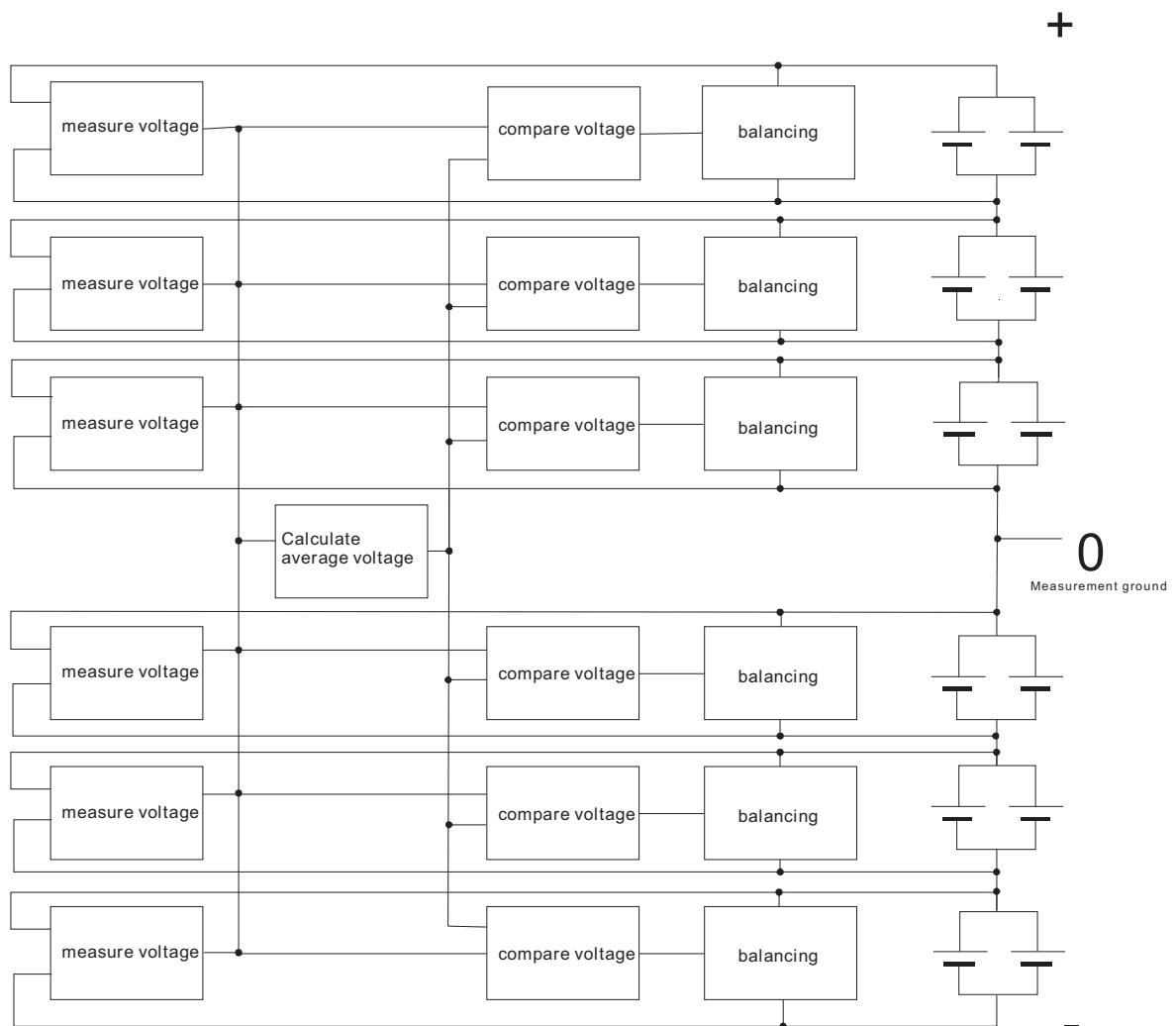


Figure 3.2 Block diagram for measurement and balancing system

The actual battery voltage shows the information for the charged and discharged battery condition. The measurement system has to evaluate the voltage for each individual battery. Based on the measured voltage for each individual battery, the average battery voltage in the battery pack is calculated. The deviation between the

average battery voltage and each individual battery voltage is calculated consecutively and evaluated. This signal is used to control the bypass load of each individual cell, or double-cell as in this case, respectively.

Figure 3.2 shows the block diagram for measurement and balancing system

In figure 3.2 the measurement ground, the total positive and the total negative potential is defined. These connection points to battery can be used as power supply of the measurement system. According to system requirements, it is necessary to add ON/OFF function by the control part.

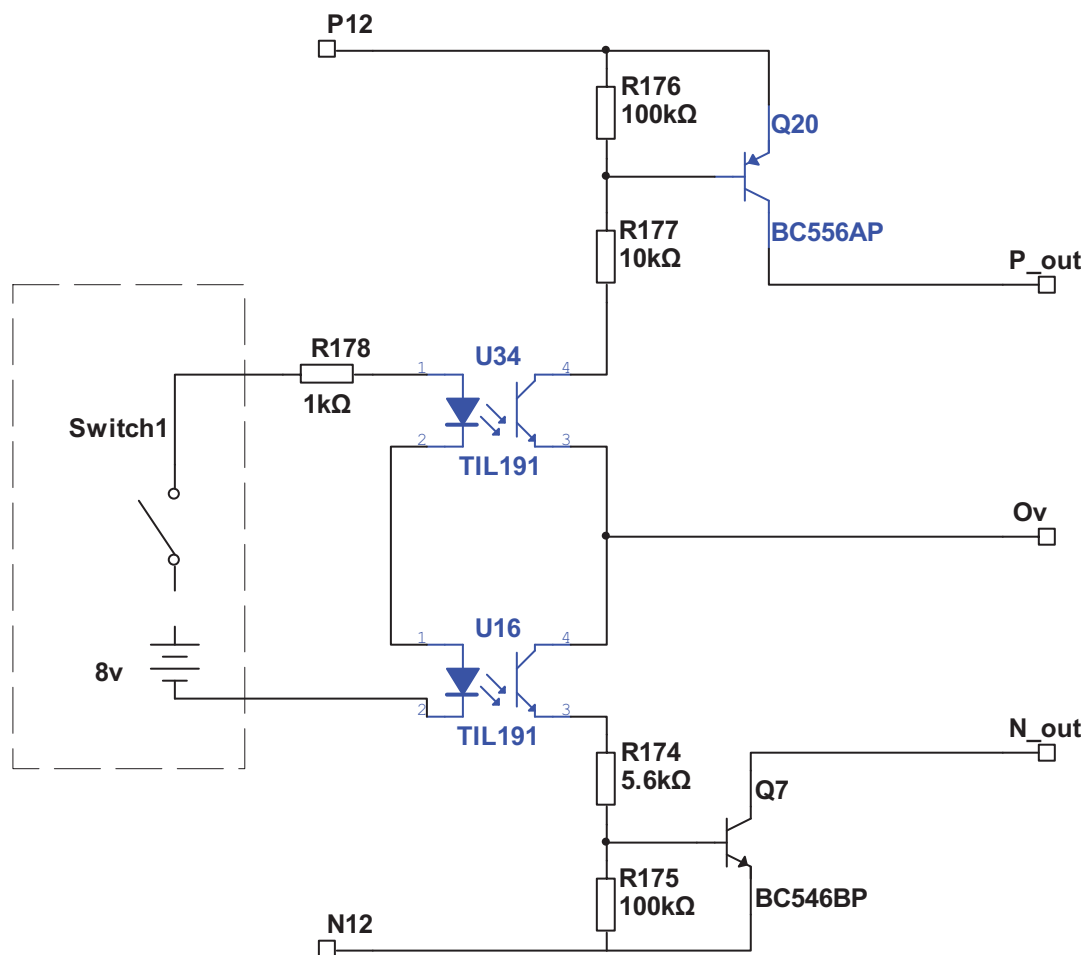


Figure 3.3 Circuit diagram for ON/OFF function

The area indicated with dashed lines, shown in Figure 3.3, is a part of a control and display module. Switch1 is the ON/OFF switch for power supply of the measurement system.

A difference amplifier measures the voltage for each individual battery. The output voltage of a difference amplifier can be calculated according to equation 3-1.

$$U_{out} = A(U_{in+} - U_{in-}) \quad (3-1)$$

A is the differential gain under feedback conditions.

Figure 3.4 shows the circuit diagram for the voltage measurement. The cell voltage is calculated.

$$U_{battery} = U_{+} - U_{-} \quad (3-2)$$

For detailed calculations refer to chapter 2.1.3.

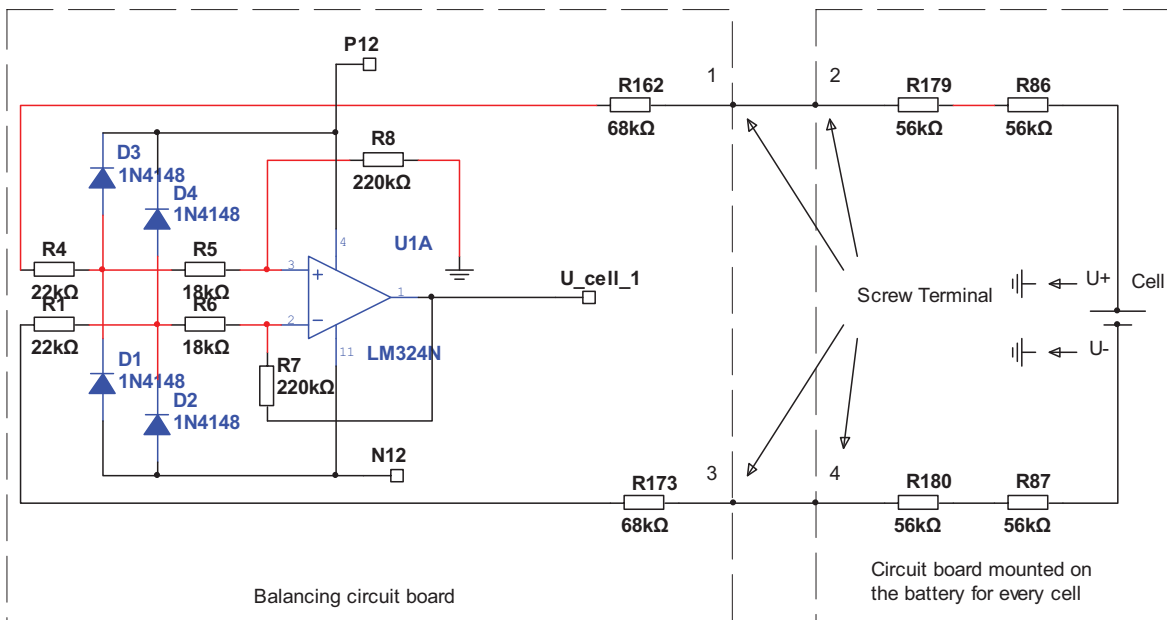


Figure 3.4 Circuit diagram for voltage measurement of cell1

When the difference amplifier circuit is connected directly to battery with a long wire, the batteries may explode or the wires start burning and/or melting if the wires are shorted. For safety reasons, it is important to split the circuit into 2 parts. One part is installed in the balancing circuit board, and the other part is installed in the circuit board, directly on the battery. Terminal 1, 2 and terminal 3, 4 are connected with wires. If the wires are shorted between cell and balancing board, there are still enough protection resistors.

All measured cell voltages are fed to the average calculator, as can be seen in Figure 3.5

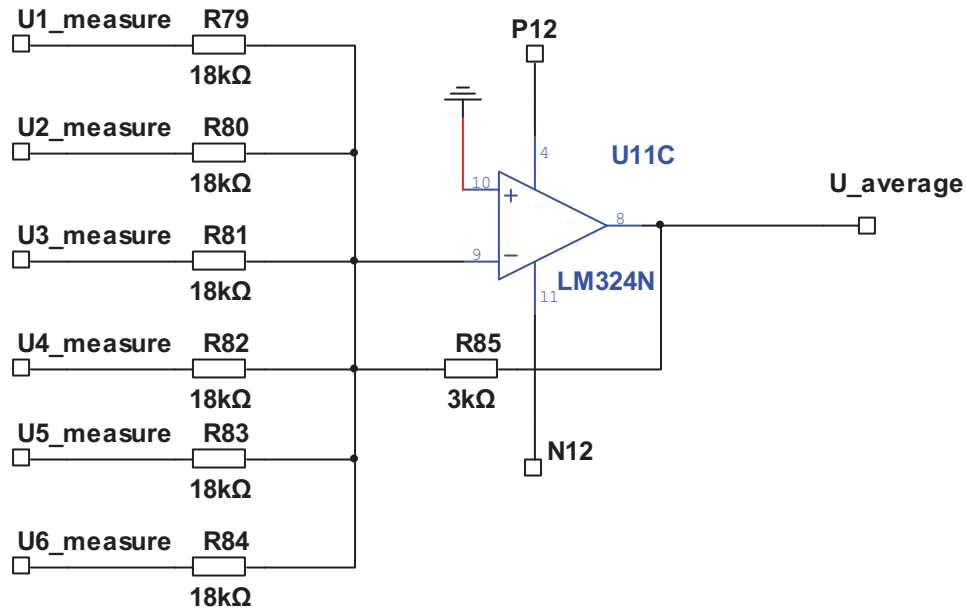


Figure 3.5 Circuit diagram of the average calculator

Since the inverting terminal of op-amp acts as a virtual ground, applying Kirchhoff's current law, following equation can be written:

$$\frac{U_1}{R_{79}} + \frac{U_2}{R_{80}} + \frac{U_3}{R_{81}} + \frac{U_4}{R_{82}} + \frac{U_5}{R_{83}} + \frac{U_6}{R_{84}} + \frac{U_{average}}{R_{85}} = 0 \quad (3-3)$$

$$R_{79}=R_{80}=R_{81}=R_{82}=R_{83}=R_{84}=18K\Omega \text{ and } R_{85}=3 K\Omega$$

$$\Rightarrow U_{average} = -\left(\frac{U_1 + U_2 + U_3 + U_4 + U_5 + U_6}{6}\right) \quad (3-4)$$

That means, the output of the average calculator is negative value of average voltage.

Then, the output signal U\_average is compared with each individual battery voltage.

The circuit diagrams are shown in Figure 3.6, Figure 3.7 and Figure 3.8.

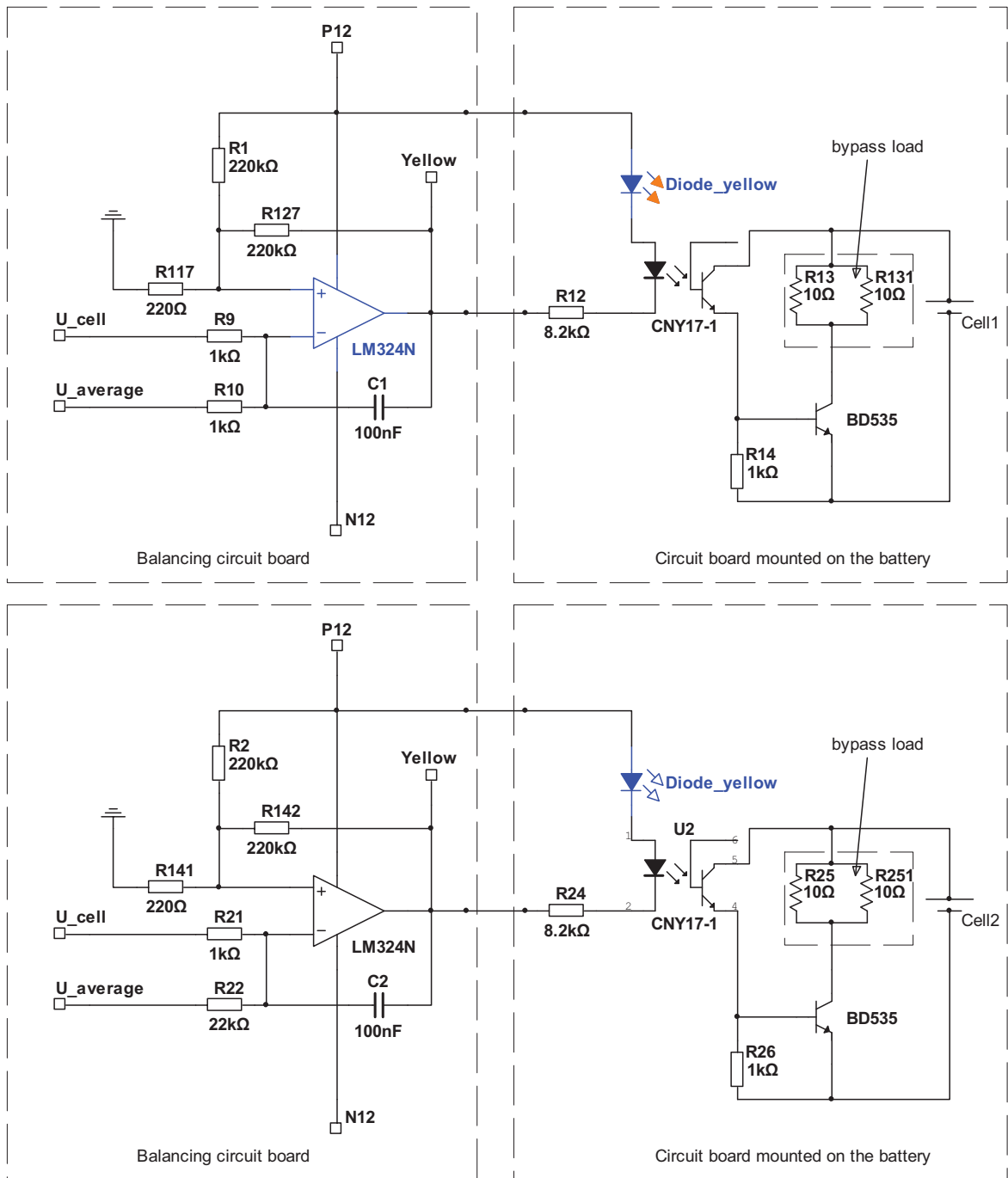


Figure 3.6 Circuit diagram bypass load controller and battery regulator for cell1 and cell2

As shown in Figure 3.6, resistor R117 and R127 are connected to the non-inverting input of the OP-AMP and operate here as a Schmitt trigger. R1 provides an offset for the Schmitt trigger as described later. The input of the Schmitt trigger is the difference between cell voltage and average voltage. The output of the Schmitt trigger is used to control the by-pass load.

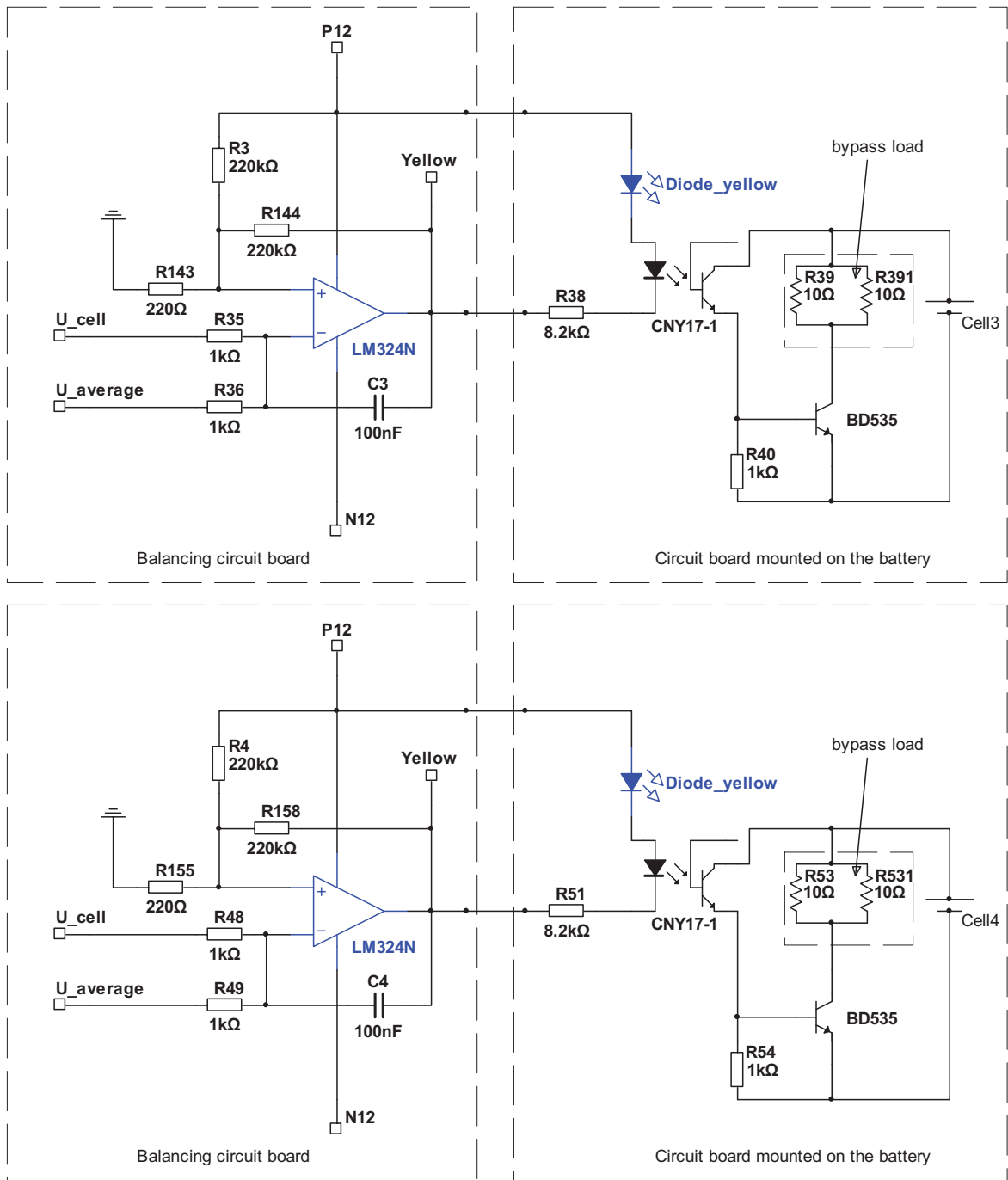


Figure 3.7 Circuit diagram bypass load controller and battery regulator for cell3 and cell4

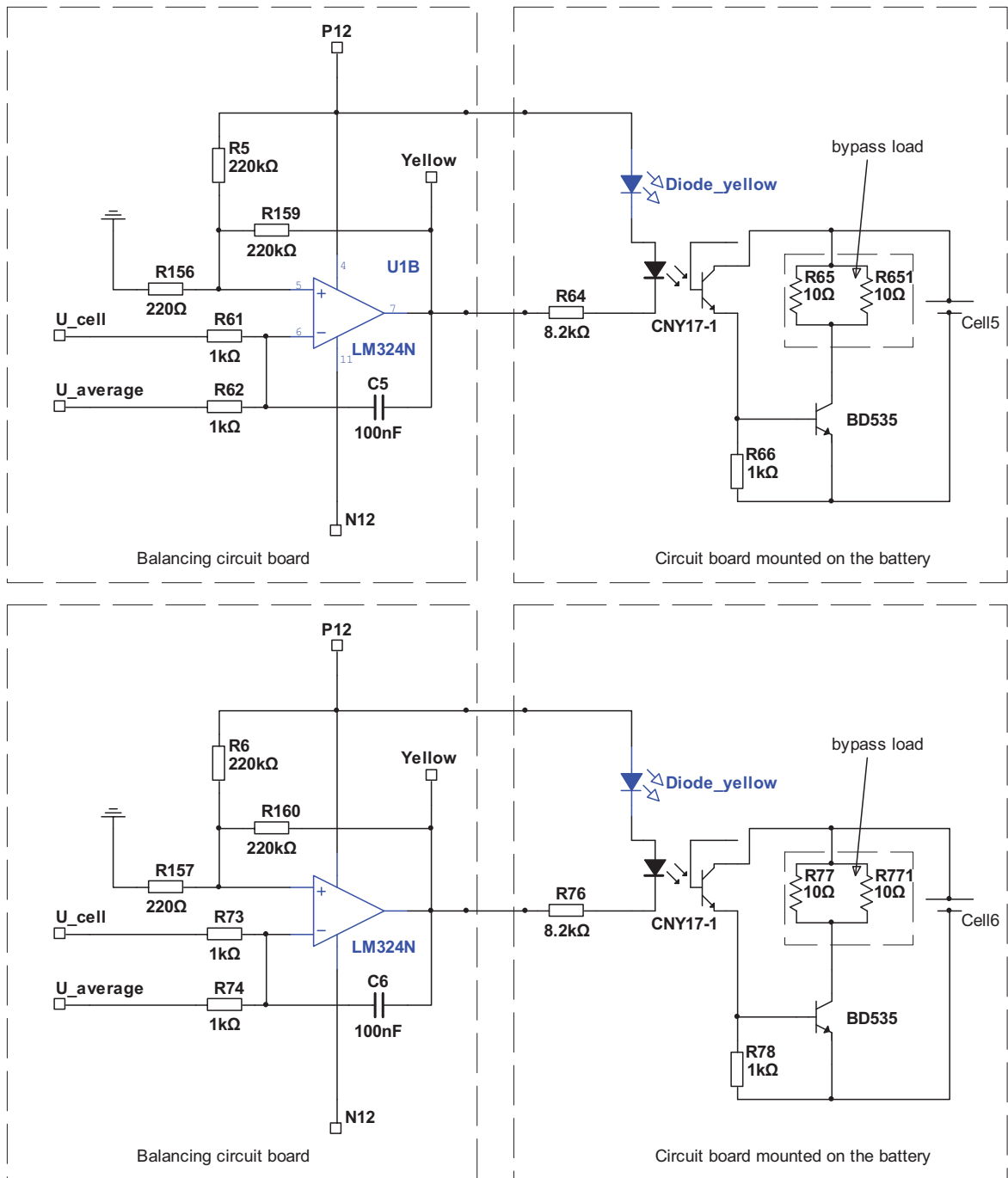


Figure 3.8 Circuit diagram bypass load controller and battery regulator for cell5 and cell6

The characteristic of a Schmitt trigger is described in chapter 2.2. Lower threshold voltage is usually a negative value. That means, battery balancing will not be stopped till the battery voltage is lower than average voltage. According to the system requirement, the battery balancing stops when the cell voltage is very close, but not lower than the average voltage. The ideal difference is between 5mV to

15mV. Because of immunity of the circuit against offset of op-amp, it is necessary to change the lower threshold voltage ( $-U_{ref}$ ) and upper threshold voltage ( $U_{ref}$ ). Therefore, a positive voltage is added to non-inverting input of the OP-AMP, via the voltage divider  $R_1$  and  $R_{117}$ .

The transfer characteristic of Schmitt trigger is changed. The new corresponding transfer characteristic is shown in figure 3.7

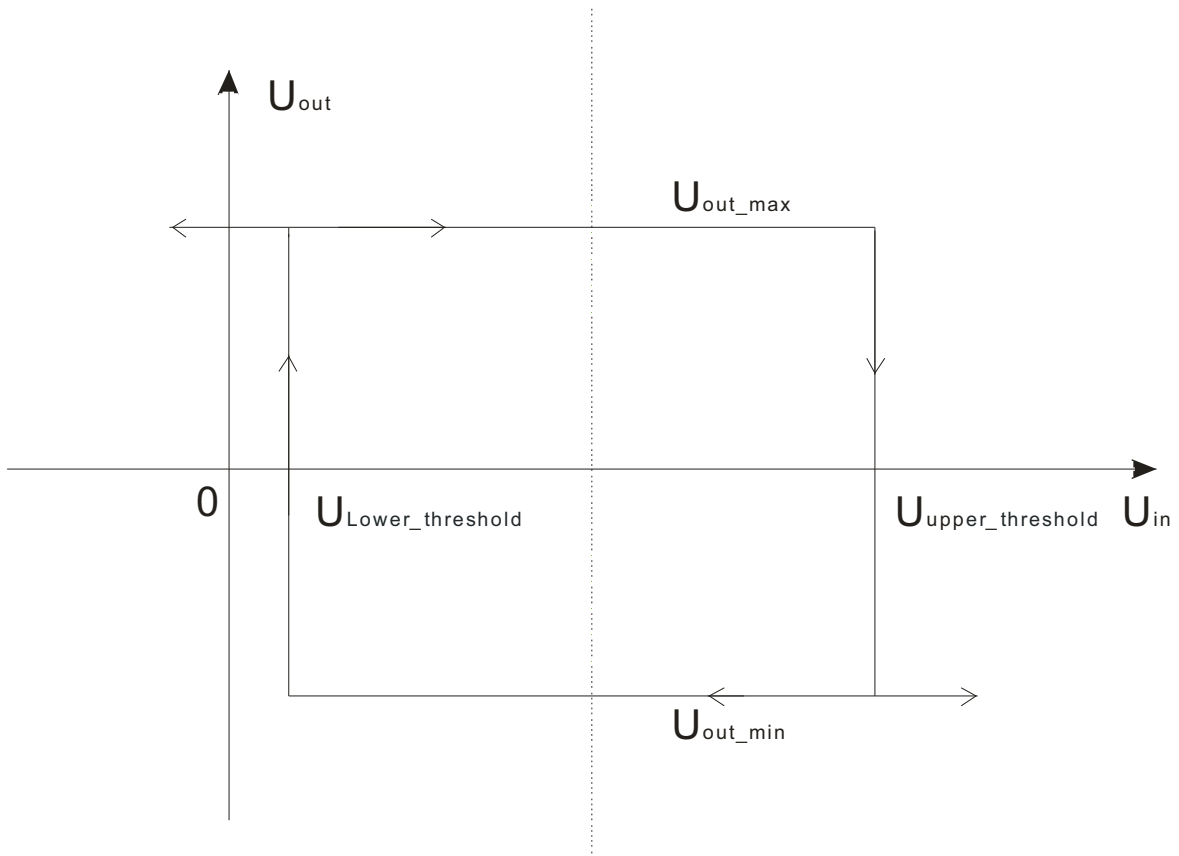


Figure 3.9 Transfer characteristic of Schmitt trigger

The output voltage of the Schmitt trigger represents the operating state of battery balancing. High level of signal means battery voltage is OK. Low level of signal means battery voltage is too high, and the bypass resistor circuit needs to be turned on.

Further, the output voltage  $U_{out}$  determines the operating state of the opto-coupler CNY17.

Figure 3.8 shows the balancing circuit board for 12 cells, 6 in series and 2 in parallel, correspondingly.



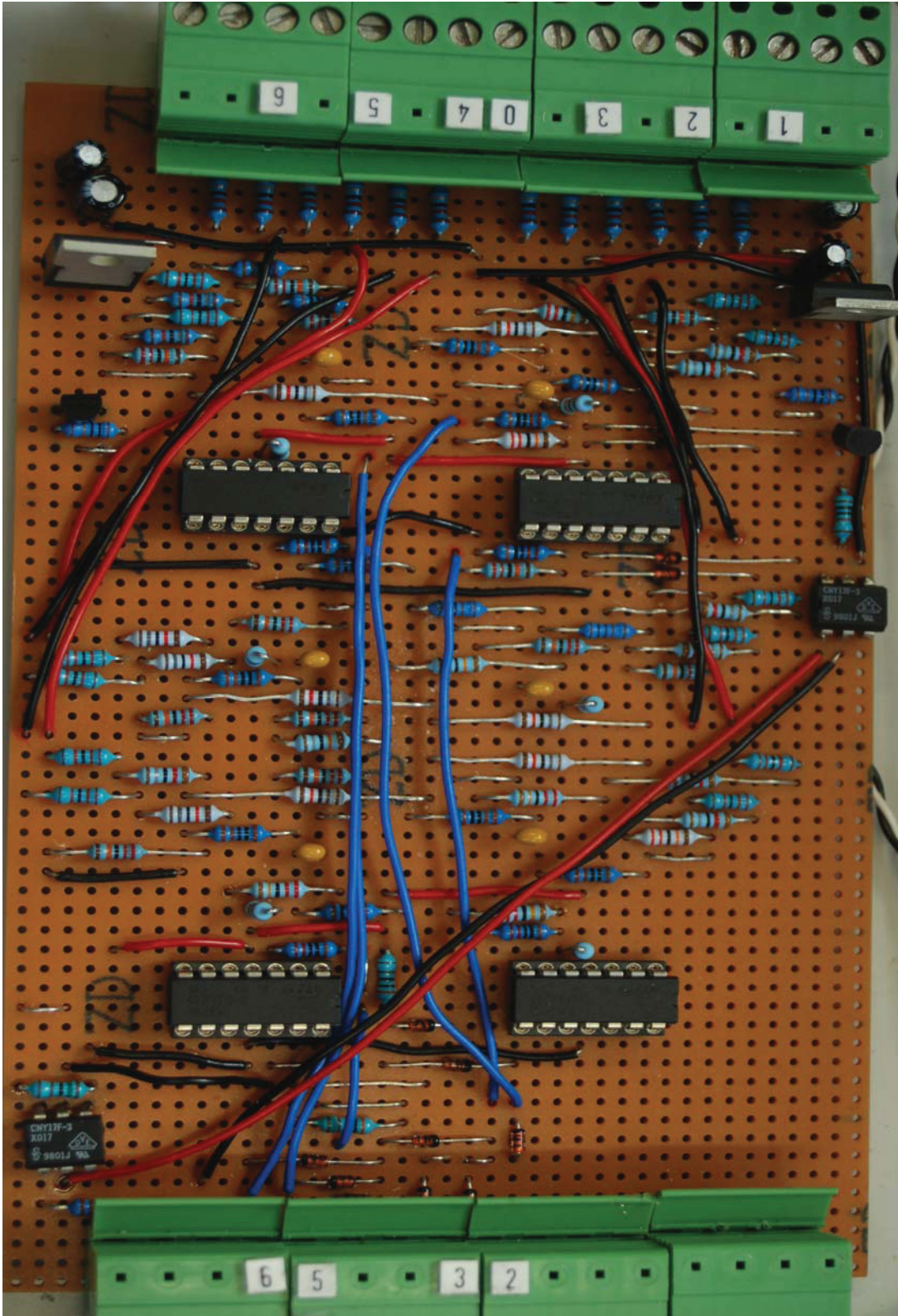


Figure 3.10 balancing circuit board for 12 batteries

The layout of balancing circuit is shown in Figure 3.9

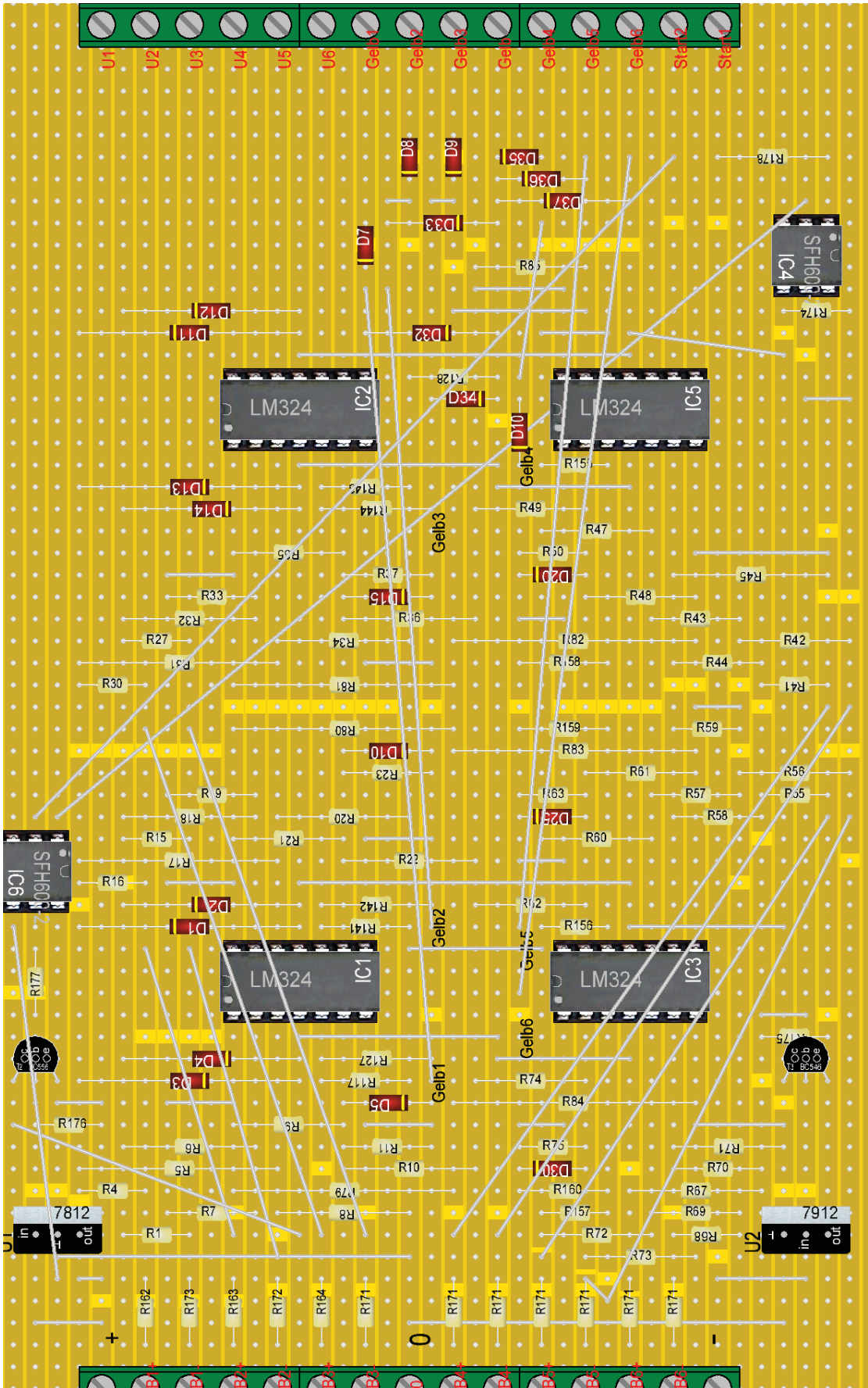


Figure 3.11 Layout of balancing circuit for 12 batteries

---

### 3.1.2 Battery regulator

The core component of the battery regulator is one transistor and a switchable bypass load. The circuit diagram is shown in figure 3.6.

The component CNY17 is an opto-coupler. An opto-coupler transfers electrical signals between two isolated circuits by using light [20]. It is used to achieve potential separation.

The output voltage of the OP-AMP, shown in figure 3.6, determines the operating state of the opto-coupler. If the op-amp output is high, no current flows through the opto-coupler and the transistor is switched off. There are no current flows through bypass load. If the op-amp output is low, current flows through the opto-coupler and the transistor is switched on.

The rated battery voltage range is from 3.0v to 4.2v. The bypass loads consist of two 10Ω resistor in parallel. Therefore, the current through bypass load can be estimated according to equation 3-5 under the condition of neglecting on-state voltage drop at the Darlington transistor.

$$I = \frac{U}{R} \quad (3-5)$$

The current I is in the range of from 0.6A to 0.84A. The opto-coupler, transistor and bypass load are installed on a small circuit board. This small circuit board is mounted directly on the battery for safety and dissipation power distribution reasons.

Figure 3.10 shows the top view of the cell. There are two screw holes at positive pole and negative pole. The area indicated with dashed lines is the size of the circuit board. The circuit board can be fixed by two screw holes.

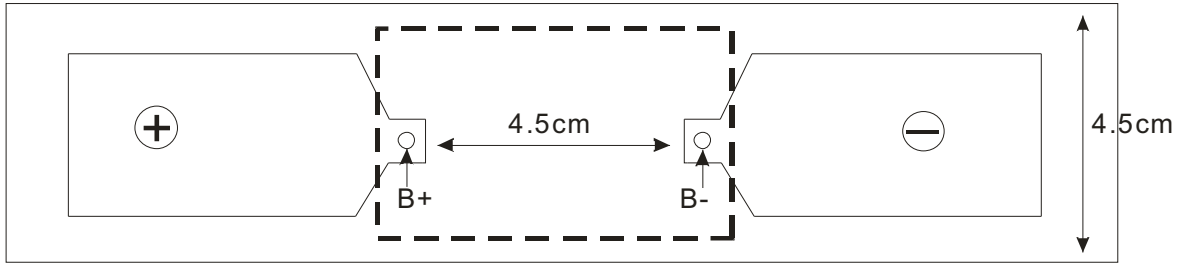


Figure 3.12 Top view of the battery

Figure 3.11 shows circuit board on the battery including protection circuit.

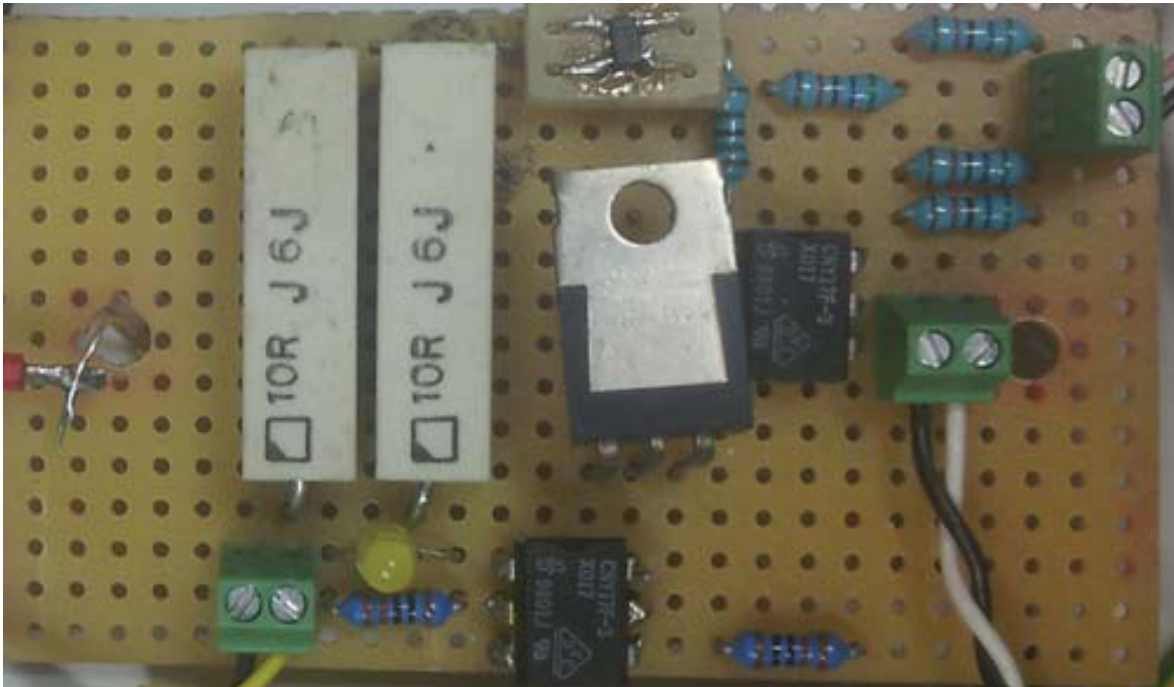


Figure 3.13 Circuit board on the battery including protection circuit

The layout of circuit board on the battery is shown in Figure 3.12

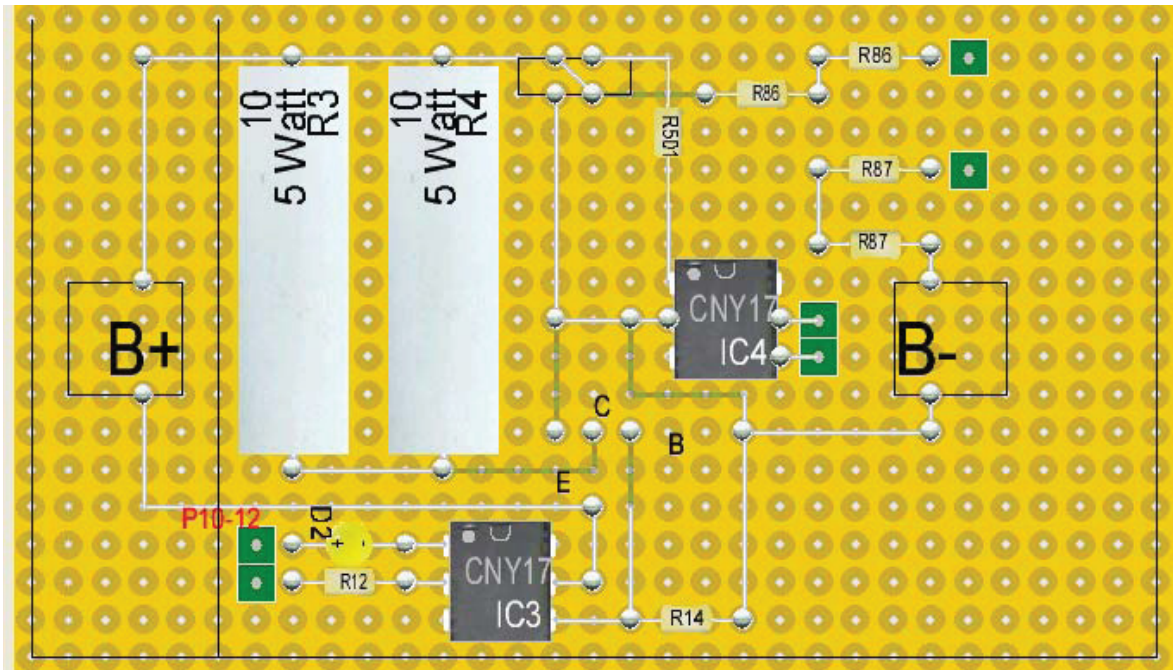


Figure 3.14 Layout of circuit board on the battery including protection circuit

In order to protect the components on the circuit board and to ensure power dissipation, it is necessary to add a cover (figure 3.13, figure 3.14, and figure 3.15). Transistor and power resistors generate a lot of heat during work. Therefore we use an aluminum cover, being used as heat sink.

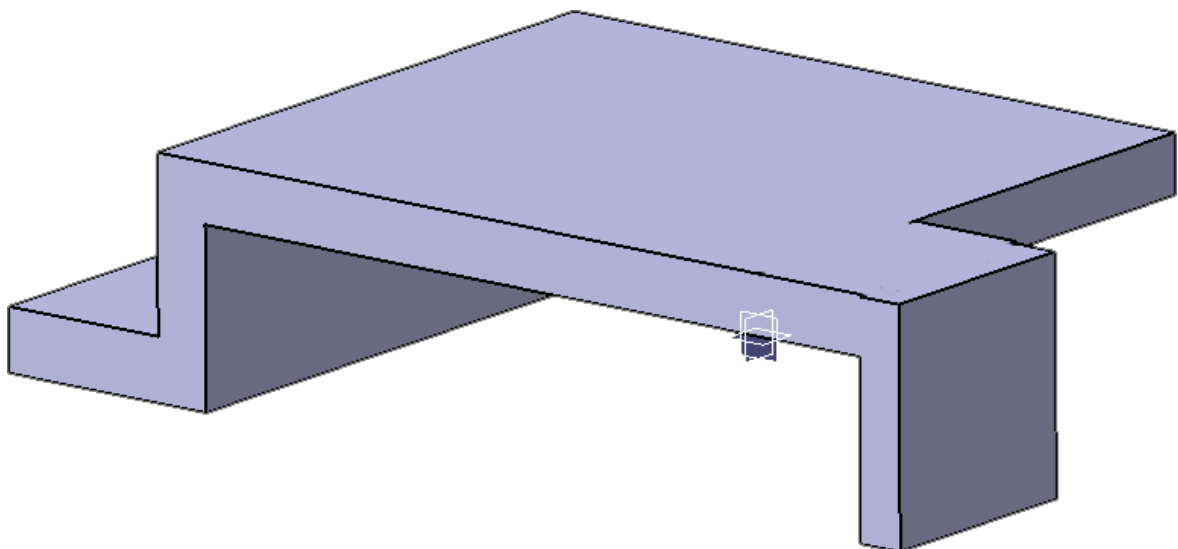


Figure 3.15 Front view of cover

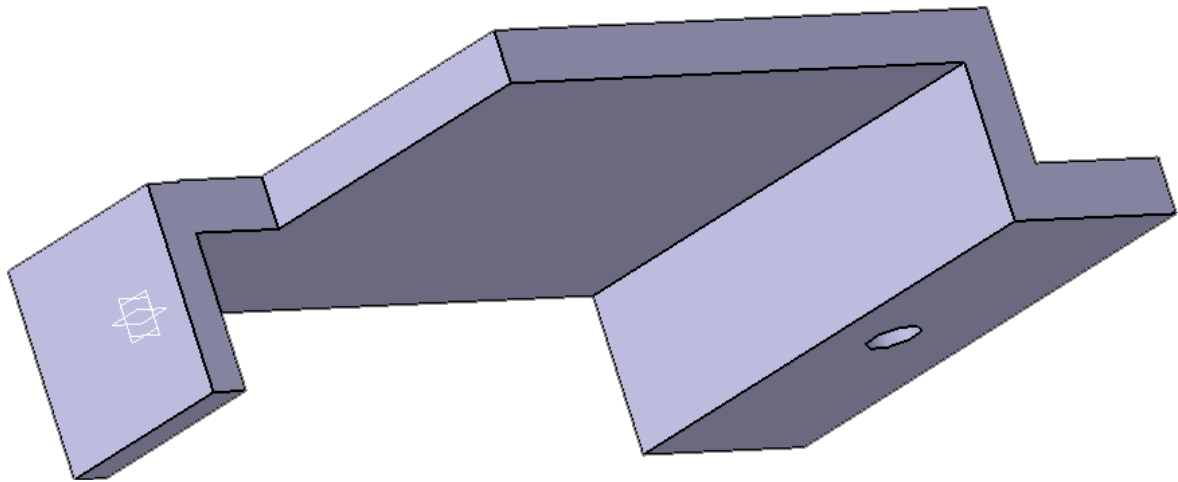


Figure 3.16 Bottom view of cover

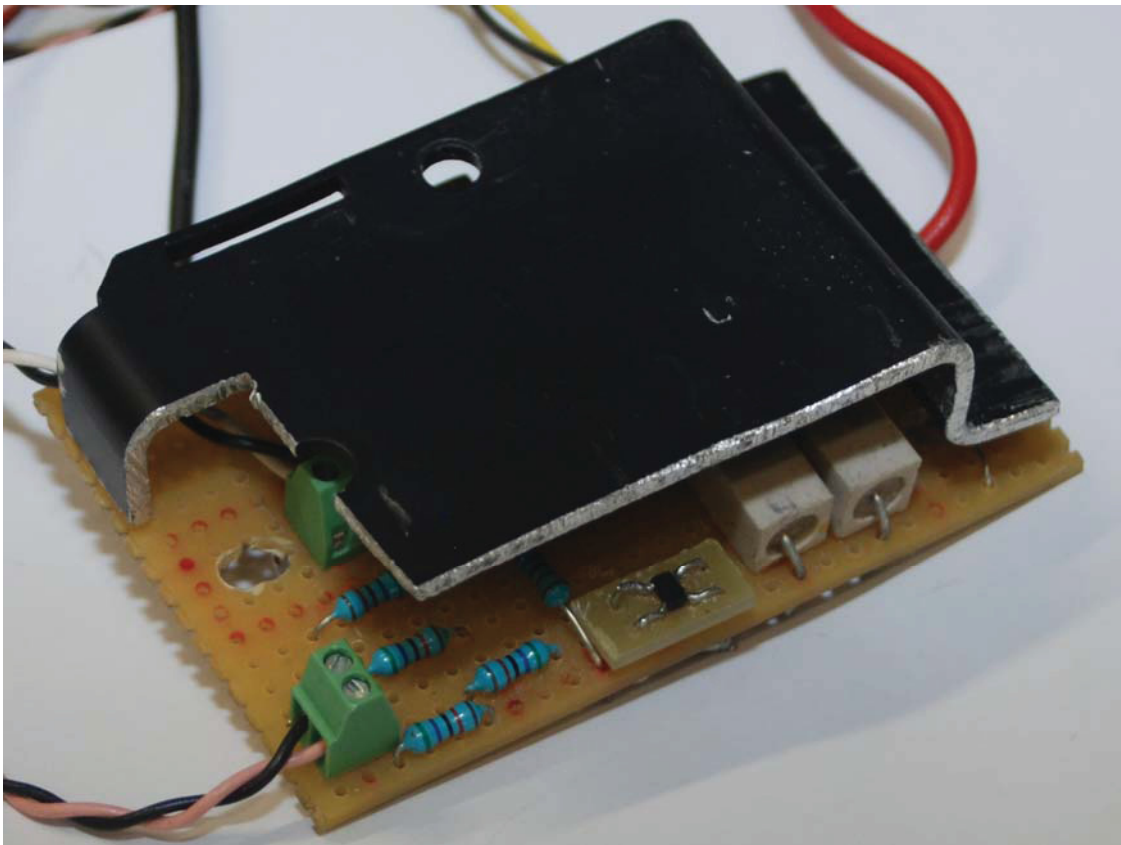


Figure 3.17 Circuit board on the battery including cover

## 3.2 Measurement System for Temperature

Temperature measurement and control of the battery system is very important. The battery pack consists of 12 cells. Each cell must work in a suitable temperature range. To ensure the safety of the battery monitoring, two separate circuits for our measurement system are used. One is the temperature measurement circuit and the other is the excessive temperature detection system. If one circuit fails, it is still possible to observe the status of the battery.

### 3.2.1 Temperature measurement circuit

Through this circuit, the temperature of each battery is measured. In chapter 2.3.1, the property of Silicon Temperature sensors is described. In order to get the temperature of the cells, KTY81-210 as temperature sensors are chosen. These sensors are mounted directly on the battery.

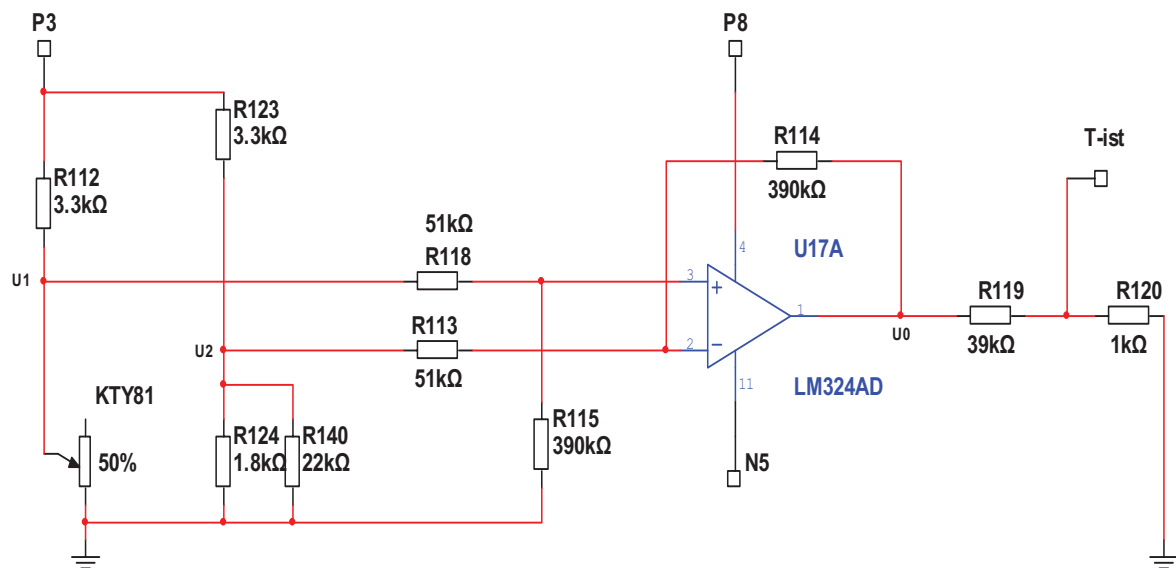


Figure 3.18 Temperature measurement circuit

The measurement range of this temperature sensor is from  $-50\text{ }^{\circ}\text{C}$  to  $100\text{ }^{\circ}\text{C}$ . This temperature range is mapped to output voltage between  $-2\text{V}$  and  $4\text{V}$ . The reference voltage is set to  $3\text{V}$ . Linearization is to be computed for this range. The DC operating voltage of this difference amplifier is  $+8\text{V}$  and  $-5\text{V}$ .

---

In order to specify the value for all of the resistors, some of the values must be prespecified. For the resistors  $R_{112}$  and  $R_{123}$ ,  $3.3k\Omega$  is chosen. The resistances  $R_{124}$ ,  $R_{115}$  and  $R_{114}$  determine the gain and the zero point.

From the datasheet of KTY81-210, the following data is obtained.

$$T=0\text{ }^{\circ}\text{C} : R_{\text{kty81}}=1630\Omega$$

$$T=100\text{ }^{\circ}\text{C} : R_{\text{kty81}}=3392\Omega$$

$$\Rightarrow U_1 \text{ at } 0\text{ }^{\circ}\text{C} = 0.99\text{V}, U_1 \text{ at } 100\text{ }^{\circ}\text{C} = 1.52\text{V}$$

$$\Rightarrow \Delta U_{\text{input}}=0.53\text{V}$$

$\Rightarrow$  The gain of the circuit results from the required output voltage

$$V = \frac{\Delta U_{\text{output}}}{\Delta U_{\text{input}}} = \frac{4\text{V}}{0.53\text{V}} = 7.57 \quad (3-6)$$

Further, the gain for the difference amplifier is given by equation 3-7

$$V = \frac{R_{114}}{R_{113}} \quad (3-7)$$

From these two equations, the value for the resistors  $R_{114}=390k\Omega$  and  $R_{113}=51k\Omega$  is chosen from the E96 series resistor table

Now the zero point must be defined. When the temperature  $T=0\text{ }^{\circ}\text{C}$ , the output voltage of the OP should be  $U_0=0\text{V}$

$$U_0=V \cdot (U_1-U_2) \quad (3-8)$$

$$\Rightarrow U_1 \text{ at } 0\text{ }^{\circ}\text{C} = U_2 \text{ at } 0\text{ }^{\circ}\text{C} \quad (3-9)$$

$$\Rightarrow R_{124} // R_{140} = R_{\text{Kty81}} \text{ at } 0\text{ }^{\circ}\text{C} = 1630\Omega$$

From the E96 series for resistors, the value for the resistors  $R_{124}=1.8k\Omega$  and  $R_{140}=22k\Omega$  are chosen.

The output voltages  $U_0$  is between  $-2\text{V}$  and  $4\text{V}$ . A LCD digital panel meter (Type



PM-438) is used to display the temperature of the batteries. This LCD voltmeter module features 200mV d.c. full scale reading, auto-zero and auto-polarity. The input voltage range should be in the range of between -199mV and 199mV. Two resistors ( $R_{119}$  and  $R_{120}$ ) are used as a voltage divider in order to get the actual Temperature T-ist, which should be in the range of -50mV to 100mV. T-ist is connected to this digital Panel Meter.

Through the above calculations we get the following theoretical results:

Table 3.1 Theoretical results of temperature measurement

Temperature(°C)	$R_{kty81}$ ( $\Omega$ )	$U_0$ (V)	T-ist (°C)
-50	1030	-2	-50
0	1630	0	0
25	2000	1	25
50	2417	2	50
100	3392	4	100

The test of the circuit is described in chapter 4. A deviation less than 10 degrees is acceptable.

### 3.2.2 Over-temperature detection system

This circuit produces an alarm signal when any cell temperature exceeds the normal operating temperature. The temperature of each cell must be monitored. Therefore 12 PTC thermistors are mounted directly to 12 batteries.

The output alarm signal is sent to the control and display module. In case of a over temperature alarm, a LED is activated and further measures can be started.

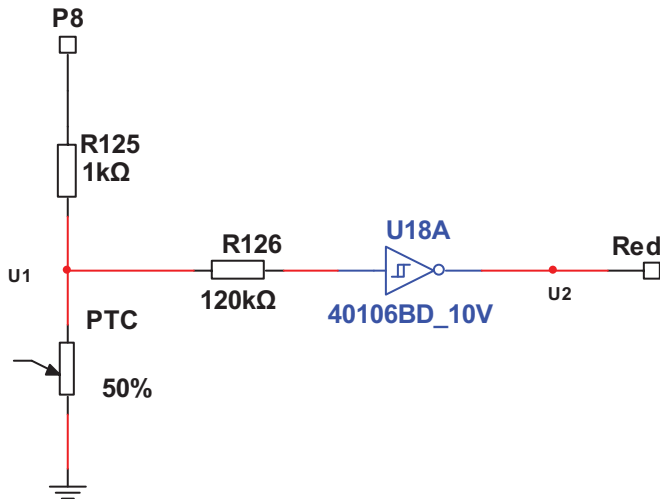


Figure 3.19 Over-temperature detect circuit

Figure 3.16 shows the use of PTC in the over-temperature detection circuit. PTC and  $1\text{K}\Omega$  resistor  $R_{125}$  are connected in series.  $R_{125}$  and PTC act as a voltage divider, Voltage  $U_1$  depends on resistance of PTC. According to the characteristics of PTC, resistance of PTC is very low when the battery is not in over-temperature condition and very high when the battery is in over-temperature condition. Voltage range of  $U_1$  is from low to high. At the same time, the output of Schmitt trigger 40106 is high or low. That means, if the battery is not over-temperature, the voltage level on  $U_2$  is high. Otherwise the voltage level is low.

There are 12 cells in the battery module. Therefore, there are 12x High/Low voltages. In order to evaluate these voltages, a diode AND logic gate is implemented. This diode AND logic is shown in figure 3.17.

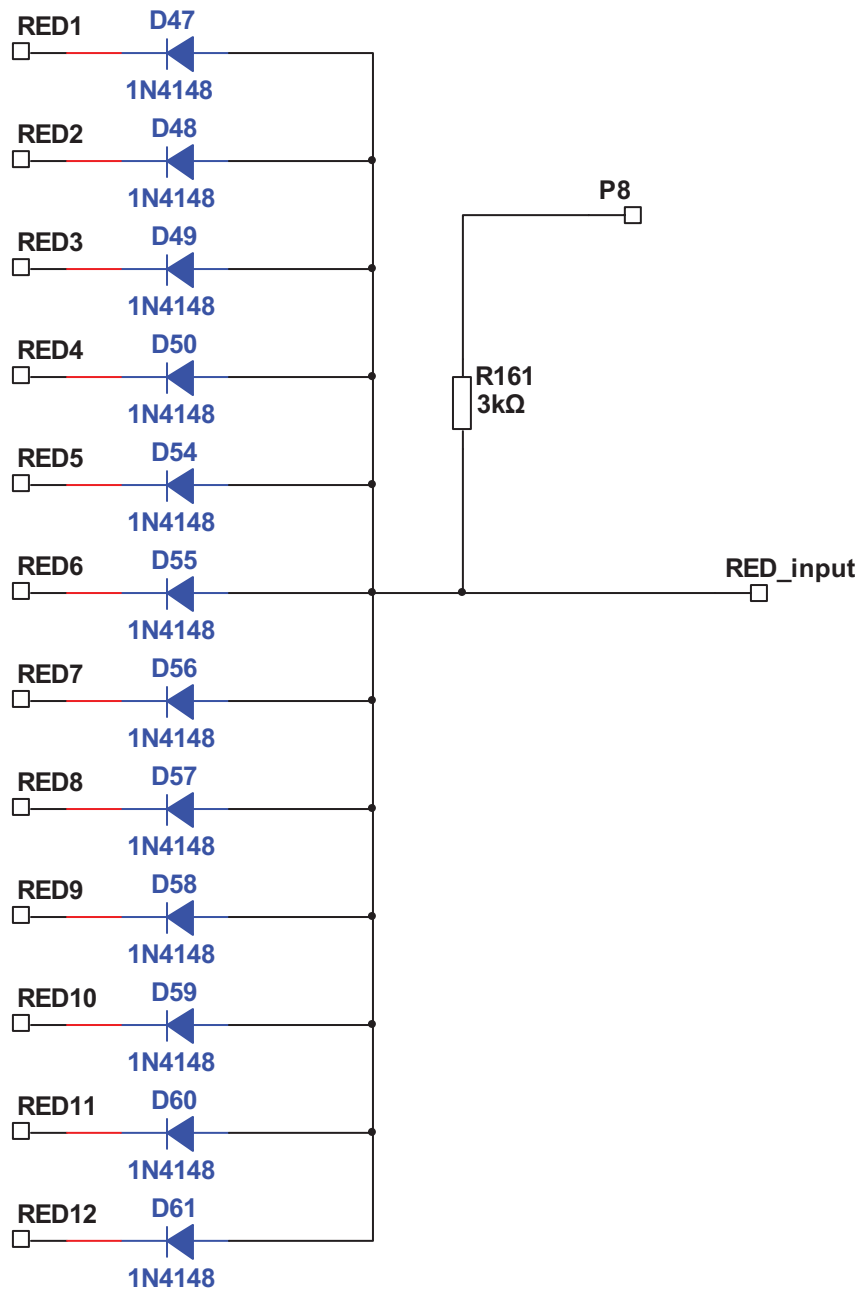


Figure 3.20 diode AND logic gate for over-temperature detect circuit

Figure 3.18 shows circuit board of measurement system for temperature

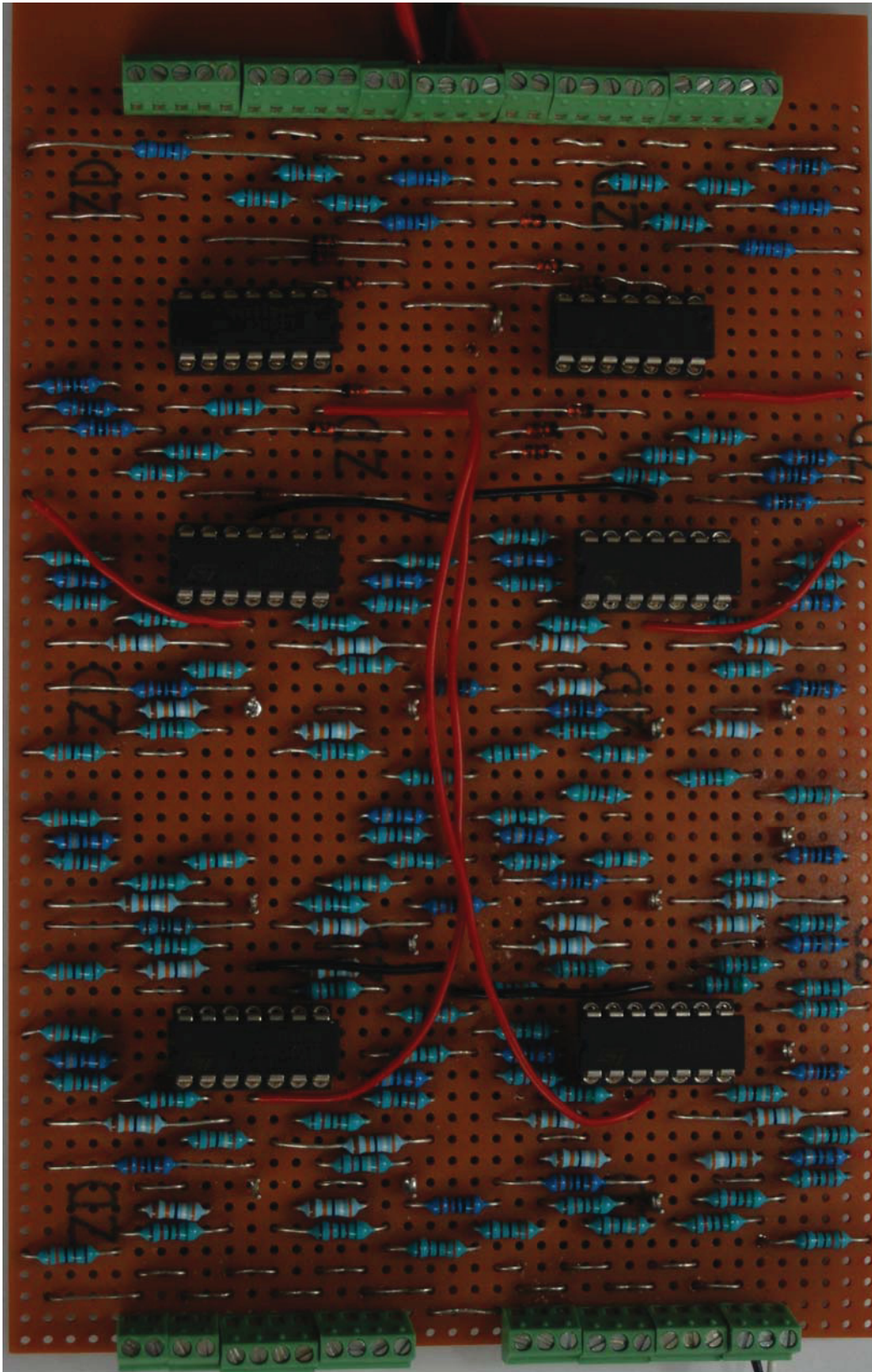


Figure 3.21 Temperature measurement circuit board

Figure 3.19 shows layout of Temperature measurement circuit board

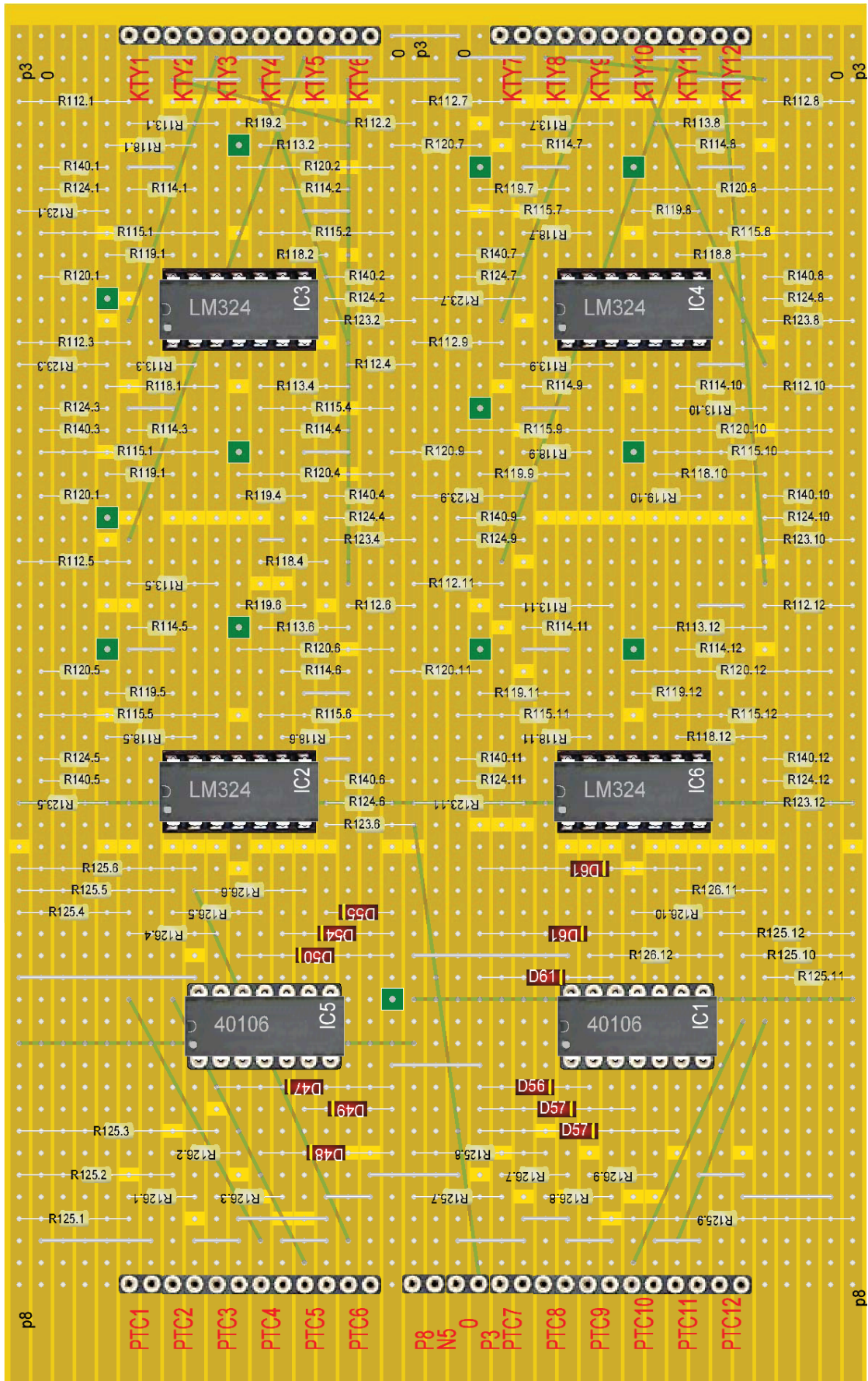


Figure 3.22 Layout of Temperature measurement circuit board

---

### 3.3 Monitoring System for Voltage of Batteries

The Lithium-ion-cell has an operating voltage range from 3.0V to 4.2V. It is important to ensure that the cells of all batteries are within this voltage range.

In chapter 2.3 the feature of window comparator is described. The window comparator MAX9065 has an upper threshold voltage of 4.2V and a lower threshold voltage of 3.0V. Therefore it is suitable for the monitoring system. The window comparator MAX9065 is chosen in this circuit.

Figure 3.20 shows the top view of MAX9065

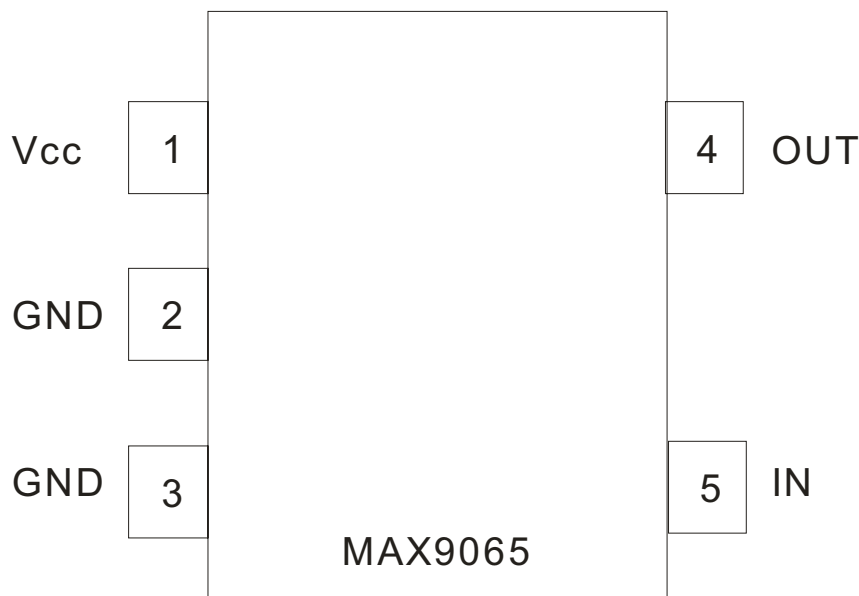


Figure 3.23 Pin configuration of Max9065 (Top view)

The dimension of integrated circuits MAX9065 is very small. It cannot be soldered in 2.54mm project board. Therefore, a mounting socket is designed for it. A schematic of the mounting socket is shown in Figure 3.21.

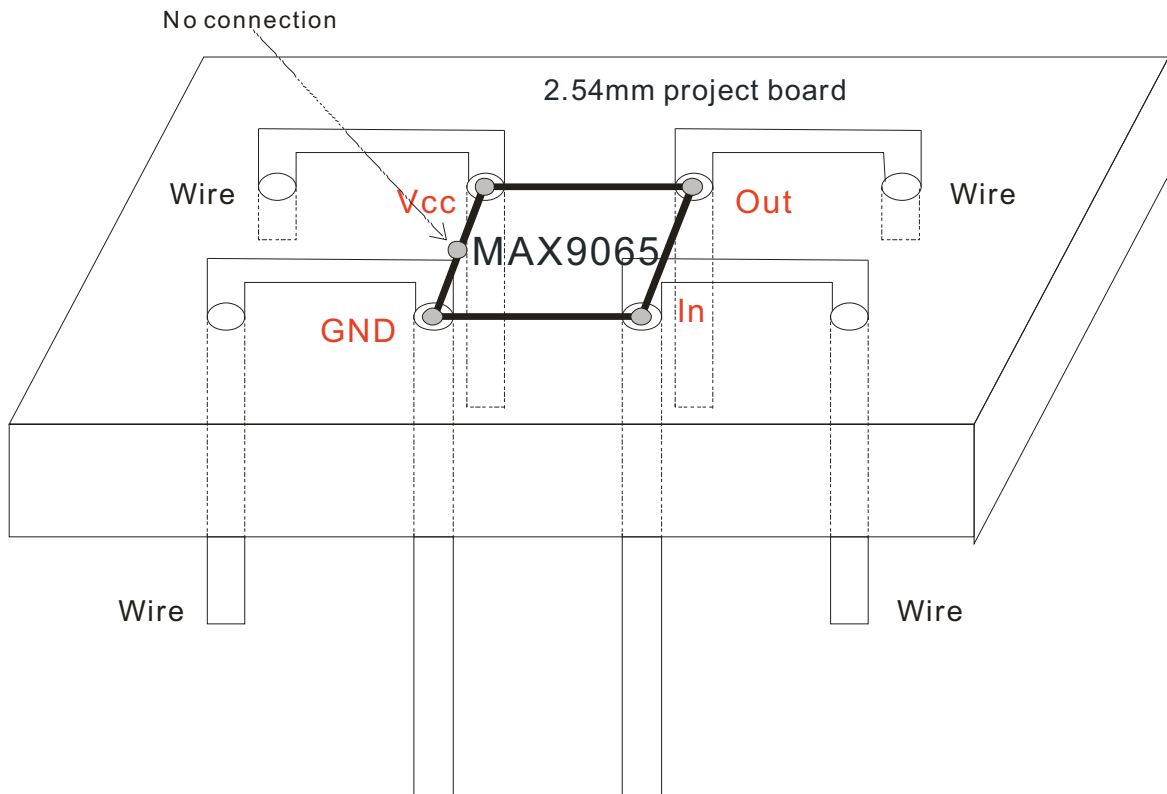


Figure 3.24 Schematic of mounting socket

As shown in figure 3.21, four wires are soldered to the 2.54mm project board. Four connection points in the middle are used as welding points. Pin 1,3,4,5 of MAX9065 are soldered to these 4 welding points. So the window comparator MAX9065 can be mounted on 2.54mm project board.

In order to measure the battery voltage accurately, the wire from battery to the input of MAX9065 should be as short as possible. Therefore, it is installed in the circuit board on the battery. The corresponding circuit is shown in Figure 3.22.

An opto-coupler is used to isolate the control signal. B\_voltage is the signal at pin 4 of the opto-coupler. The output signal of MAX9065 is low when the input voltage is above 3.0V and below 4.2V. When the signal B\_voltage is high, the output signal of MAX9065 is high.

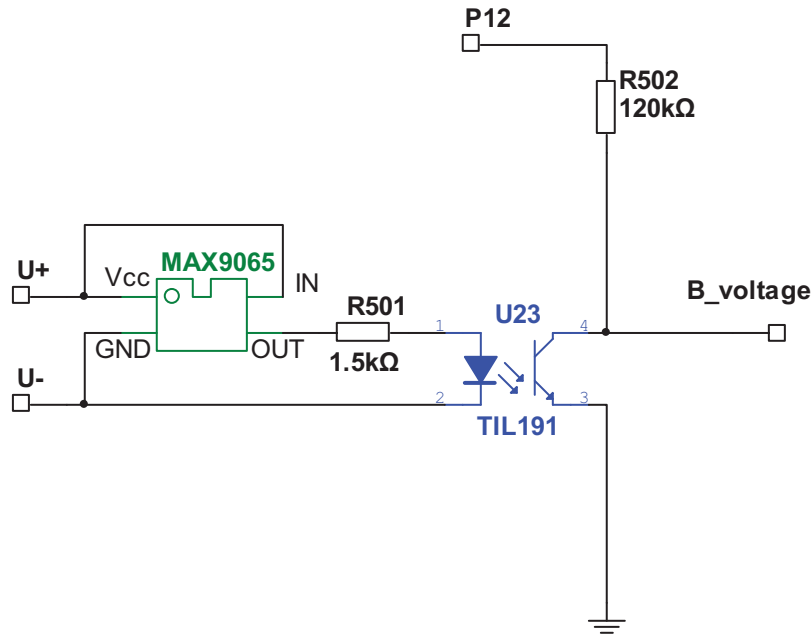


Figure 3.25 Voltage range monitoring circuit

There are 12 batteries in the battery pack. Always two batteries are connected in parallel. So, six voltage range monitoring circuits are required. All output signals of the voltage range monitoring circuits are fed to the voltage status display circuit board, as shown in Figure 3.26. LEDs are used to display the status of the battery voltage. The following table shows the logical relationship between the battery voltage and the LEDs.

Table 3.2 Logical relationship between the battery voltage and the LEDs

Battery voltage U(V)	RED Led	Green_1 Led
$3.0v \leq U \leq 4.2v$	OFF	ON
$U < 3.0v$	ON	OFF
$U > 4.2v$	ON	OFF

If the battery voltage is out of range, it is necessary to record and show this status with an indicator. A circuit containing a RS flip flop circuit can achieve this function.



In chapter 2.4.2, this circuit is introduced. Two NAND gates of a quad 2-input NAND Schmitt trigger integrated circuit 4093, shown in Figure 3.26, can be wired to form a RS flip flop.

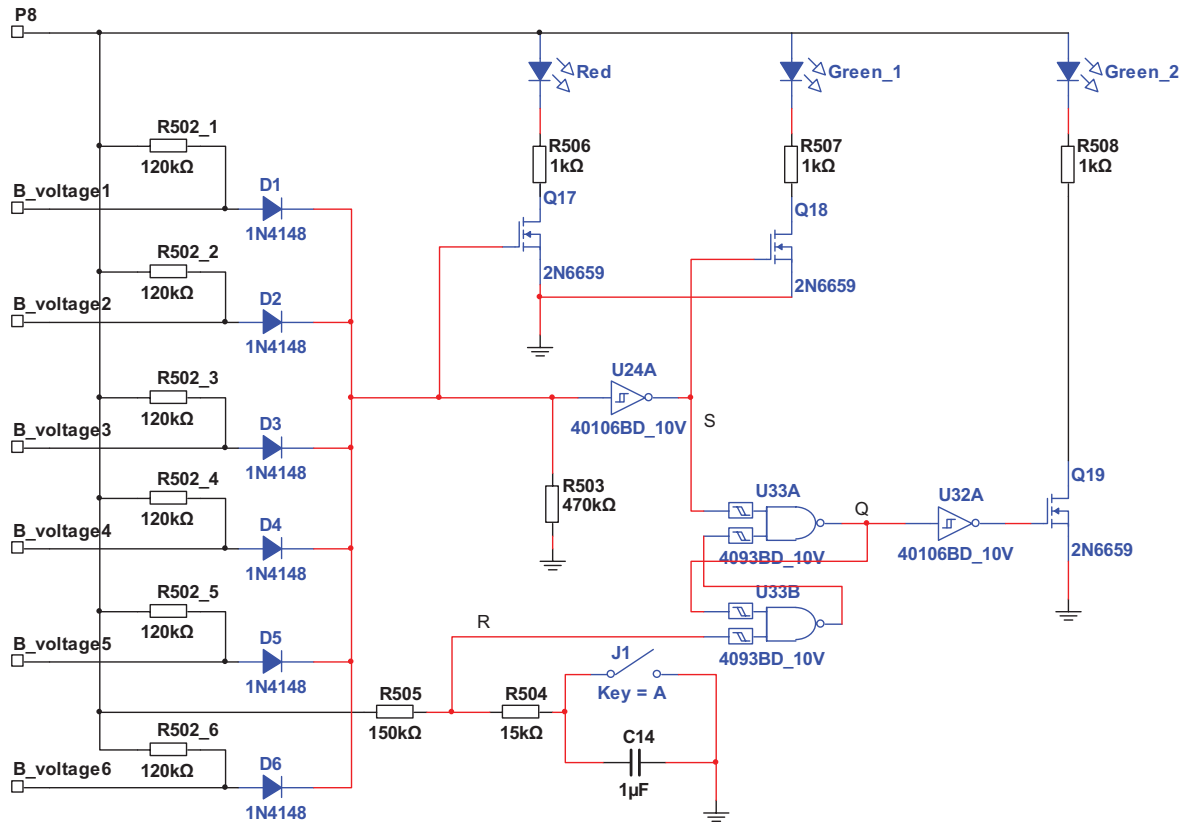


Figure 3.26 Voltage status display circuit

This RS flip flop consists of two inputs, the set input S and the reset input R. When any of the cell voltages is out of range, LED 'Red' in Figure 3.26 is on and LED Green\_1 in Figure 3.26 is off. The low voltage level is applied to input S and the outputs of RS flip flop swings to high voltage level. The LED Green\_2 is also off. This status means, some cell voltage is out of range. The voltages of each cell are measured.

If the problem has been resolved, high voltage level is applied to input S. LED Red is off and LED Green\_1 is on. Because of the memory property of the RS flip flop circuit, the output of RS flip flop remains at high voltage level. The LED Green\_2 is still off.

---

Switch J1 in Figure 3.26 is a pushbutton switch. If the button of switch J1 is pushed, a low voltage pulse is applied to input S. This pulse causes the output to switch to the low voltage level. Then LED Green\_2 is now turned on.

Figure 3.27 shows circuit board of voltage monitoring system.

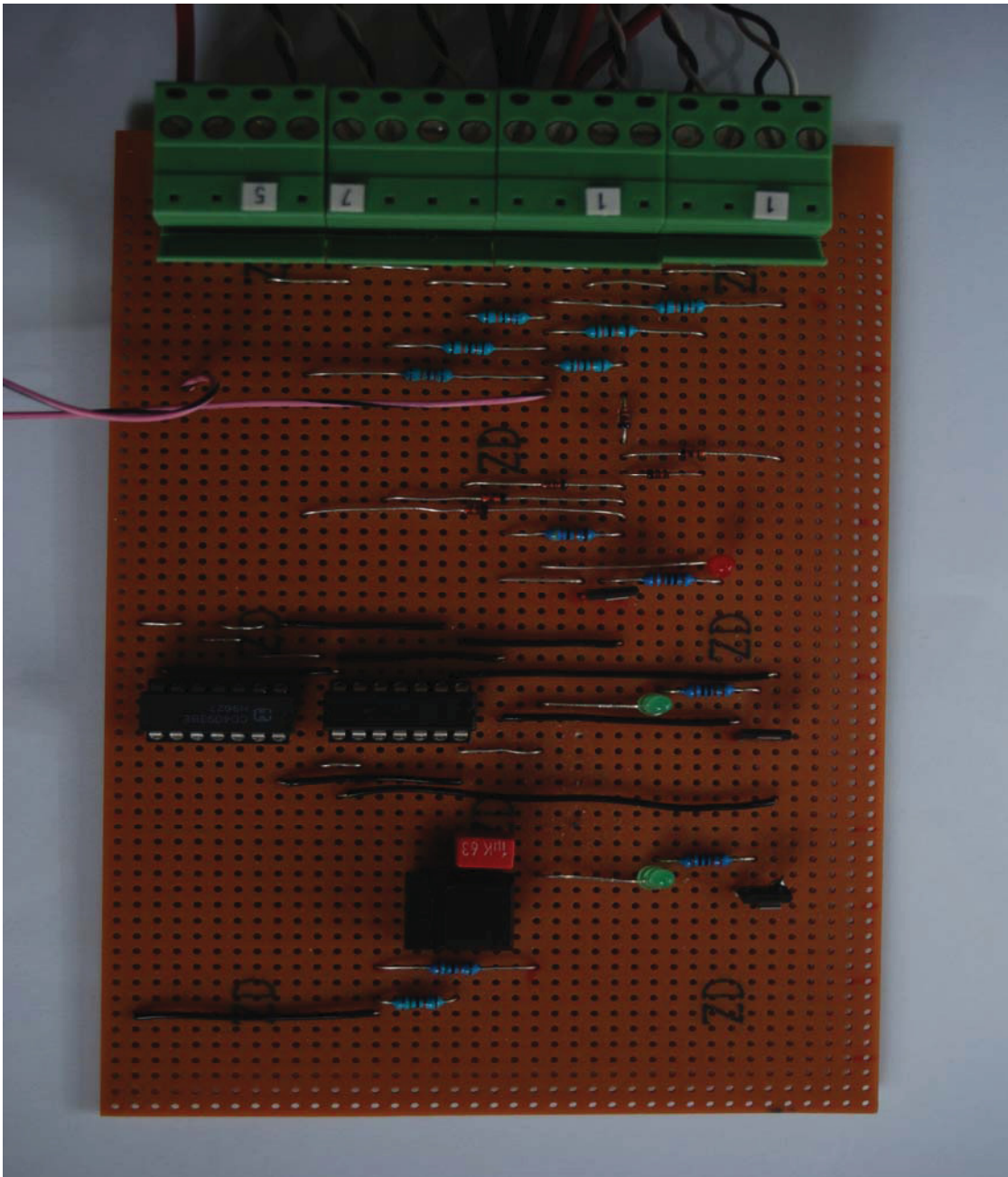


Figure 3.27 Circuit board of voltage monitoring system

Figure 3.28 shows the layout of voltage monitoring system.

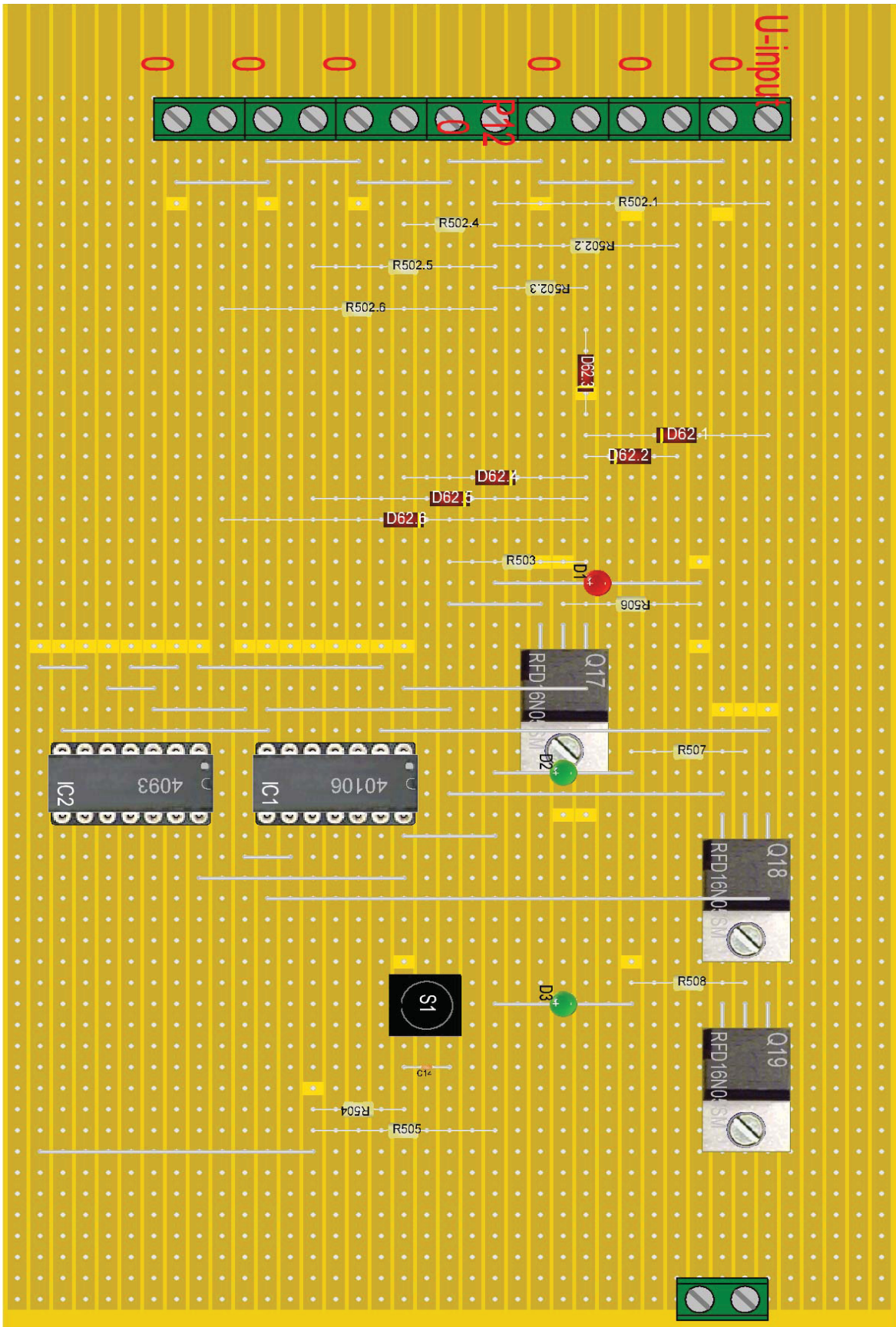


Figure 3.28 Layout of the voltage monitoring system

---

### 3.4 Control and Display Module

A control and display module has to be easy to use and self-understanding. The operating status of the entire system should be displayed very clearly.

The first important function is the ON/OFF-function of the balancer. As shown in Figure 3.3, Switch1 is the ON/OFF switch for the battery balancing. When the switch is OFF, the power supply of the balancer is interrupted. Further the electric power consumption will be reduced to a minimum.

In the circuit shown in Figure 3.6, the output signal “Yellow” is the control signal for the bypass load. There are six pairs of parallel connected batteries. When any bypass load turns on, the Yellow LED on the display module should also turn on. Therefore an AND logic gate is used. The diodes D32, D33, D34, D35, D36, D37 and resistor R128 in Figure 3.29 form a AND logic gate. The output of the AND logic gate must be transferred to the display module. The power supply of the display module is a Lead-acid car board battery at 12 Volts and the power supply of balancing module is the lithium-ion battery module or lithium-ion pack. The reference ground of these two power supply system is different. An opto-coupler is used to transfer this control signal. The corresponding circuit is shown in Figure 3.29.

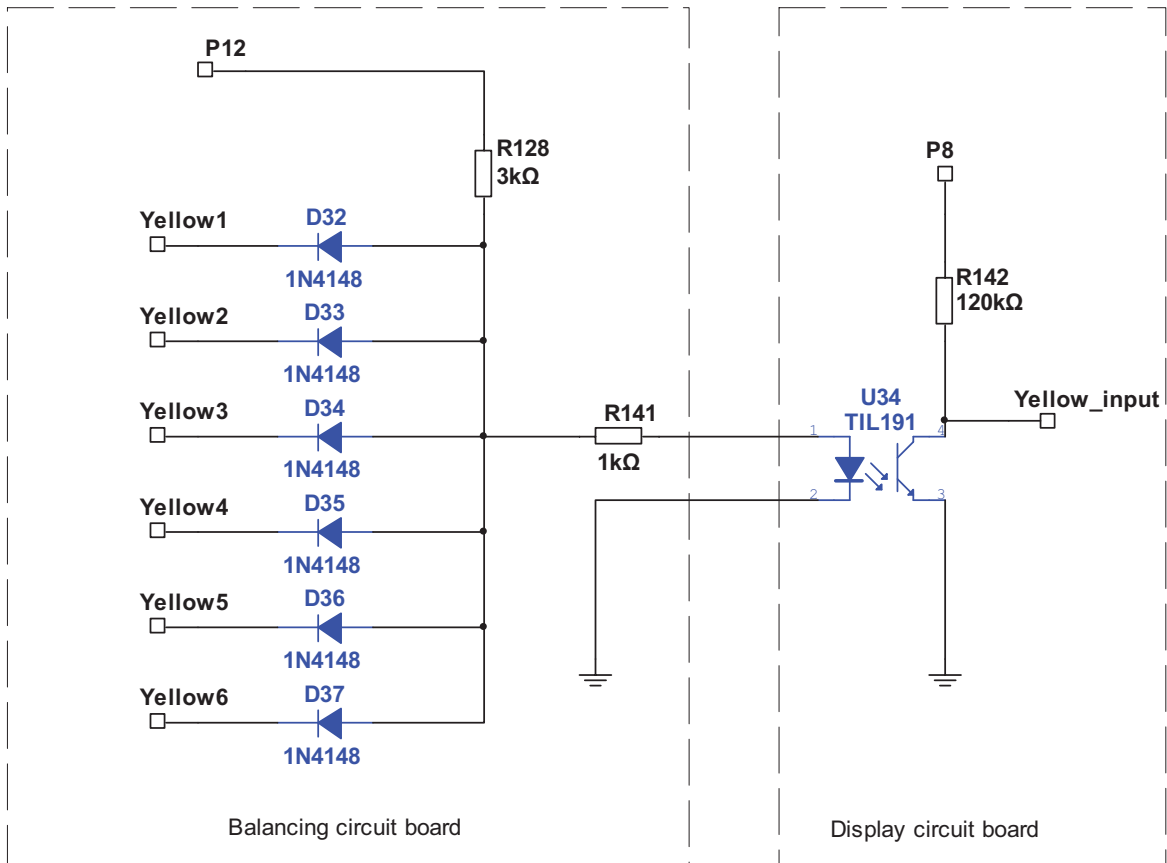


Figure 3.29 AND logic gate for Yellow LED control circuit

LEDs are used as status indicators in the display module.

Table 3.3 Overview of status indicators

Status indicator	Status description
Green LED	Green means everything is working fine
Red LED	Over temperature or battery voltage is out of range
Yellow LED	Battery balancing is working

Green LED is ON only when Red LED and Yellow LED are OFF. The schematic shown in Figure 3.30 can archive this requirement.

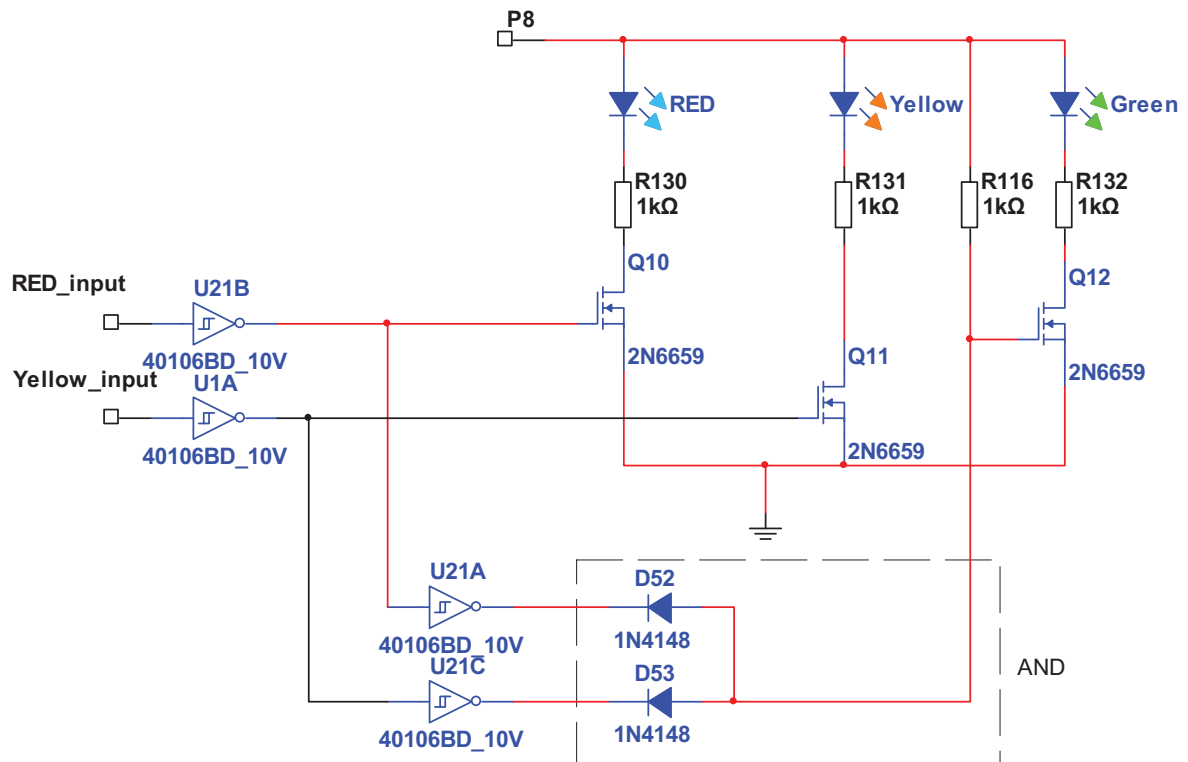


Figure 3.30 LED control circuit in display module

The diodes D52, D53 and the resistor R116 in Figure 3.30 also form an AND logic gate. The output of the AND logic gate applies to the gate-source voltage  $V_{GS}$  of the transistor Q12, as shown in Figure 3.30. A HIGH output results only if both inputs to the AND gate are HIGH. If only one input to the AND gate is LOW, which corresponds to a HIGH level at the U21A, or U21C, respectively, inverter input, a LOW output results. If  $V_{GS}$  of the transistor Q12 is high, a drain current flows and the Green LED is ON.

Figure 3.31 shows the layout of the display module.

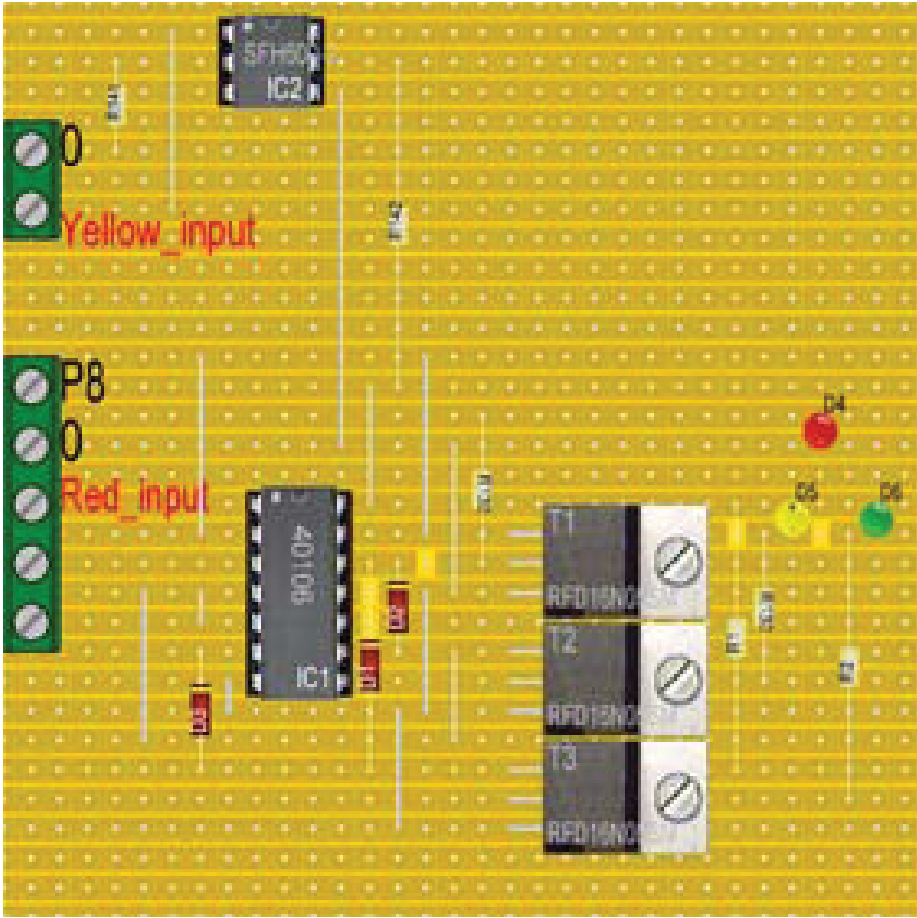


Figure 3.31 Layout of display module

Figure 3.32 shows the photo of the display module

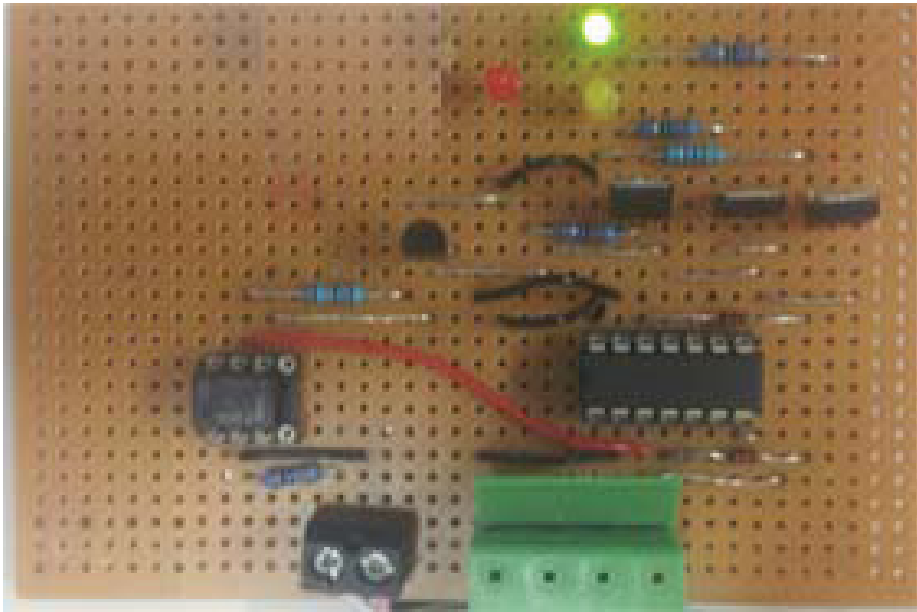


Figure 3.32 Circuit board of the display module

### 3.5 Power Supply Module

There are two separated power supply systems in this system. One power supply is using the 24V lithium-ion battery pack to be balanced. The other power supply is using 12V Lead-acid car board battery. The battery voltage is drifting with time and SOC condition. It is necessary to have a stable voltage source.

A voltage stabilizer is used to create a stable voltage. A lithium-ion battery pack is the power source of the voltage measurement and balancing circuit. The amplifiers in the voltage measurement and balancing circuit need to operate in the range of  $\pm 12V$  DC. Positive voltage regulator LM7812 and negative voltage regulator LM7912 are used to create stable  $\pm 12V$  in DC and act as voltage limiter. Figure 3.33 shows the circuit diagram of the  $\pm 12V$  power supply for the voltage measurement and balancing circuit.

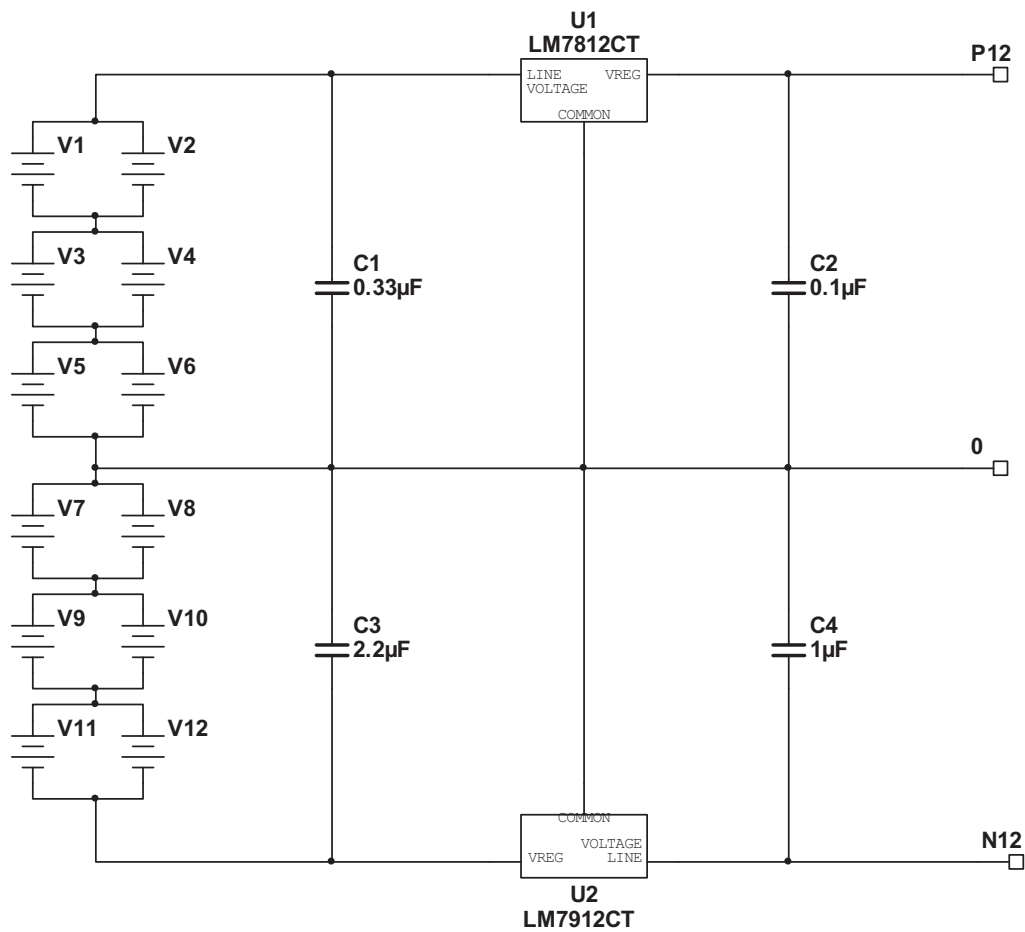


Figure 3.33 Circuit diagram of  $\pm 12V$  voltage limiter module



The other power source is a 12V car board battery typically Lead-acid. Temperature measurement and display circuit need a power supply of +8V, +3V and -5V. A charge pump is used to create a negative voltage, as shown in Figure 3.34.

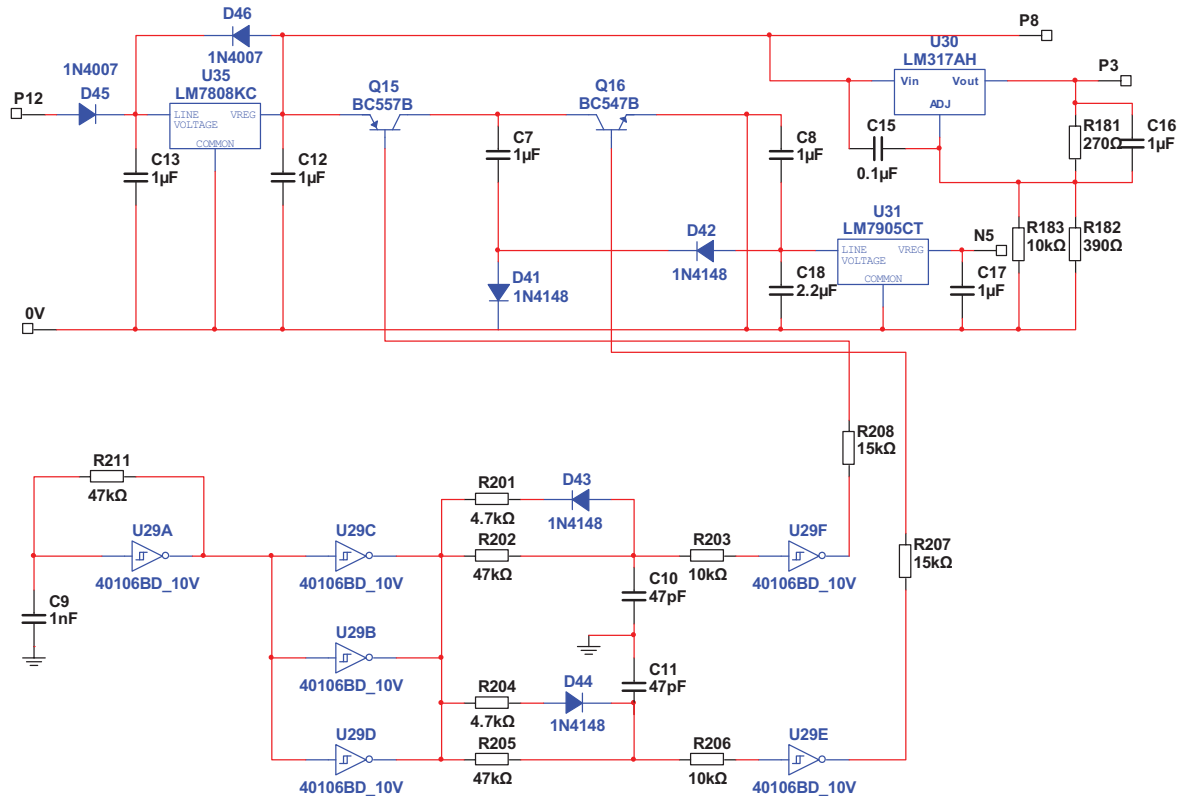


Figure 3.34 Circuit diagram of +8V, +3V and -5V power supply module

Capacitor C9, resistor R211 and Schmitt trigger U29A act as astable multivibrator and generator a rectangular wave. The control signals of Q15 and Q16 are the outputs of Schmitt trigger U29F and U29E. Due to the time delay of capacitor C10 and C11, these two signals are not in HIGH level at the same time.

Characteristics of charge pumps are introduced in chapter 2.5. Similar to the situation described in Figure 2.16 and Figure 2.17, the transistors Q15 and Q16 in Figure 3.34 act as switch, as well as diodes D41 and D42. The positive input voltage is inverted through capacitor C7 and C8 to the negative voltage. A negative voltage stabilizer LM7905 is chosen to create -5V DC.

The value of the resistors  $R_{181}$ ,  $R_{182}$  and  $R_{183}$  are set to following values.

$R_{181}=270\Omega$ ,  $R_{182}=390\Omega$  and  $R_{183}=10K\Omega$

The output voltage of the stabilizer LM317 can be calculated according to equation 3-10

$$V_o \approx 1.25V\left(1 + \frac{R_{181}}{R_{182} \parallel R_{183}}\right) \quad (3-10)$$

$$\Rightarrow V_o = 3V$$

The circuit layout of power supply module is shown in Figure 3.35.

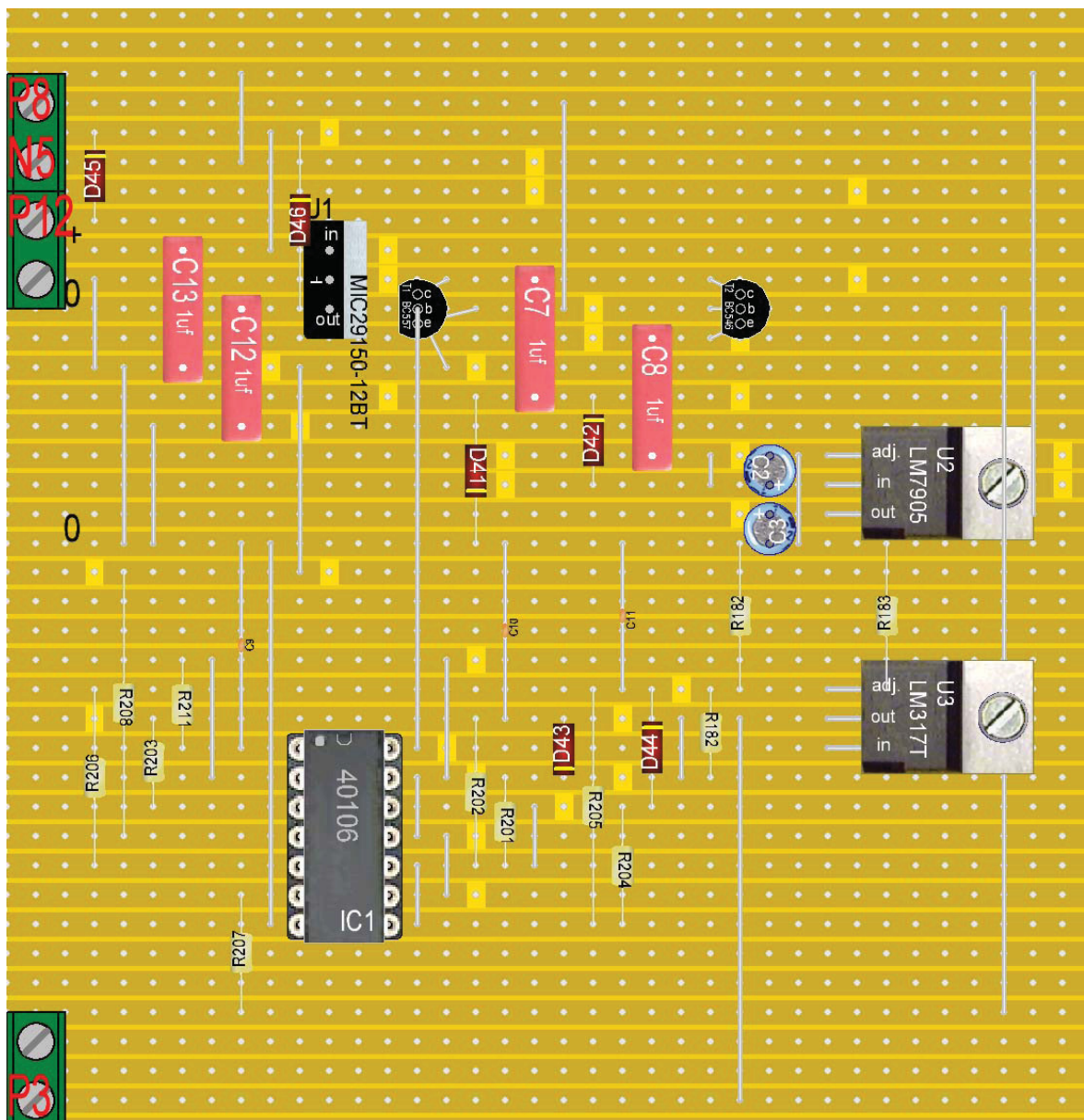


Figure 3.35 Layout of power supply module

---

## 4 Electric Circuit Testing and Commissioning

All of the functional modules are described and established in previous chapters.

In this chapter, the system is tested according the following steps:

1. Use Laboratory power supply instead of the battery pack to test the function of each electronics module
2. Use Laboratory power supply instead of the battery pack to test the entire balancing system, including the protection measurement system
3. Use battery pack to test the entire balancing system

### 4.1 Testing Function Modules

#### 4.1.1 Battery voltage measurement

Accurate voltage measurement is a prerequisite to ensure a correct operation of the whole system. The battery pack consists of 12 cells, 6 cells are connected in series: each other cell has another cell in parallel to increase capacity. Six battery voltage measurement circuits are used. A differential amplifier measures voltage for each individual cell.

The output voltage of the practical differential amplifier depends not only on the difference voltage. It depends also on the common mode rejection ratio. The operational amplifier common-mode rejection ratio (CMRR) is the ratio between the common-mode gain and the differential mode gain.

The common-mode testing procedure of the differential amplifier is used to evaluate the impact of unwanted input signals on the output. The matching of the resistors influences the CMRR. With this test procedure the influence of the resistors tolerances can be determined as well.

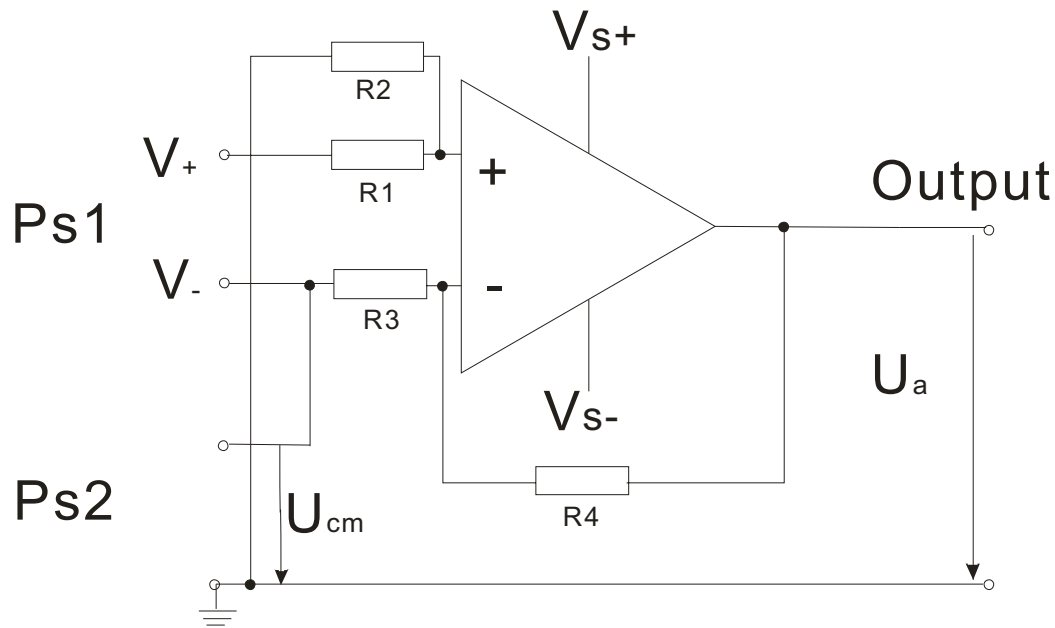


Figure 4.1 Schematic diagram of common mode testing

As shown in Figure 4.1, two power supplies (Ps1 and Ps2) are used for the testing. Ps1 is set to 4.0V and supplies both inputs of  $V_+$  and  $V_-$ . Ps2 is used to produce the voltage  $U_{cm}$ . The voltage  $U_{cm}$  is applied to the inverting input to produce a common mode signal. The value of  $U_{cm}$  is changed from 0V to 16V, while the output voltage of the differential amplifier  $U_a$  is measured. An amplifier with infinite CMRR would have no change in output.

The realized battery voltage measurement system, where the  $U_{cm}$  has to be determined is shown in Figure 4.2.

$$R1=R86+R179+R162+R4+R5 \quad (4-1)$$

$$R2=R8 \quad (4-2)$$

$$R3=R87+R180+R173+R1+R6 \quad (4-3)$$

$$R4=R7 \quad (4-4)$$

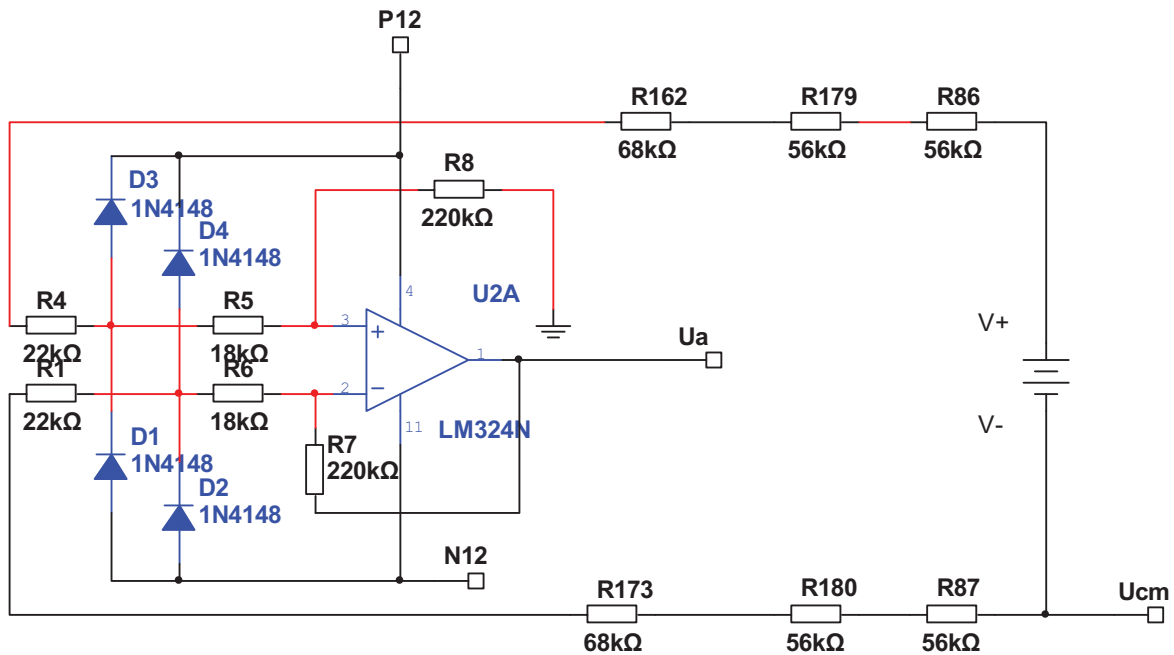


Figure 4.2 Circuit diagram for the test of common-mode

Table 4.1 output voltages of differential amplifier under different  $U_{cm}$  voltage level

$U_{cm}(V)$	$U_{a1}(V)$	$U_{a2}(V)$	$U_{a3}(V)$	$U_{a4}(V)$	$U_{a5}(V)$	$U_{a6}(V)$
0	3.968	4.007	3.993	4.013	4.001	4.005
2	3.962	4.007	3.990	4.004	3.997	4.005
4	3.956	4.007	3.988	3.995	3.994	4.005
6	3.950	4.007	3.985	3.985	3.991	4.005
8	3.944	4.007	3.983	3.976	3.988	4.005
10	3.938	4.008	3.981	3.967	3.985	4.005
12	3.933	4.008	3.978	3.957	3.982	4.006
14	3.927	4.008	3.976	3.948	3.979	4.006
16	3.921	4.008	3.973	3.939	3.966	4.006

As shown in Figure 4.1  $U_{cm}$  is the common mode voltage.  $U_{a1}$ ,  $U_{a2}$ ,  $U_{a3}$ ,  $U_{a4}$ ,  $U_{a5}$  and  $U_{a6}$  are the output voltage of the differential amplifier from each battery cell voltage measurement circuit.  $U_{diff}$  is defined as the difference between maximum and minimum output voltage of the differential amplifier. The  $U_{diff}$  of each battery voltage measurement circuit is shown in Table 4.2

Table 4.2  $U_{diff}$  of each battery voltage measurement circuit

	1	2	3	4	5	6
$U_{diff}(mV)$	47	1	20	74	35	1

A difference voltage 10mV is considered an acceptable value. The measurement  $U_{diff}$  in battery voltage measurement circuit 1, 3, 4 and 5 were much higher. These errors are because of the resistor tolerance. By replacing resistors, the  $U_{diff}$  was reduced to acceptable values in these circuits. The final result is shown in Table 4.3

Table 4.3 match of the resistors in measurement circuit

	Before(K $\Omega$ )	After(K $\Omega$ )
R7	219.97	219.68
R8	218.9	219.71
R33	219.46	219.96
R34	219.12	219.91
R45	221.22	219.99
R47	219.54	219.98
R59	219.97	219.57
R60	219.56	219.57

After the resistors were replaced, the previous testing procedure was repeated again. The testing result is shown in Table 4.4 and Table 4.5 respectively

Table 4.4 output voltages of differential amplifier (improved)

$U_{cm}(V)$	$U_{a1}(V)$		$U_{a3}(V)$	$U_{a4}(V)$	$U_{a5}(V)$
0	4.000		4.007	4.004	4.001
2	4.000		4.006	4.003	4.000
4	4.000		4.005	4.002	3.998
6	3.999		4.004	4.000	3.997
8	3.998		4.003	3.999	3.996
10	3.998		4.002	3.997	3.995
12	3.997		4.001	3.996	3.994
14	3.996		4.000	3.995	3.992
16	3.996		3.999	3.994	3.991

Table 4.5  $U_{diff}$  of battery voltage measurement circuit (improved)

Moduel	1		3	4	5
$U_{diff}(mV)$	4		8	10	10

After the changing of resistors, the outputs of voltage measurement circuit become

much precise. The ratio match of the resistors is as important as the CMRR of the op amp.

The cell voltage range is defined from 3V to 4.2V. One power supply is used to simulate cell voltage. The power supply is adjusted in following steps: 2.5V, 2.9V, 3.0V, 3.2V, 3.5V, 3.8V, 4.0V, 4.1V, 4.2V and 4.3V. The cell voltage is measured for each six voltage measurement circuits. The testing result is shown in Table 4.6. The simulated cell voltage is shown in column "Target". B1, B2, B3, B4, B5, B6 are voltages measured from each voltage measurement circuit.

Table 4.6 cell voltage measurement,

<b>Target (V)</b>	<b>B1(V)</b>	<b>B2(V)</b>	<b>B3(V)</b>	<b>B4(V)</b>	<b>B5(V)</b>	<b>B6(V)</b>
2.5	2.526	2.524	2.536	2.563	2.535	2.526
2.9	2.927	2.291	2.928	2.955	2.929	2.924
3	3.016	3.025	3.038	3.009	3.001	3.021
3.2	3.212	3.227	3.239	3.229	3.246	3.218
3.5	3.517	3.518	3.537	3.534	3.549	3.519
3.8	3.797	3.813	3.825	3.804	3.842	3.815
4	3.999	4.011	4.008	4.016	4.008	4.007
4.1	4.104	4.113	4.109	4.098	4.095	4.085
4.2	4.195	4.216	4.224	4.194	4.205	4.189
4.3	4.295	4.301	4.315	4.294	4.289	4.279
4.4	4.397	4.391	4.387	4.395	4.398	4.385
Max. error	0.026	0.027	0.038	0.063	0.049	0.026
op.range error	0.017	0.027	0.038	0.034	0.049	0.021

---

## 4.1.2 Voltage monitoring module

In chapter 3.3 the function of monitoring system for voltage of batteries is described and established. In this chapter, each voltage monitoring module is tested.

As shown in Figure 4.3, six power supplies are used to simulate the 12 cells in the battery pack. Six voltage monitoring modules are used in the monitoring system.



Figure 4.3 The connection of six power supplies

The connection of power supplies, monitoring modules and display module is shown in Figure 4.4.

The testing result is shown in Table 4.7. B1, B2, B3, B4, B5 and B6 are the output voltage of 6 power supplies. The column named “Green” indicates the green LED. The column named “Red” indicates the red LED. The symbol  $\surd$  means LED ON and the symbol  $\times$  means LED OFF. Reset is the status of reset function. When all cells voltage are in the operation range (3.0V- 4.2V), press the reset button, the second green LED is ON, as shown in Figure 3.26



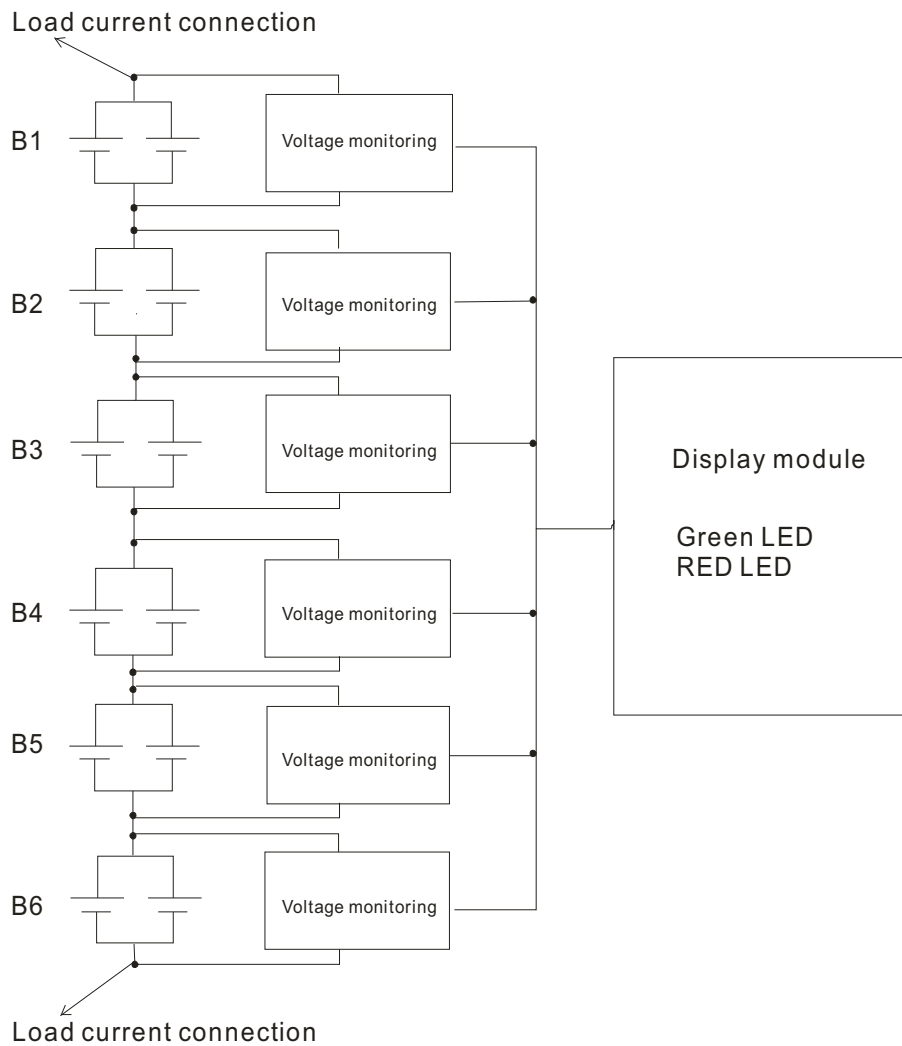


Figure 4.4 Block diagram for voltage monitoring system

Table 4.7 Test result of voltage monitoring system

Test	B1	B2	B3	B4	B5	B6	Green	Red	Reset
1	4.0	4.0	4.0	4.0	4.0	4.0	✓	×	
2	<b>4.3</b>	4.0	4.0	4.0	4.0	4.0	×	✓	✓
3	3.2	4.0	4.0	4.0	4.0	4.0	✓	×	
4	<b>2.9</b>	4.0	4.0	4.0	4.0	4.0	×	✓	✓
5	4.0	<b>4.3</b>	4.0	4.0	4.0	4.0	×	✓	✓
6	4.0	3.2	4.0	4.0	4.0	4.0	✓	×	
7	4.0	<b>2.9</b>	4.0	4.0	4.0	4.0	×	✓	✓
8	3.5	4.0	4.0	4.0	4.0	4.0	✓	×	
9	3.5	3.5	<b>4.3</b>	4.0	4.0	4.0	×	✓	✓
10	3.6	3.8	3.2	4.0	4.0	4.0	✓	×	
11	3.6	3.8	<b>2.9</b>	4.0	4.0	4.0	×	✓	✓
12	3.6	3.8	4.0	3.8	4.0	4.0	✓	×	

13	3.6	3.8	4.0	<b>4.3</b>	4.0	4.0	×	✓	✓
14	3.6	3.8	4.1	3.2	4.0	4.0	✓	×	
15	3.6	3.8	4.1	<b>2.9</b>	4.0	4.0	×	✓	✓
16	3.1	3.8	4.1	4.0	4.0	4.0	✓	×	
17	3.1	3.8	4.1	4.0	<b>4.3</b>	4.0	×	✓	✓
18	3.1	3.8	4.1	4.0	3.2	4.0	✓	×	
19	3.1	3.8	4.1	4.0	<b>2.9</b>	4.0	×	✓	✓
20	3.1	3.8	4.1	4.0	4.0	4.1	✓	×	
21	3.1	3.8	4.1	4.0	4.0	<b>4.3</b>	×	✓	✓
22	3.1	3.8	4.1	4.0	4.0	3.2	✓	×	
23	3.1	3.8	4.1	4.0	4.0	<b>2.9</b>	×	✓	✓
24	3.1	3.8	4.3	4.0	4.0	<b>2.9</b>	×	✓	✓
25	3.1	3.8	4.3	4.3	4.0	<b>2.9</b>	×	✓	✓

#### 4.1.3 Temperature measurement and over-temperature detection

In chapter 3.2 the functions of temperature measurement and over-temperature detection system are described and established. In this chapter, these two systems are tested.

There are 12 cells in the battery pack. The 12 temperature measurement modules and the 12 over-temperature detection modules are used. A variable resistor is used to simulate the behavior of the PTC and KTY at different temperatures.

$R_{ptc}$  is the resistance of PTC. The resistance of PTC changes according to the temperature. This test simulates the following process: the temperature changes from low to high and then from high to low. The outputs of the Schmitt trigger “40106” is used to control the display module. The output H (High) means the temperature is within allowable limits. If the output is L (Low), the temperature is too high (over-temperature).

The testing result is shown in Table 4.8

Table 4.8 Testing of over-temperature detection

Test	1	2	3	4	5	6	7	8
$R_{ptc}$ ( $\Omega$ )	176	1248	1432	2085	3200	775	479	60
Cell1								
Input (40106) V	1.1	4.3	4.6	5.3	5.9	3.4	2.5	0.4
Output (40106)	H	H	L	L	L	H	H	H
Cell2								
Input (40106) V	1.2	4.3	4.6	5.3	5.9	3.4	2.5	0.5
Output (40106)	H	H	L	L	L	H	H	H
Cell3								
Input (40106) V	1.1	4.3	4.6	5.3	5.9	3.4	2.5	0.4
Output (40106)	H	H	L	L	L	H	H	H
Cell4								
Input (40106) V	1.2	4.4	4.6	5.3	5.9	3.4	2.6	0.5
Output (40106)	H	H	L	L	L	H	H	H
Cell5								
Input (40106) V	1.1	4.3	4.6	5.4	5.9	3.4	2.5	0.4
Output (40106)	H	H	L	L	L	H	H	H
Cell5								
Input (40106) V	1.2	4.3	4.6	5.3	5.9	3.4	2.5	0.4
Output (40106)	H	H	L	L	L	H	H	H
Cell6								
Input (40106) V	1.1	4.3	4.7	5.3	5.9	3.4	2.5	0.4
Output (40106)	H	H	L	L	L	H	H	H
Cell7								
Input (40106) V	1.1	4.3	4.6	5.3	5.9	3.4	2.5	0.4
Output (40106)	H	H	L	L	L	H	H	H
Cell8								
Input (40106) V	1.2	4.3	4.7	5.3	5.9	3.5	2.5	0.4
Output (40106)	H	H	L	L	L	H	H	H

Cell9								
Input (40106) V	1.1	4.3	4.6	5.2	5.9	3.4	2.5	0.3
Output (40106)	H	H	L	L	L	H	H	H
Cell10								
Input (40106) V	1.1	4.3	4.6	5.3	5.9	3.4	2.5	0.4
Output (40106)	H	H	L	L	L	H	H	H
Cell11								
Input (40106) V	1.1	4.2	4.6	5.3	5.9	3.4	2.5	0.4
Output (40106)	H	H	L	L	L	H	H	H
Cell12								
Input (40106) V	1.2	4.3	4.6	5.4	5.9	3.5	2.5	0.4
Output (40106)	H	H	L	L	L	H	H	H

According to the testing result from Table 4.8 , the input-output characteristic of Schmitt trigger 40106 is shown in Figure 4.5.

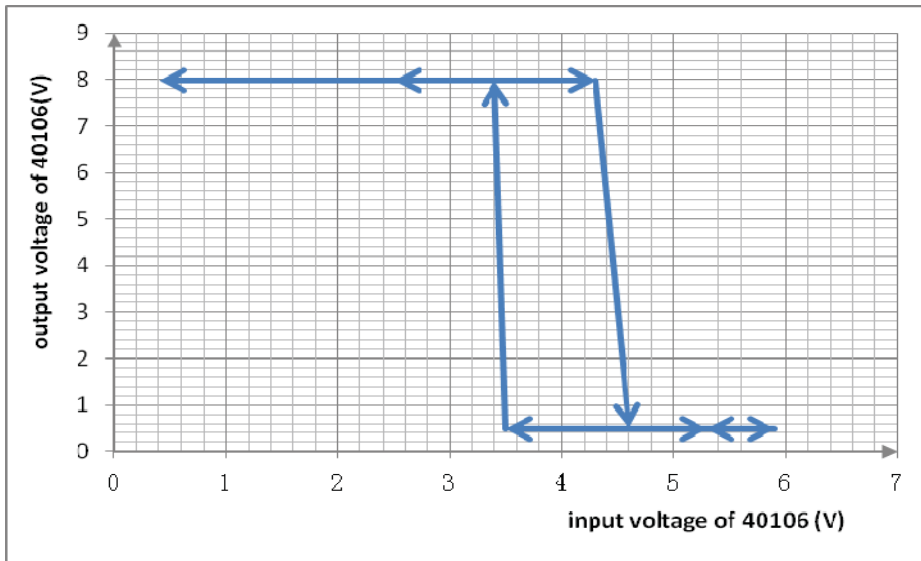


Figure 4.5 Input/output characteristic of Schmitt trigger 40106

As shown in Figure 4.5, the positive-going threshold voltage is 4.6V and the negative-going threshold voltage is 3.4V. The corresponding switch resistance of PTC is about 1432Ω.

The measurement range of temperature sensor KTY-81 is from -50 °C to 100 °C.

The testing result of temperature is shown in Table 4.9.  $R_{kty}$  is the resistance of KTY

at corresponding target temperature. From Temp\_cell1 to Temp\_cell12 is the value displayed in LCD digital Panel Meter.

Table 4.9 Temperature measurement testing result

Target (°C)	-50	-30	-10	0	25	50	80	100
R <sub>ky</sub> (Ω)	980	1247	1495	1630	2000	2417	2980	3392
Temp_cell1	-56.45	-31.11	-9.79	0.92	27.29	52.75	81.78	99.48
Temp_cell2	-56.58	-31.38	-10.18	0.49	26.72	51.99	80.89	98.53
Temp_cell3	-56.09	-30.72	-9.32	1.44	27.89	53.41	82.54	100.29
Temp_cell4	-56.92	-31.60	-10.25	0.48	26.87	52.32	81.37	99.09
Temp_cell5	-56.83	-31.40	-9.97	0.81	27.31	52.85	82.04	99.82
Temp_cell6	-57.44	-32.06	-10.64	0.12	26.62	52.12	81.29	99.07
Temp_cell7	-56.68	-31.33	-9.94	0.79	27.25	52.70	81.82	99.53
Temp_cell8	-56.50	-31.22	-9.94	0.85	27.22	52.62	81.69	99.40
Temp_cell9	-56.13	-30.83	-9.51	1.33	27.75	53.17	82.27	100.01
Temp_cell10	-56.31	-31.01	-9.78	1.12	27.37	52.76	81.80	99.51
Temp_cell11	-55.35	-30.09	-8.86	2.00	28.24	53.58	82.57	100.27
Temp_cell12	-56.12	-30.78	-9.48	1.43	27.75	53.19	82.30	100.05

Deviations between actual and indicated temperatures are always less than 4K.

## 4.2 Testing Entire Balancing System with Power Supply

In chapter 3.1 the function of battery balancing system is described and established. In this chapter, this battery balancing systems is tested.

The core function of balancing system is shown in Figure 3.6. The output of operational amplifier is the control signal for by-pass load, as shown in Figure 3.6. Therefore, the input and output of the operational amplifier are recorded to evaluate the balancing system. The schematic diagram of signal measurement is shown in Figure 4.6.

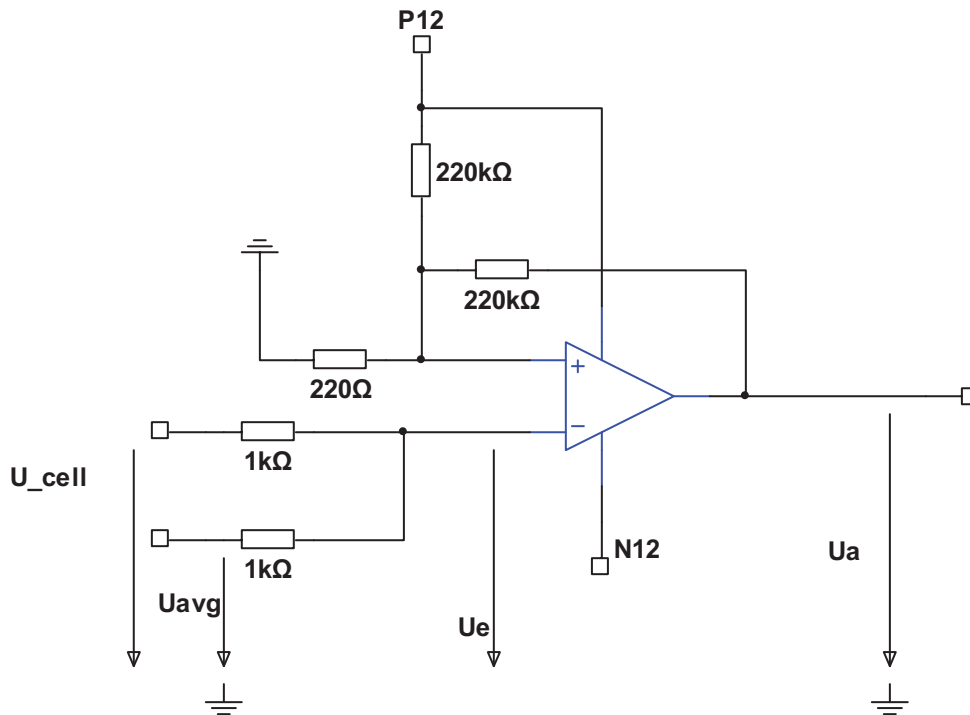


Figure 4.6 Schematic diagram of signal measurement

$U_{cell}$  is the cell voltage measured by voltage measurement system.  $U_{avg}$  is the average voltage of the battery pack.  $U_e$  is the voltage on the inverting input.  $U_a$  is the output voltage.

The six power supplies are used to simulate cells in the battery pack. The output voltage of one power supply is changed. The output voltage of other 5 power supplies is kept on same value.  $U_{cell}$ ,  $U_{avg}$ ,  $U_e$  and  $U_a$  are measured.

There are six balancing modules in the balancing system. This was done for all six balancing modules.

Table 4.10 shows the test result of balancing module No.1

Table 4.10 Testing of balancing module, No.1

$U_{cell1}$ (V)	$U_{avg}$ (V)	$U_e$ (mV)	$U_a$ (V)
4.011	4.047	-17.150	9.237
4.028	4.050	-10.210	9.249
4.052	4.054	0.030	9.272

4.062	4.056	4.160	9.281
4.074	4.058	8.860	9.291
4.091	4.061	15.960	9.308
4.100	4.064	18.850	9.318
4.108	4.072	19.150	-8.880
4.132	4.076	28.980	-8.860
4.111	4.072	20.210	-8.870
4.100	4.070	15.750	-8.870
4.090	4.069	11.790	-8.870
4.069	4.052	8.880	-8.870
4.058	4.050	4.710	-8.870
4.051	4.049	2.790	9.240
4.042	4.048	-2.170	9.230

According to the test result from Table 4.10, the relationship between  $U_e$  and  $U_a$  is shown in Figure 4.7.

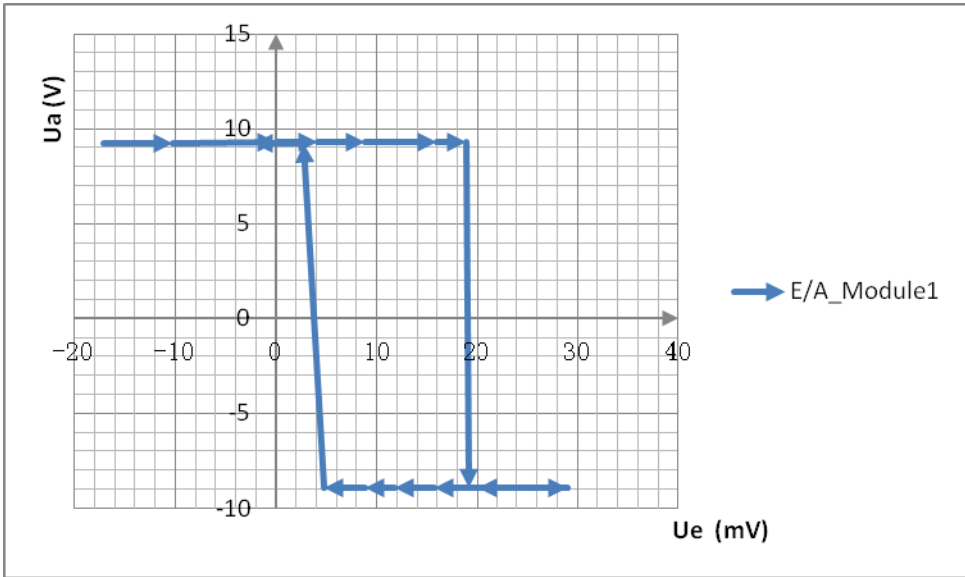


Figure 4.7 Relationship between  $U_e$  and  $U_a$  for balancing module No.1

As shown in Table 4.10, the output voltage of the first power supply  $U_{cell1}$  is varied in the range from 4.011V to 4.132V. The simulated cell voltage of the other five modules are kept the same. When the voltage  $U_e$  is 19.150mV, the output voltage  $U_a$  is -8.88V. This means a too high cell voltage and the battery balancer is start working until the voltage  $U_e$  is 2.79mV. The voltage  $U_{cell1}$  is 2mV higher than the

average voltage of the battery pack. All of the cell voltages are balanced. For the balancing module No.1, the lower threshold voltage is 2mV and upper threshold voltage is 19.150mV. The upper threshold voltage is the voltage when the balancing module is activated. The lower threshold voltage is the voltage when the balancing process is stopped.

Table 4.11 shows the test result of balancing module No.2

Table 4.11 Testing of balancing module, No.2

$U_{\text{cell}2}$ (V)	$U_{\text{avg}}$ (V)	$U_e$ (mV)	$U_a$ (V)
4.028	4.045	-19.210	9.182
4.039	4.046	-13.990	9.194
4.048	4.048	-10.190	9.205
4.060	4.049	-4.880	9.219
4.074	4.052	0.540	9.232
4.091	4.054	7.480	9.249
4.112	4.058	16.290	9.272
4.126	4.060	22.290	9.286
4.157	4.065	35.250	9.305
4.160	4.065	36.660	-10.243
4.203	4.073	54.440	-10.254
4.145	4.063	30.340	-10.244
4.129	4.059	23.800	-10.245
4.100	4.058	16.100	-10.238
4.088	4.057	15.590	9.276

According to the test result from Table 4.11, the relationship between  $U_e$  and  $U_a$  is shown in Figure 4.8. For the balancing module No.2, the lower threshold voltage is 15.59mV and upper threshold voltage is 36.66mV.



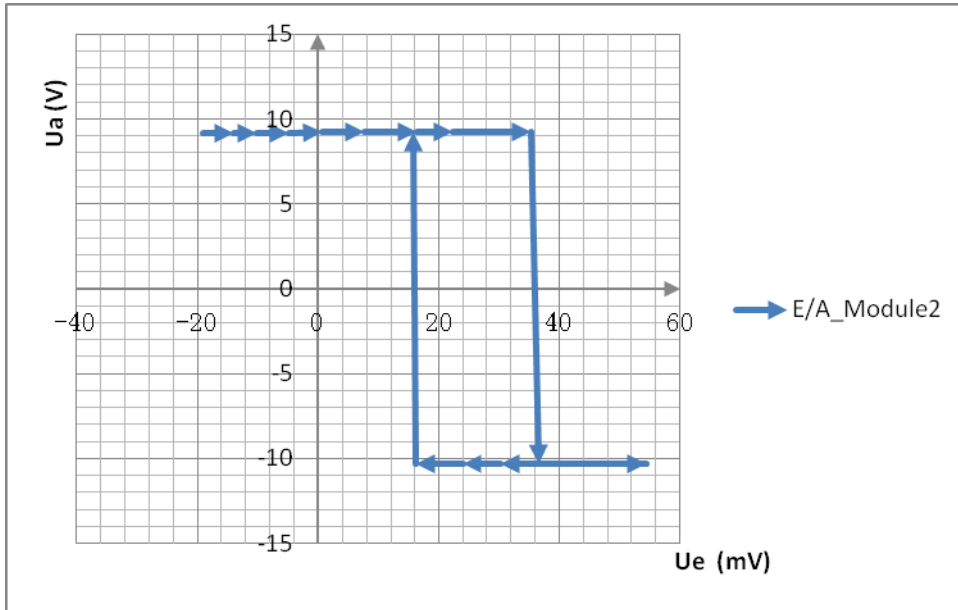


Figure 4.8 Relationship between  $U_e$  and  $U_a$  for balancing module No. 2

Table 4.12 shows the test result of balancing module No.3

Table 4.12 Testing of balancing module, No.3

$U_{cell3}$ (V)	$U_{avg}$ (V)	$U_e$ (mV)	$U_a$ (V)
4.044	4.042	-2.450	9.169
4.066	4.045	6.870	9.190
4.078	4.047	11.820	9.204
4.088	4.049	16.470	9.219
4.097	4.050	19.980	9.227
4.103	4.051	22.520	-10.246
4.139	4.057	37.540	-10.186
4.098	4.050	20.750	-10.230
4.076	4.046	11.420	-10.240
4.064	4.045	4.230	-10.238
4.056	4.043	3.200	9.196
4.037	4.040	-4.870	9.177

According to the test result from Table 4.12, the relationship between  $U_e$  and  $U_a$  is shown in Figure 4.9. For the balancing module No.3, the lower threshold voltage is 3.2mV and upper threshold voltage is 22.52mV.

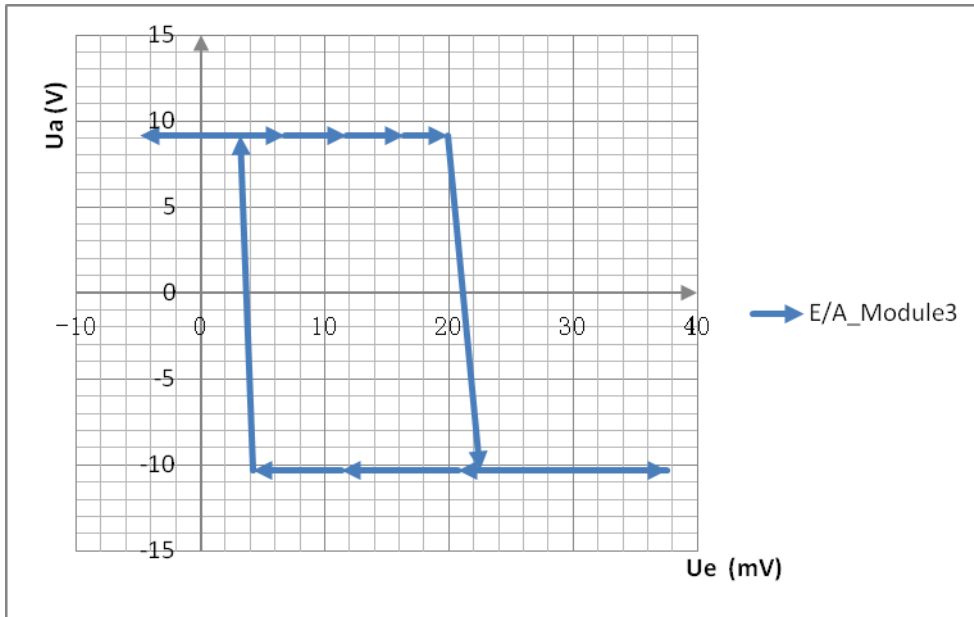


Figure 4.9 Relationship between  $U_e$  and  $U_a$  for balancing module No.3

Table 4.13 shows the test result of balancing module No.4

Table 4.13 Testing of balancing module, No.4

$U_{\text{cell4}}$ (V)	$U_{\text{avg}}$ (V)	$U_e$ (mV)	$U_a$ (V)
4.034	4.041	-2.770	9.277
4.052	4.044	4.670	9.276
4.082	4.049	17.620	9.279
4.095	4.051	22.580	9.279
4.098	4.052	24.190	-10.222
4.123	4.056	34.820	-10.272
4.096	4.051	23.650	-10.252
4.072	4.047	13.620	-10.220
4.053	4.044	8.260	-10.202
4.049	4.044	5.860	9.285
4.037	4.041	-1.150	9.283

According to the test result from Table 4.13, the relationship between  $U_e$  and  $U_a$  is shown in Figure 4.10. For the balancing module No.4, the lower threshold voltage is 5.86mV and upper threshold voltage is 24.19mV.

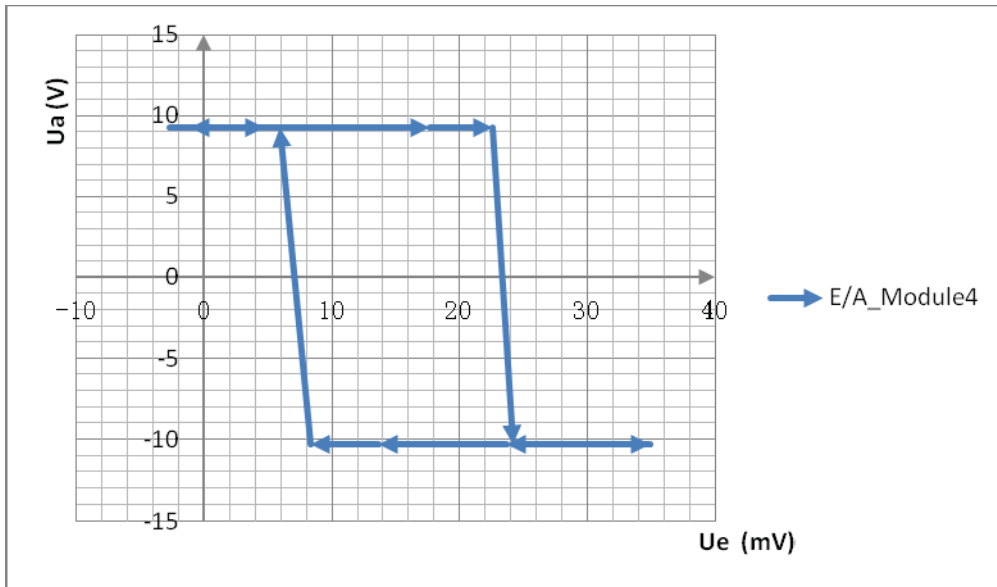


Figure 4.10 Relationship between  $U_e$  and  $U_a$  for balancing module No.4

Table 4.14 shows the test result of balancing module No.5

Table 4.14 Testing of balancing module, No.5

$U_{cell5}$ (V)	$U_{avg}$ (V)	$U_e$ (mV)	$U_a$ (V)
4.023	4.045	-9.370	9.164
4.050	4.050	4.220	9.175
4.073	4.053	11.150	9.179
4.083	4.055	15.490	9.181
4.095	4.056	20.660	9.185
4.106	4.058	25.180	9.185
4.124	4.061	33.400	9.187
4.130	4.062	35.760	-10.382
4.198	4.073	64.200	-10.444
4.130	4.062	35.870	-10.379
4.088	4.054	18.360	-10.335
4.081	4.053	15.370	9.191
4.056	4.049	4.960	9.191

According to the test result from Table 4.14, the relationship between  $U_e$  and  $U_a$  is shown in Figure 4.11. For the balancing module No.5, the lower threshold voltage is 15.37mV and upper threshold voltage is 35.76mV.

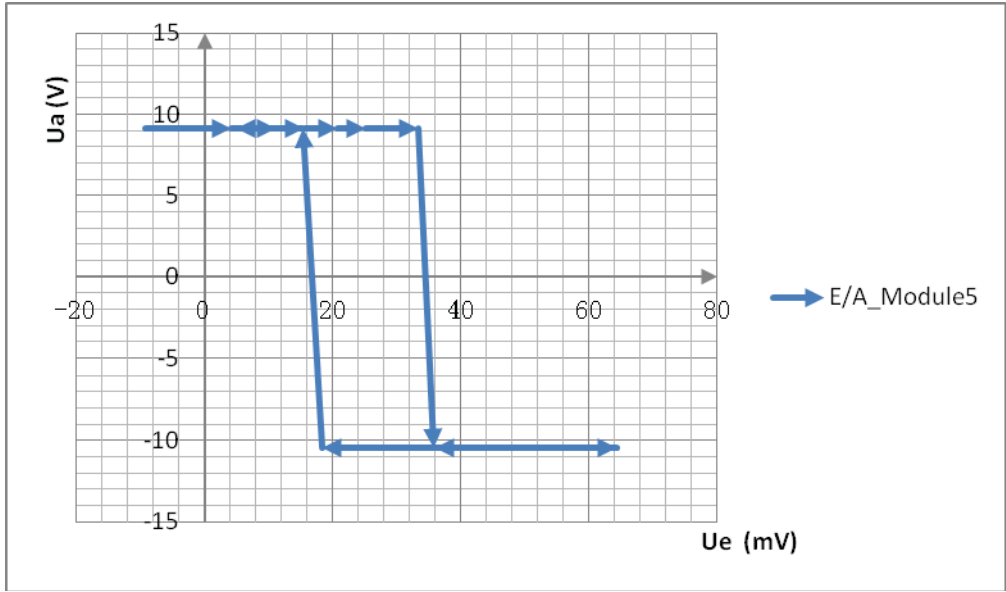


Figure 4.11 Relationship between Ue and Ua for balancing module No.5

Table 4.15 shows the test result of balancing module No.6

Table 4.15 Testing of balancing module, No.6

$U_{b_6}$ (V)	$U_{avg}$ (V)	$U_e$ (mV)	$U_a$ (V)
4.033	4.046	-4.890	9.180
4.065	4.051	8.700	9.183
4.081	4.053	15.030	9.187
4.098	4.056	22.410	9.189
4.100	4.056	23.400	-10.353
4.126	4.061	34.110	-10.377
4.100	4.056	23.500	-10.344
4.086	4.054	17.800	-10.346
4.057	4.049	5.380	-10.296
4.054	4.048	4.550	9.195
4.029	4.044	-5.860	9.194

According to the test result from Table 4.15, the relationship between Ue and Ua is shown in Figure 4.12. For the balancing module No.6, the lower threshold voltage is 4.55mV and upper threshold voltage is 23.40mV.

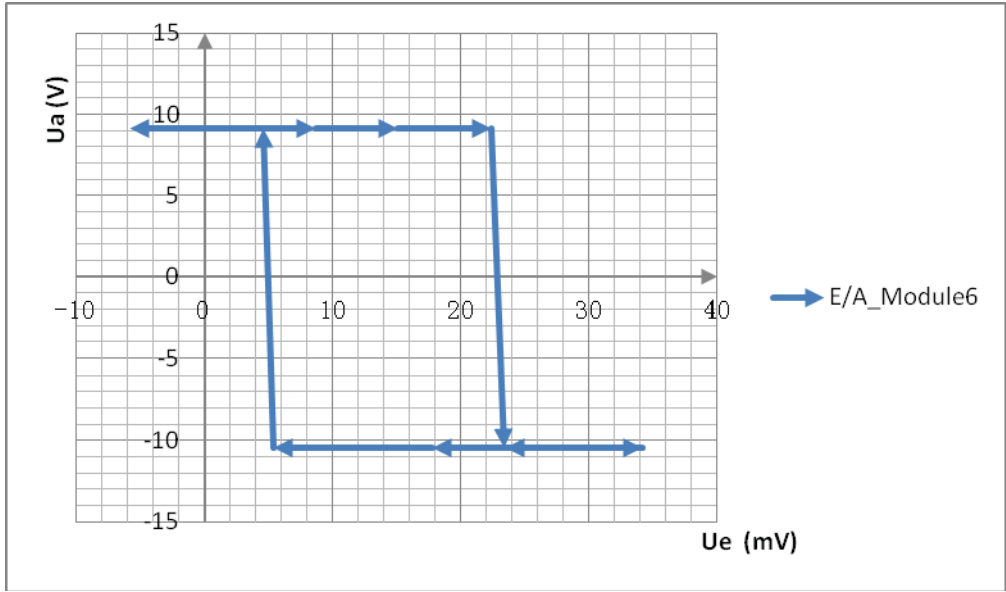


Figure 4.12 Relationship between  $U_e$  and  $U_a$  for balancing module No.6

In the ideal balancing situation, the lower threshold voltage is 15mV and the upper threshold voltage is 35mV.

Table 4.16 Comparison of the lower threshold voltage and the upper threshold voltage from module 1 to module 6

Module	1	2	3	4	5	6
Low(mV)	2.790	15.590	3.200	5.860	15.370	4.550
High(mV)	19.15	36.66	22.52	24.19	35.76	23.4

As shown in Table 4.16, the balancing modules 2 and 5 have almost same value as the ideal balancing situation. The balancing modules 1, 3, 4 and 6 have less lower threshold voltage and upper threshold voltage. That means, these balancing modules start working earlier and stop working later than the ideal balancing situation. The deviation is around 10 to 15 mV. This deviation is depending on component values of the resistors. The standard tolerance for resistors is 1%. Therefore, the deviation around 10 to 15mV is acceptable.

According to the testing result of all six balancing module, the relationship between  $U_e$  and  $U_a$  compared with the ideal curve is shown in

Figure 4.13.

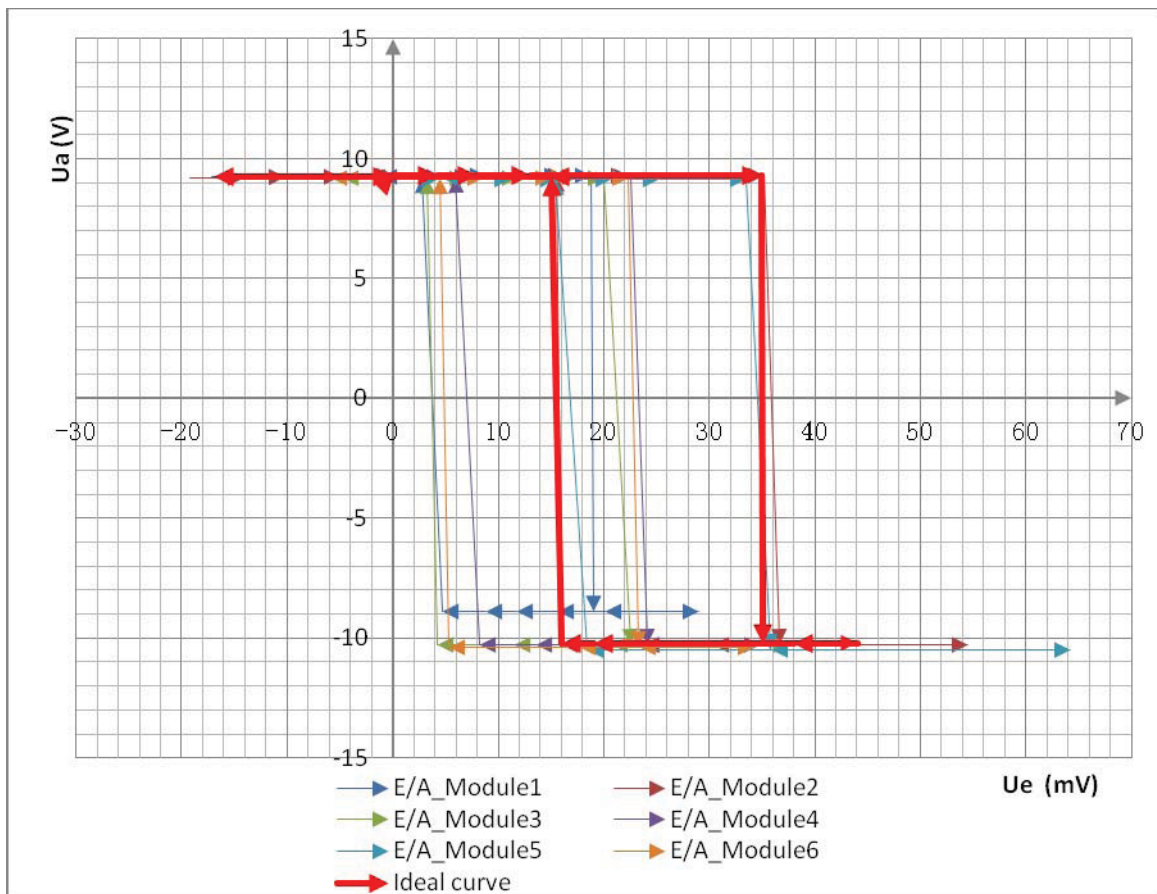


Figure 4.13 Relationship between  $U_e$  and  $U_a$  for all six balancing modules comparing with the ideal curve

### 4.3 Balancing System Installation and Commissioning

In chapter 4.2, the function of 6 battery-balancing modules are tested with power supplies. In this chapter, these 6 battery-balancing modules are tested with the battery pack, as shown in Figure 4.15.

There are 12 cells in the battery pack. Each 2 cells are parallel connected. The metal plates are used to connect cell pairs in series. The connection inside of the battery pack is shown in Figure 4.14

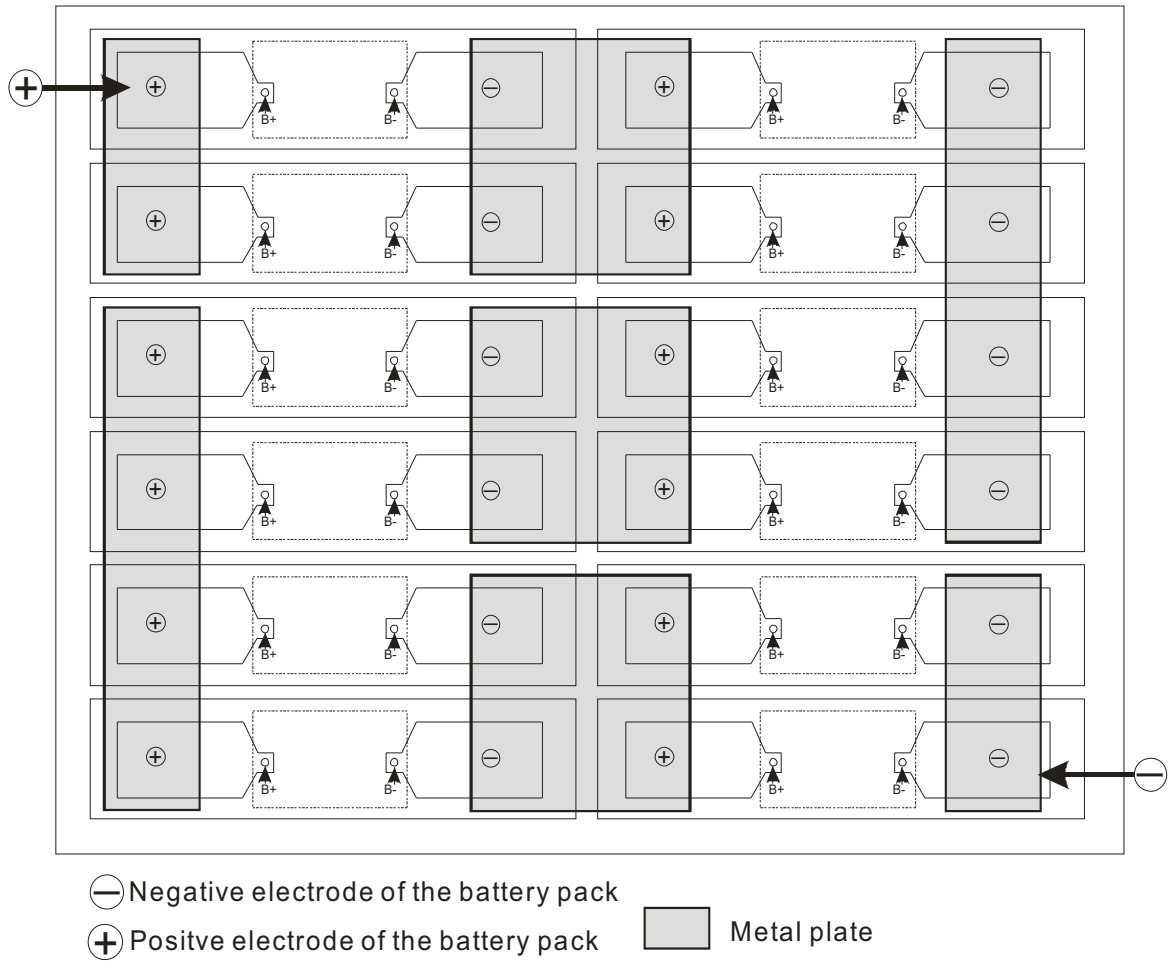


Figure 4.14 The connection inside of the battery pack, TOP view

The cell voltages in the battery pack are balanced before the test, the voltages are shown in Table 4.17.

Table 4.17 Cell voltages in the battery pack before test

Cell 1	Cell 2	Cell 3	Cell 4	Cell 5	Cell 6
3.864V	3.852V	3.856V	3.854V	3.859V	3.855V



Figure 4.15 battery pack and 6 circuit boards on the battery

Each cell is tested in following steps:

1. Charging with a power supply until the balance-module is started.
2. Stop the charging process
3. Waiting until the balance-module is stopped

Table 4.18 Comparison of the lower threshold voltage and the upper threshold voltage from module

1 to module 6

Moduel	1	2	3	4	5	6
low	5.680	17.350	8.480	6.650	19.980	6.350
high	17.34	33.31	22.77	18.97	30.38	28.54

According to the testing result of all six balancing module, the relationship between  $U_e$  and  $U_a$  comparing with the ideal curve is shown in Figure 4.16



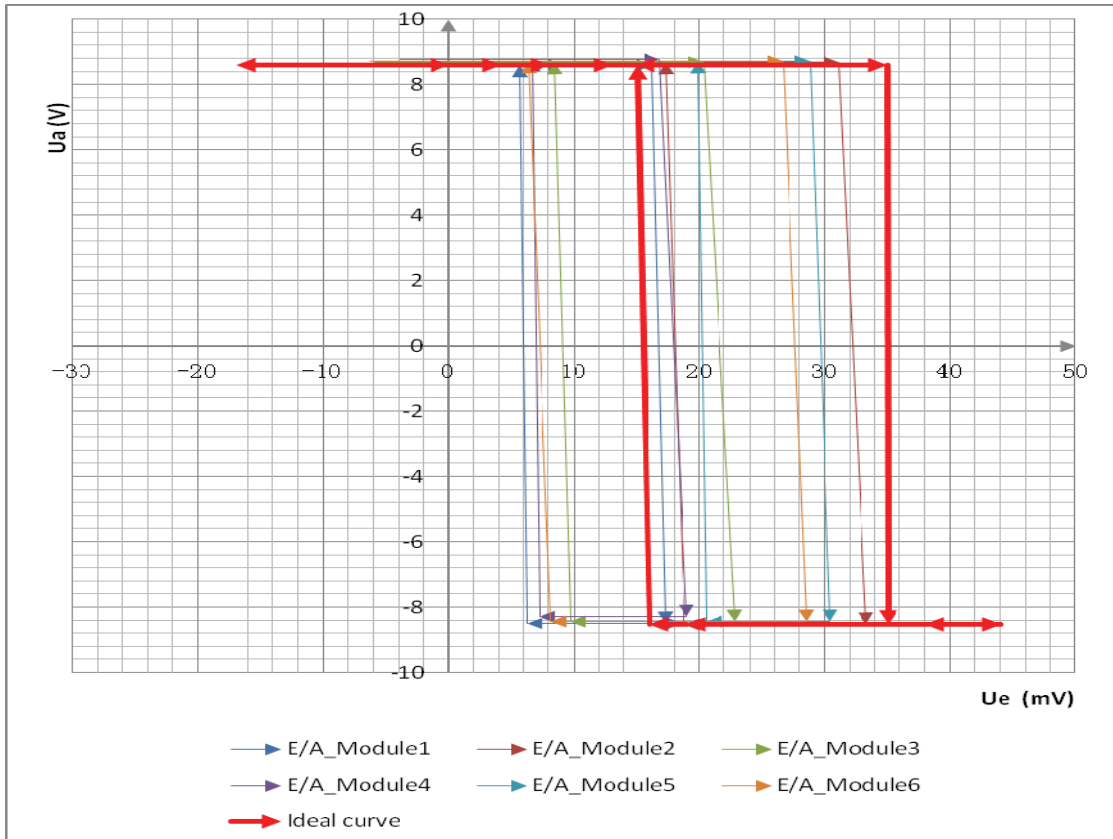


Figure 4.16 Relationship between  $U_e$  and  $U_a$  for all six balancing modules comparing with the ideal curve

Table 4.19 Cell voltages in the battery pack after test and the difference from average voltage

	Cell1	Cell2	Cell3	Cell4	Cell5	Cell6
Voltage	3.881	3.905	3.880	3.870	3.901	3.893
$\Delta U$	-7.3	16.7	-8.3	-18.3	12.6	4.7

As shown in Table 4.19,  $\Delta U$  is the difference between the cell voltage and the average voltage of the battery cell. The voltage differences of 6 cells are less than 19mV. That means, all of the 6 cell voltages in the battery pack is balanced.

---

## 5 Conclusion

In the future, the Lithium-ion battery has broad prospects in the field of electric vehicles. As energy storage device, the performance of the Lithium-ion battery is a key factor for the usability of electric vehicles. The battery management system is used for battery safety, as well as for communication with vehicle management system. The way how to extend the battery life and improve the battery efficiency is the key issue of the battery management system. Therefore, the research of battery management technologies and systems has great significance. The study focuses on a balancing system for a Lithium-ion battery pack.

In this thesis, first of all the characteristics of Lithium-ion batteries are introduced. The reason of cell unbalancing is explained and the aim of battery balancing is defined. In the second part of the thesis, several essential electronic circuits such as operational amplifier, window comparator, Schmitt trigger, temperature sensors, diode transistor logic circuits and charge pump are introduced.

After this section, function modules of the balancing system are designed and established. There are following modules in the system:

- Voltage measurement and battery regulator module,
- Temperature measurement and over-temperature detection module,
- Monitoring module for battery over-voltage(over-voltage protection),
- Control and display module,
- Power supply module.

Finally, all the function modules are assembled and tested in two phases. The first phase is testing the balancing system by using of power supplies as cell replacements because of safety (electronic current limiting). In the second phase, testing the balancing system with real battery pack is accomplished. All the critical voltages during the test are recorded and analyzed. Through analysis of these data, it could be proved that the balancing system has achieved the task of the thesis: all

---

the cell voltages in the battery pack are balanced after completion of the balancing process. The balancer can be turned off by control signals in order to save energy during standstill of the electric vehicle, for instance. Also the function of over-voltage and over-temperature protection units fulfill the requirements according to results of extensive tests.

Follow-up work should be done in implementing the described battery module balancer and protector for every module in the battery pack of an electric vehicle and in testing the system in practical operation.

---

## 6 Directory

### 6.1 Literature

- [1] Franz W. Peren, Das Elektroauto und sein Markt, Campus Verlag; Auflage: 1 (14. Mai 1997), ISBN-13: 978-3593357003
- [2] Jung-Ki Park, Principles and applications of lithium secondary batteries. Wiley-VCH Verlag, ISBN 978-3-527-33151-2
- [3] Gholam-Abbas Nazri, Lithium Batteries: Science and Technology, Gianfranco Pistoia, Springer 2009, ISBN 978-1-4020-7628-2
- [4] Lucien F. Trueb, Batterien and Akkumulatoren: Mobile Energiequellen für Heute und Morgen, Springer DE, ISBN 3-540-62997-1
- [5] Roger L. Freemann, Fundamentals of Telecommunications, Published by John Wiley & Sons, Inc., Hoboken, ISBN 0-471-71045-8
- [6] International Energy Agency (DE-588) 114056-5, Electric vehicles, S. 108
- [7] Proceedings: September 18-22, 2005 in Berlin, S 78
- [8] Davide Andrea, Battery Management Systems for Large Lithium Ion Battery Packs, Artech house, ISBN 978-1-60807-104-3
- [9] Wupper horst, Professionelle Schaltungstechnik mit Operationsverstärkern, Franzis-Verlag, Poing, 1994, ISBN 3-7723-6732-1
- [10] Maxim Integrated Products, "Ultra-Small, Low-Power, Window comparator in 4 UCSP and 5 SOT23" MAX9065 datasheet, 19-4224; Rev 2; 1/11
- [11] N.P. Deshpande, Electronic devices & circuits, Principles and Applications, Tata McGraw-Hill, ISBN 978-0-07-061711-7
- [12] Jacob Fraden, Handbook of Modern Sensors, Physics, Designs, and Applications, Fourth Edition, Springer, ISBN 978-1-4419-6465-6
- [13] Klaus Beuth, Digitaltechnik 9., überarbeitete Auflage, Vogel Buchverlag, ISBN 3-8023-1440-9

- 
- [14] Stanley W. Amos, Transistorschaltungen: Entwurf und Arbeitsweise, ISBN 3-527-28295-5
- [15] Lutz v. Wangenheim, Aktive Filter in RC- und SC-Technik: Grundlagen Berechnungsverfahren Schaltungstechnik, Hüthig Buch Verlag Heidelberg, ISBN 3-7785-1894-1
- [16] Fachkunde Industrieelektronik und Informationstechnik, 7 überarbeitete Auflage, Verlag Europa-Lehrmittel, ISBN 3-8085-3247-5
- [17] Georg Becke & Eilhard Haseloff, Digitaler Schaltungsentwurf in Theorie und Praxis: Das TTL Kochbuch, Texas Instruments, ISBN 3-88078-093-5
- [18] Agnes F. McBrewster, Frederic P. Vandome, John Miller, Charge pump, Betascript Publishing, ISBN 6-1337-5922-4
- [19] Tietze, U.; Schenk, Ch.: Halbleiter-Schaltungstechnik. Auflage 12, 2002, Verlag Springer, ISBN 978-3540428497
- [20] R.M. Marston, Optoelectronics circuits manual, 2 edition, Newnes, ISBN 0-7506-4166-5

## 6.2 Tables

Table 1.1 Battery Specific energy Comparison [6].....	5
Table 2.1 input and output voltages of AND logic gate .....	25
Table 2.2 Truth table of AND logic gate .....	25
Table 2.3 input and output voltages of OR logic gate .....	27
Table 2.4 Truth table of OR logic gate [17] .....	27
Table 2.5 input and output voltages of NOT logic gate .....	28
Table 2.6 Truth table of NOT logic gate [17] .....	28
Table 2.7 Truth table for RS flip flop using two NAND gates .....	29
Table 2.8 Truth table for RS flip flop using two NOR gates.....	30
Table 3.1 Theoretical results of temperature measurement .....	49
Table 3.2 Logical relationship between the battery voltage and the LEDs.....	56

---

Table 3.3 Overview of status indicators .....	61
Table 4.1 output voltages of differential amplifier under different $U_{cm}$ voltage level.....	69
Table 4.2 $U_{diff}$ of each battery voltage measurement circuit.....	69
Table 4.3 match of the resistors in measurement circuit.....	70
Table 4.4 output voltages of differential amplifier (improved) .....	70
Table 4.5 $U_{diff}$ of battery voltage measurement circuit (improved) .....	70
Table 4.6 cell voltage measurement, .....	71
Table 4.7 Test result of voltage monitoring system .....	73
Table 4.8 Testing of over-temperature detection .....	75
Table 4.9 Temperature measurement testing result.....	77
Table 4.10 Testing of balancing module, No.1 .....	78
Table 4.11 Testing of balancing module, No.2 .....	80
Table 4.12 Testing of balancing module, No.3.....	81
Table 4.13 Testing of balancing module, No.4.....	82
Table 4.14 Testing of balancing module, No.5.....	83
Table 4.15 Testing of balancing module, No.6.....	84
Table 4.16 Comparison of the lower threshold voltage and the upper threshold voltage from module 1 to module 6 .....	85
Table 4.17 Cell voltages in the battery pack before test .....	87
Table 4.18 Comparison of the lower threshold voltage and the upper threshold voltage from module 1 to module 6 .....	88
Table 4.19 Cell voltages in the battery pack after test and the difference from average voltage.....	89

### 6.3 Figures

Figure 1.1 Operating Principle of Lithium-ion Battery [3] .....	2
---	---

---

Figure 1.2 equivalent circuit of a lithium-ion battery .....	3
Figure 1.3 3 Battery pack with 3 cells in series .....	6
Figure 1.4 Discharging without Battery Balancing.....	7
Figure 1.5 Charging without Battery Balancing .....	7
Figure 1.6 Schematic diagram of simple passive Battery balancing device ....	9
Figure 2.1 Symbol of operational amplifier .....	12
Figure 2.2 Amplifier with voltage output [19].....	13
Figure 2.3 Non-inverting amplifier [14] .....	14
Figure 2.4 Inverting amplifier [14].....	15
Figure 2.5 Difference Amplifier [15] .....	16
Figure 2.6 function of the window comparator [9].....	18
Figure 2.7 Inverting Schmitt Trigger [19] .....	19
Figure 2.8 Transfer characteristic of Schmitt Trigger .....	20
Figure 2.9 R/T curve of KTY81/210.....	22
Figure 2.10 RT curve of PTC thermistor.....	23
Figure 2.11 The schematic diagram for the two-input AND gate .....	24
Figure 2.12 Typical DTL Circuit of AND logic gate.....	24
Figure 2.13 The schematic diagram for the two-input OR gate .....	26
Figure 2.14 Typical DTL Circuit of OR logic gate.....	26
Figure 2.15 Schematic diagram for NOT gate .....	27
Figure 2.16 Typical DTL Circuit of NOT logic gate .....	28
Figure 2.17 Basic flip-flop circuit with NAND gates [16] .....	29
Figure 2.18 Basic flip-flop circuit with NOR gates [16] .....	30
Figure 2.19 Voltage inverter employing the charge pump principle [19], state 1: charging of C1.....	31
Figure 2.20 Voltage inverter employing the charge pump principle [19], state 2: discharging of C1 .....	31

---

Figure 3.1 Battery pack connection diagram .....	33
Figure 3.2 Block diagram for measurement and balancing system .....	33
Figure 3.3 Circuit diagram for ON/OFF function .....	34
Figure 3.4 Circuit diagram for voltage measurement of cell1 .....	35
Figure 3.5 Circuit diagram of the average calculator .....	36
Figure 3.6 Circuit diagram bypass load controller and battery regulator for cell1 and cell2.....	37
Figure 3.7 Circuit diagram bypass load controller and battery regulator for cell3 and cell4.....	38
Figure 3.8 Circuit diagram bypass load controller and battery regulator for cell5 and cell6.....	39
Figure 3.9 Transfer characteristic of Schmitt trigger .....	40
Figure 3.10 balancing circuit board for 12 batteries .....	41
Figure 3.11 Layout of balancing circuit for 12 batteries .....	42
Figure 3.12 Top view of the battery .....	44
Figure 3.13 Circuit board on the battery including protection circuit.....	44
Figure 3.14 Layout of circuit board on the battery including protection circuit	45
Figure 3.15 Front view of cover .....	45
Figure 3.16 Bottom view of cover .....	46
Figure 3.17 Circuit board on the battery including cover .....	46
Figure 3.18 Temperature measurement circuit.....	47
Figure 3.19 Over-temperature detect circuit.....	50
Figure 3.20 diode AND logic gate for over-temperature detect circuit.....	51
Figure 3.21 Temperature measurement circuit board.....	52
Figure 3.22 Layout of Temperature measurement circuit board .....	53
Figure 3.23 Pin configuration of Max9065 (Top view) .....	54
Figure 3.24 Schematic of mounting socket.....	55
Figure 3.25 Voltage range monitoring circuit .....	56



---

Figure 3.26 Voltage status display circuit .....	57
Figure 3.27 Circuit board of voltage monitoring system .....	58
Figure 3.28 Layout of the voltage monitoring system .....	59
Figure 3.29 AND logic gate for Yellow LED control circuit .....	61
Figure 3.30 LED control circuit in display module .....	62
Figure 3.31 Layout of display module .....	63
Figure 3.32 Circuit board of the display module .....	63
Figure 3.33 Circuit diagram of $\pm 12V$ voltage limiter module .....	64
Figure 3.34 Circuit diagram of +8V, +3V and -5V power supply module .....	65
Figure 3.35 Layout of power supply module.....	66
Figure 4.1 Schematic diagram of common mode testing .....	68
Figure 4.2 Circuit diagram for the test of common-mode .....	69
Figure 4.3 The connection of six power supplies .....	72
Figure 4.4 Block diagram for voltage monitoring system.....	73
Figure 4.5 Input/output characteristic of Schmitt trigger 40106 .....	76
Figure 4.6 Schematic diagram of signal measurement .....	78
Figure 4.7 Relationship between $U_e$ and $U_a$ for balancing module No.1 .....	79
Figure 4.8 Relationship between $U_e$ and $U_a$ for balancing module No. 2 .....	81
Figure 4.9 Relationship between $U_e$ and $U_a$ for balancing module No.3 .....	82
Figure 4.10 Relationship between $U_e$ and $U_a$ for balancing module No.4 ....	83
Figure 4.11 Relationship between $U_e$ and $U_a$ for balancing module No.5 ....	84
Figure 4.12 Relationship between $U_e$ and $U_a$ for balancing module No.6 ....	85
Figure 4.13 Relationship between $U_e$ and $U_a$ for all six balancing modules comparing with the ideal curve.....	86
Figure 4.14 The connection inside of the battery pack, TOP view.....	87
Figure 4.15 battery pack and 6 circuit boards on the battery.....	88
Figure 4.16 Relationship between $U_e$ and $U_a$ for all six balancing modules comparing with the ideal curve.....	89

---

## 6.4 List of Symbols

U: Voltage

E: electromotive force

I: electric current

R: resistor

GND: ground

A.h: amp-hour

$V_{s+}$ : positive supply voltage

$V_{s-}$ : negative supply voltage

T: temperature